VEHICLE NOISE SOURCE HEIGHTS & SUB-SOURCE SPECTRA

Florida Atlantic University
Department of Ocean Engineering

Robert K. Coulson

FL-ER-63-96

VEHICLE NOISE SOURCE HEIGHTS
& SUB-SOURCE SPECTRA

Final Report

Robert K. Coulson
November 1996

Center for Acoustics & Vibration
Department of Ocean Engineering
Florida Atlantic University
Boca Raton, Fl 33431

This is the final report for work under Florida Department of Transportation
HPR Study # 0709, contract # B-9077

1. Report No. FL-ER-63-96 PB97-132328	3. Recipient's Catalog No.
4. Title & Subtitle: Vehicle Noise Source Heights & Sub-Source Spectra	5. Report Date: December, 1996
	6. Performing Organization Code: 1610-061-02
7. Authors(s): Robert K. Coulson	8. Performing Organization Report No.
9. Performing Organization Name and Address: Florida Atlantic University, Department of Ocean Engineering, Boca Raton, Florida 33431-0991	10. Work Unit No. (TRAIS)
	11. Contract or Grant No.: B-9077
12. Sponsoring Agency Name and Address: Florida Department of Transportation, Environmental Management Office, 605 Suwannee Street, Mail Station 37, Tallahassee, Florida 32399-0450	13. Type of Report and Period Covered: Final
	14. Sponsoring Agency Code: 99700-7613-119

15. Supplementary Notes

Prepared in cooperation with the Federal Highway Administration

16. Abstract

This report describes a turn-key system that was developed and implemented to collect the vehicle source height database for incorporation into the new Traffic Noise Model; 'TNM.' A total of 2500 individual vehicle pass-byes were measured with this system at 16 different sites around Florida and this data is presented in the form of averaged curves for each vehicle type.

The dependence of source height on speed, pavement type, road grade and acceleration state is also shown for 10 different types of vehicles. The effect of these roadway conditions on the vehicle source heights is small compared to the typical variation in the whole data set. A recommendation is therefore made that the overall average of the data for each vehicle type be used in the TNM model and that variations with speed, pavement, grade and acceleration can be neglected. The data collection system and algorithm used to obtain the source heights is described and the accuracy is demonstrated experimentally with known sources. The measured vehicle source heights are further verified using an alternate Matched Field Processing algorithm which produced very similar results. It is also shown that the single equivalent source height model for a distribution of sources is more accurate than the two sub-source model when used in barrier attenuation calculations.

17. Key Words: Noise, Source Height, Traffic Noise, Sound Spectra	18. Distribution Statement: No restrictions. This document is available to the public through the National Technical Information Service Springfield, VA 22161

19. Security Classif. (of this report)	20. Security Classif. (of this page)	21. No. of Page	22. Price
Unclassified	Unclassified	105	

NOTICE

The opinions, findings and conclusions expressed in this publication are those of the authors and not necessarily those of the Department of Transportation or the U.S. Department of Transportation.

Prepared in cooperation with the State of Florida Department of Transportation and the U.S. Department of Transportation.

TABLE OF CONTENTS

METRIC CONVERSION FACTORS

Approximate Conversions from Metric Measures

Symbol	When You Know	Multiply By	To Find	Symbol
cm	centimeters	0.3937	inches	in
m	meters	3.281	feet	ft
m	meters	1.094	yards	yd
km	kilometers	0.6214	miles	mi
kph	kilometers per hour	0.6214	miles per hour	mph

Approximate Conversions to Metric Measures

Symbol	When You Know	Multiply By	To Find	Symbol
in	inches	2.540	centimeters	cm
ft	feet	0.3048	meters	m
yd	yards	0.9144	meters	m
mi	miles	1.609	kilometers	km
mph	miles per hour	1.609	kilometers per hour	kph

1. INTRODUCTION

The Federal Highway Administration is collecting a highway noise data base for the development of noise level regression equations. These data and equations are to provide the acoustic foundation for the new Traffic Noise Model 'TNM'. In addition to the collection of Reference Energy Mean Emission Level (REMEL) data, this test plan also requires the collection of an extensive data base of frequency dependent vehicle noise source heights covering the many vehicle classes and possible roadway parameters. These source heights will be used, along with the emission spectra, to apportion the total energy between two sub-sources whose heights will be specified for each vehicle class. As part of a previous Florida Department of Transportation sponsored project [1], Florida Atlantic University (FAU) developed and tested a methodology and processing algorithm that would calculate the single equivalent noise source height, as a function of frequency, for any vehicle using data recorded from a vertical array of microphones in a vehicle pass-by situation. However, this method involved collecting data and trigger signals on a tape recorder and subsequent downloading and analysis of this data in the laboratory which proved to be very time consuming. Therefore a total of only 100 pass byes were recorded and analysed, all from the same site. The TNM database requires the collection of over 1000 pass byes covering many combinations of vehicle type, speed, acceleration, road grade and road materials. Having had experience with this kind of data collection and analysis FAU proposed and was requisitioned to develop a more 'turn-key', rapid data acquisition and analysis system and to subsequently collect the large database for incorporation into 'TNM'.

This report describes the 'turn-key' system that was developed and the analysis algorithm used to compute the frequency dependent single equivalent noise source heights and sub-source spectra. A total of 2500 individual vehicle pass-byes have been measured at 16 different sites in Florida and this data is presented in the form of averaged plots for all the different vehicle types and possible roadway parameters. The data is also included on diskette and the format of these data files is described.

During the course of this study the inaccuracies of this methodology were addressed and some improvements were made to the algorithm. These changes and their effect on the data are also discussed. Two additional studies were also performed by Graduate students as Masters thesis topics. The first of these studies involves the development of a matched field processing method for the calculation of single equivalent source heights. The matched field results are more accurate but unfortunately more computer intensive. However they show very similar results to those measured with the turn-key system using the same time series data . The second graduate student study addresses the errors introduced into the TNM model by the concept of replacing a distribution of sources as a single equivalent source or as two arbitrary sub-sources. This study concludes that the single equivalent source model produces significantly smaller errors in the overall propagation attenuation calculations than the two sub-source model which tends to underestimate the transmission losses. Summaries of both these studies are included in this report along with some of their most important results.

2. THEORETICAL ANALYSIS

2.1. Introduction

A typical highway vehicle noise spectrum includes contributions from a number of noise sources such as tire, engine, exhaust, gear box, and aerodynamic noise. Each of these sources originate from different locations above the roadway and have different source strengths and frequency content. Since it is not possible to identify the location and spectrum of each source the concept of an equivalent single source is introduced [2]. The single equivalent source height is defined as the position at which the distributed sources could be replaced by a single point source to reproduce the same far field over the largest possible solid angle. With this frequency dependent source height and the emission spectra it is then relatively simple to model the sound propagation from the roadway to an observer over various types of terrain or noise barrier. In an attempt to reduce the anticipated errors in the propagation model involved with modeling a distribution of sources as a single source the FHWA decided to divide the total emission energy amongst two sub-sources of given heights and calculate their propagation individually before summing them at the observer position. These vehicle sub-source spectra are apportioned from the overall spectra using the measured single equivalent source height and the second acoustic moments.

2.2. Single Equivalent Source Height calculation

Using a binaural source location technique it is possible to obtain the centroid of any source distribution and the total source strength which is the sum of the component source strengths. It was shown by Kinns [4] that the equivalent source position of an arbitrary uncorrelated distribution of omnidirectional sound radiators may be obtained from the coherence and phase spectra of a closely spaced pair of microphones. If two microphones lie in a plane containing the axis of the line sources, the power and cross spectra of the microphone signals can be measured. The cross spectrum in the far field is then expressed as the combination of the cross spectrum of each source component in the source region and a transfer function related to the range difference between the source and each microphone. The relation between coherence spectra and multipole moments of the source region can also be obtained. The first and second moments give the source centroid and scale. Glegg & Yoon extended this concept to sources distributed in height above a hard surface. The full development of the theoretical equations can be found in [2] & [3] where it is shown that the acoustic moments of a distribution of sources are directly related to the far field. They then demonstrate that the acoustic centroid of the distribution can be defined and that by replacing it with a point source with an equivalent source strength an equivalent far field can be created. Using cross spectral analysis to define the far field they derive an expression to locate the equivalent source height.

The cross spectral density of sources distributed over a given volume is defined as;

$$C_m = \int_V Q_e(\bar{y},\omega) G(\bar{y},\bar{x}_m) d\bar{y} \tag{2.1}$$

where C_m is the cross spectral density between a microphone at $\bar{x}_0$ and a microphone at $\bar{x}_m$ and Q_e is the source strength. The transfer function $G(\bar{y},\bar{x}_m)$ is calculated from the geometry shown in figure 1 and the complex reflection coefficient γ as;

$$G(\bar{y},\bar{x}_m) = (1+\gamma)\left(\frac{e^{ik(r_+ - r_0)}}{r_+ r_0} + \gamma^* \frac{e^{ik(r_- - r_0)}}{r_- r_0} \right) \tag{2.2}$$

Glegg and Yoon then use a Taylor series expansion of the function $G(\bar{y},\bar{x}_m)$ to estimate the cross spectral density. By choosing a reference point at y_0 on the reflecting plane, the cross spectral estimate is expressed as a sum of acoustic multipole moments about the reflecting plane. This expansion and resulting equation are shown in reference [1]. A similar Taylor series expansion of $G(y_0 + \bar{z}, x_m)$ can be performed for a point source at $y = \bar{y}_0 + \bar{z}$ where $\bar{z} = (y_e, 0, 0)$ and y_e is the equivalent source height or position of the acoustic centroid for the distributed sources above the plane. A comparison between the two series reveals that for small values of the argument $y_e k h_m / r$ (k is the wavenumber) the fields are the same when $y_e = \sqrt{\mathrm{Re}\,\mu^{(2)}}$, where $\mu^{(2)}$ is the second acoustic multipole moment. The validity of the derivation is dependent on the far field assumption defined by the relationships;

$$(r_+ r_0)^{-1} \cong (r_- r_0)^{-1} \cong (rR)^{-1} \tag{2.3}$$

where $r_{\pm} = \sqrt{(y_e \mp h_m)^2 + R^2}$, $r_0 = \sqrt{(y_e)^2 + R^2}$, $r = \sqrt{(h_m)^2 + R^2}$ and $R >> y_e$. (see figure 1.) The cross spectral estimate C_m is then given by;

$$C_m \cong \overline{C}_m = \overline{Q}_T G(\overline{y}_0 + \overline{z}, \overline{x}_m) = \overline{Q}_T G(\overline{y}_0, \overline{x}_m) \cos(k y_e h_m / r) \tag{2.4}$$

where $\overline{Q}_T$ is the total equivalent source strength of all the individual sources in the distribution and is defined as;

$$\overline{Q}_T = \int Q_e(\overline{y}, \omega) d\overline{y} \tag{2.5}$$

The estimated autospectral density C_0 is then;

$$C_0 \cong \overline{C}_0 = \overline{Q}_T G(y_0, x_0) \tag{2.6}$$

and the resulting frequency response function is defined as;

$$H(x_m, \omega) = \frac{C_m}{C_0} \cong \frac{G(y_0, x_m)}{G(y_0, x_0)} \cos(k y_e h_m / r) \tag{2.7}$$

By normalizing the cross spectral density with the autospectral density this function is independent of source strength. The frequency response function describes the sound field as a simple geometric function. Given the range between the array and the axis of the source, the height of the source becomes the only unknown variable. The measurement model D_m is extracted from equation 2.7 and is defined as;

$$D_m = \mathrm{Re}\left[\frac{C_m G(\overline{y}_0, \overline{x}_0)}{C_0 G(\overline{y}_0, \overline{x}_m)}\right] \approx \cos(y_e k h_m / r) \tag{2.8}$$

which yields the equivalent source height as;

$$y_e = \cos^{-1}\left(\frac{D_m r}{k h_m}\right) \tag{2.9}$$

This shows that by measuring the cross spectrum C_m between two microphones in an array we can find the equivalent source height. However there are limitations because ; (1.) $\cos^{-1}(x)$ is multi-valued and (2.) when $D_m \approx 1$ the measurement is sensitive to noise. These points will be discussed in sections 2.3 & 2.4.

2.3. Error Bias Limitations

For a single omnidirectional point source in the absence of extraneous noise only one pair of microphones would be necessary to define the source height up to the frequency where $ky_e h_m / r = \pi$. However in the case of highway vehicles measured in a roadside environment there are several bias errors introduced by the following;

1.) Measurement noise at the reference microphone
2.) Insufficient averaging
3.) Microphone spacing and range
4.) Geometrical near field effects and ground reflection
5.) Source size
6.) Directivity and horizontal distribution
7.) Doppler amplitude and frequency distortion

In [2] each of these errors is analysed in detail and it is shown that a total normalized error of ± 15% in estimated source height can be achieved if the limits for the value of D_m are;

$$0 \le D_m \le 0.75 \tag{2.10}$$

and the signal to noise ratio s/n > 10 dB. The lower limit in equation 2.10 or high frequency limit is determined by the point where the truncated Taylor series expansions for the distributed and single sources converge. The number of terms required in the series to reach an acceptable convergence depends on the extent of the source distribution. Since the number of terms used is fixed the error introduced will increase as the source size increases. The upper bound in equation 2.10 or low frequency limit is controlled by noise contaminating the autospectrum estimate. In the absence of noise $|D_m|$ approaches 1 at low frequencies. However when noise is introduced the autospectrum contains an error term which causes an underestimate of D_m and thus an overestimate of the source height. This effect increases with D_m as can be seen in figure 2.4 and will be discussed in section 2.4.2.

2.4. Microphone Pair Selection & Spacing

The limits set by equation 2.10 produce a region of validity for a given pair of microphones with a given separation. Therefore smaller microphone spacings must be used at higher frequencies and higher source heights. An array of microphones is therefore necessary to cover the broad ranges of both frequency and possible source height.

Equation 2.10 is the criteria used to select the pair of microphones, for a particular frequency, from which to calculate the source height. Figure 2.2 shows the range of frequencies and source heights that can be measured by each microphone pair in the array while satisfying the condition set in equation 2.10. The heights of the microphones in the array are chosen so that their useful regions overlap one another and together cover as much of the frequency/source height range as possible without leaving any gaps.

The D_m functions of equation 2.8 are cosine functions whose values may pass through the range specified in equation 2.10 several times in the frequency range of interest, causing some ambiguity. The approximations used in this analysis are only correct for the region where each curve *first* passes through the limits of equation 2.10 Theoretical D_m curves for each microphone in the array paired with the reference ground level microphone are shown in figure 2.3 for a source height of 1m. It can be seen in this figure that for a given frequency there may be two, (or more with real data), microphone pairs that satisfy the condition that D_m lies in the range $0 \leq D_m \leq 0.75$. A criteria for choosing which pair to use to calculate the source height at a given frequency must therefore be established.

2.4.1. Lowest Pair Criteria: When the original methodology was developed by Glegg & Yoon [2] the processing power of computers was much more limited than with today's technology. Manipulation of large arrays of data was slow so to overcome the ambiguity caused by the periodic nature of the D_m functions a simple criteria was established where no data indexing and truncation was necessary. It was simply assumed that if the value of D_m for microphone m lies in the correct range then the value of D_m for microphone (m-1) will always be larger (microphone m being higher than microphone m-1). The correct microphone could therefore be uniquely defined as being the *lowest* microphone for which the data satisfies equation 2.10. Figure 2.3(a) shows theoretical D_m curves for a 1m source height for the 1m tall 8 element array used in the first half of this study. The thicker solid line on figure 2.3(a) shows the portion of each curve that would be used for the source height calculation with this lowest pair criteria.

2.4.2. Highest Pair Criteria: In the second half of this study the inaccuracies of the method were addressed and it became evident that this method was significantly overestimating the source height particularly for relatively low sources. In the original study the limits set in equation 2.10 ensure errors of less than ±15% for a signal to noise ratio of 10 dB. These later studies revealed that the most dominant error was caused by the noise in the signals and that this error increases with increasing values of D_m and decreasing signal to noise ratio. Figure 2.4 shows this relationship and it can be seen that, for a signal to noise ratio of 10 dB, the normalized error is zero when $D_m = 0$ and increases to about +15% when $D_m = 0.75$ and that higher noise levels further increase the error. In figure 2.3(a) it can be seen that using the lowest pair criteria biases the D_m values to the higher end of the limits of equation 2.10 where the overestimates are greatest. This effect is compounded by the large overlap between the adjacent microphone pairs in such a compact array. It was decided therefore to change the microphone selection criteria to a bias toward the highest pair that satisfy equation 2.10. The thicker solid line in figure 2.3(b) shows the sections of each curve that would be used with this selection criteria and it can be seen that the D_m values are now biased toward the more accurate lower end of the range defined in equation 2.10. With this method it is necessary to truncate each D_m curve the first time it crosses the $D_m = 0$ line to avoid the ambiguities produced by the periodic D_m functions.

As mentioned previously, the original microphone spacing and array height were determined so that the effective ranges of frequency and source height that can be measured by each microphone pair overlap considerably. This was done to ensure that with real data there would be no drop outs or frequencies at which none of the microphone pairs satisfied equation 2.10. However by raising the height of the array it is possible to measure lower sources at lower frequencies and the effect of the overlap on the bias toward one end of the D_m range is reduced. The few dropouts that do occur can simply be omitted from the one third octave averaging without any detrimental effects to the data. A new taller array was used to collect data in the second half of this study using the highest pair criteria. This method was shown to produce significantly more accurate measurements of sources of known heights particularly for low sources at low frequencies as will be shown in section 4.3.1. Theoretical D_m curves for this array are shown in figure 2.3(b) where the thicker solid line shows the region of each curve that would be used to measure a source of height 1m.

2.5. Sub-Source Strength Calculation

To obtain the source spectra at the two desired sub-source heights we must consider the definition of the equivalent source height y_e and it's relation to the sub-source spectra [4] through the equations;

$$Q_T y_e^2 = Q_1 y_1^2 + Q_2 y_2^2 \tag{2.11}$$

and

$$Q_T = Q_1 + Q_2 \tag{2.12}$$

where Q_1 and Q_2 are the sub-source strengths and Q_T is the vehicles total source strength. The sub-source heights are y_1 and y_2 and are defined, by FHWA, as 0 m & 3.66 m for heavy trucks and 0 m and 1.52 m for all other vehicle types. These equations can be solved to obtain the sub-source strengths using the relationships;

$$Q_2 = \frac{Q_T\left(y_e^2 - y_1^2\right)}{\left(y_2^2 - y_1^2\right)} \tag{2.13}$$

$$Q_1 = Q_T - Q_2 \tag{2.14}$$

If r is defined as the ratio of the strengths of the two sub-sources then;

$$r = \frac{Q_2}{Q_1} = \frac{y_e^2 - y_1^2}{y_2^2 - y_e^2} \tag{2.15}$$

The total source strength Q_T can be expressed in terms of the measured auto spectral density C_0 at the reference microphone;

$$Q_T = \frac{C_0(4\pi r_0)^2}{4} \tag{2.16}$$

The sub-source spectra can then be calculated using equations 2.13 & 2.14. From these two equations it can also be seen that for this method of energy apportioning to be applicable y_1 and y_2 must be chosen so that;

$$y_1 < y_e < y_2 \tag{2.17}$$

This concept of redistributing the total energy of the single equivalent source between two sub-sources at predetermined heights is incorporated into TNM. This is done as a safety factor designed to ensure that there is no overestimation of the barrier attenuation caused by bringing some of the energy of higher sources in the distribution down to the equivalent source height.

3. THE SOURCE HEIGHT DATA COLLECTION SYSTEM

The measurement apparatus used to collect and analyze the vehicle pass-by data is shown in figure 3.1. The system consists of a vertical array of 8 microphones who's axes are distributed between ground level and a height of 1m. The microphones are interfaced to the data acquisition and analysis system which consists of 3 National Instruments dynamic signal acquisition boards mounted in an ACER Minitower Workstation with a Pentium Microprocessor.

The measurement arrangement is shown in figures 3.2 & 3.3. The array is located 7.5 meters from the center of the traffic lane being measured and the computer equipment and operator are located in a support van downstream from the array. The data acquisition is initiated by a trigger signal that is generated when a vehicle's front tires break the first infrared light beam, which crosses the highway 2.5 meters before the arrays axis to closest point of approach (CPA). The data acquisition period is determined by the time before a second trigger signal is generated when the same vehicle's front tires cross the second light beam positioned 2.5 meters past the CPA.

Two National Instruments AT2150C four channel 16 bit signal acquisition boards are used for the simultaneous analog to digital conversion of the 8 microphone signals. The trigger signal from the first infrared beam is applied to the digital trigger channel of one of these boards and this is sent over the RTSI bus to trigger acquisition on the other boards simultaneously. Since it is not possible to terminate acquisition on these boards using a digital trigger, the second trigger signal is simultaneously acquired, along with the microphone signals, on a National Instruments DSP2200 four channel digital signal processing accelerator board and this signal is subsequently used to determine the truncation point of the microphone signals so that only data collected between the two triggers is analysed. The time period between the two triggers also yields the vehicle speed through the trap and this is verified at setup using a radar gun.

The data acquisition, analysis, presentation and storage are controlled and the signal processing performed using software written on National Instruments LABVIEW 3.1.1 Graphical Programming for Instrumentation platform. The microphone signals are analysed using the algorithm described in [3] which is summarized in section 2 of this report. The main computer screen, shown in figure 3.4, displays the following information: The raw time series data from each microphone, the vehicle speed, overall noise level in dB(A), 1/3 octave spectrum, 1/3 octave spectra at each sub-source, the calculated discrete source heights and the 1/3 octave band averaged source heights. The parameter D_m [3], used by the program to decide which pair of microphones to use to calculate the source height for each particular frequency, is also shown. As discussed in section 2 this function is the cross-power spectrum of each microphone in the array with the base reference microphone normalized with the auto-power spectrum of the reference microphone. It also includes the Green's functions which are a function of the propagation path lengths and ground reflection coefficient. This information is useful in deciding whether a particular pass-by is a clean measurement. Since the D_m curves are cosine functions it is relatively easy to see whether or not they contain an excessive noise component. The whole process of data collection, reduction and storage is performed in less than a minute allowing for almost real time on site evaluation of the data.

Calibration of the system is conducted at the beginning and end of each measurement session. A Bruel & Kjaer type 4231A sound level calibrator is used to calibrate each microphone. A separate calibration program is used to calculate a calibration factor for each channel which is subsequently entered into the measurement program. The background noise level is recorded and a wind speed meter is kept available to monitor natural wind speed. Measurements are not taken if the wind speed exceeds 11 kph.

3.1. Roadside Setup

Care was exercised in choosing test sites. The following characteristics were considered:

(1) Roadside Conditions: The ground between the vehicles and the microphone array must be a hard reflecting surface. It must also be level so that the base of the array is at the same height as the roadway. Turnouts, median turnabouts, wide hard shoulders, closed traffic lanes and driveways make good sites.

(2) Uniform Vehicle Speed: Unless accelerating or decelerating vehicles are to be studied, a stretch of highway where the vehicles have reached a uniform cruising speed should be selected.

(3) Low Background Noise: The site should be away from other noise sources such as industrial plants, railway lines, airports, other busy roadways, buzzing power lines etc. The generator should be situated as far away from the array as possible. It should be further down stream

from the support vehicle and placed behind an obstacle or thick vegetation. An acoustic enclosure should be used if possible.

(4) Varied Vehicle Types: If possible roadways with a high percentage of heavier vehicles should be chosen to allow for the collection of data with a more even distribution of vehicle types.

(5) Optimum Traffic Density: The traffic density should be sufficiently low to ensure a reasonable number of isolated vehicle pass-byes. Measurements should not be taken if there is another vehicle within 50 meters. For this reason it is helpful to have a clear view of the roadway for several hundred meters in both directions. Sites where the support vehicle can be located close to the roadside are preferable.

(6) Wind Speed: Wind speed should be monitored and measurements should not be taken if it is greater than 11 kph.

Care should also be taken not to affect the traffic flow. Placing the support vehicle/personnel, traffic cones and light beams too close to the roadway may cause vehicles to decelerate or change to the wrong lane. The use of a radar gun is a useful check for the speed trap but, for the same reason, try to keep it out of sight !

3.2. System Software Operating Instructions

The whole system can be set up and operated by one or two people and requires the minimum of operator input. The operator first runs the program 'MICROPHONE CALIBRATION.VI' which determines the calibration factors for each microphone channel. These values are then entered into the main program 'SOURCE HEIGHTS.VI' when it is initiated. This program is then used to acquire and store the vehicle noise data and process it into source heights and sub-source spectra.

Note: *If you are setting up a new system it is necessary to first initialize the boards correctly so that the software addresses them in the correct order. Figure 3.5 shows the board numbers that should be assigned to each board. This step is performed using the LABVIEW program 'WDAQconf' and **must** be completed before either of these programs can be run.*

3.2.1. Microphone Calibration: The microphones should be calibrated at the start of a measurement session and should be checked again before you quit for the day.

In extreme hot/cold conditions it may also be advisable to check the calibration periodically throughout the day. The program '*MICROPHONE CALIBRATION.VI*' is used to find the calibration factors that are necessary inputs to the '*SOURCE HEIGHT.VI*' program. The program displays the microphone voltage, the averaged spectrum of that voltage and the 1/3 octave spectrum levels. The calibration procedure is as follows;

1) Open the program '*MICROPHONE CALIBRATION.VI*'. You will see a display similar to that in figure 3.6.
2) Place the B&K calibrator over microphone number 1 and turn it on.
3) Set the 'Microphone number' control to 1 and click the 'enter' button in the top left corner of the screen. (not shown)
4) Wait for a quiet period between vehicle passes then click on the 'run' arrow in the top left corner of the screen to start the program. The program performs an iteration of the calibration factor for channel 1 until the maximum level at 1000 Hz is 94 dB. At this point the program will stop.
5) Write down the 'Calibration Factor', for that channel, shown on the right of the screen.
6) Repeat steps 2 to 5 for the other seven microphones, making certain to change and enter the corresponding 'Microphone number'.

3.1.2. Source Heights: Once the microphone calibration factors have been found you are ready to collect source height data with the program 'SOURCE HEIGHT.VI'. This program displays each microphone signal, the discrete and 1/3 octave averaged source heights, the spectrum and 1/3 octave averaged spectrum levels and the 1/3 octave sub-source spectra. Also shown are the vehicle speed, overall level and the event number. The main window of this program is shown in Figure 3.4. The following steps will guide you through the data collection procedure;

1) Open the file '*SOURCE HEIGHT.VI*'. A window similar to figure 3.4 should appear.
2) Click on the 'run' arrow to start the program and the screen will change to one similar to that in figure 3.7
3) Enter the calibration factors for each microphone in the corresponding spaces on the left side of the window. Check, and change if necessary, the inputs on the

right making sure to update the name of the file where you wish to write the results from that session.

4) Click on the 'Continue' button and the window will change back to that in figure 3.4 and the trigger window will appear.

5) When the vehicle that you wish to measure is within a few seconds of the first light-beam trigger click on the 'Arm Trigger' button. The program will now capture the signal from the passing vehicle as it proceeds through the two triggers.

6) Once the signals and source heights have plotted in their relative windows of figure 3.4 a window similar to that shown in figure 3.8 will appear telling you to select the vehicle type that you just measured.

7) Select the corresponding vehicle type by dragging down on the selection bar arrow then click on the 'OK' button.

8) Once the sub-source heights have been calculated and displayed a window similar to that in figure 3.9 will appear. This window displays the results that can be written to file. Make any necessary changes to the 4 parameters in the center box and then, if you are happy with the result and wish to save the data string to file, click on the 'YES' button. The data will be appended as another row to the file named in step 3. If you do not wish to save this result simply click on the 'Abort' button. Whichever button you select the window will then return to that in figure 3.4 with the 'Arm Trigger' dialogue box.

9) Repeat steps 5 through 8 for subsequent vehicle passes.

If you wish to stop the program you may do so by clicking on the 'Abort' button in either of steps 4 or 5 and then clicking on the stop button in the top left corner of the screen.

4. THE MEASURED SOURCE HEIGHT DATA

4.1. Introduction

At the time of inception of this project the impetus was on collecting an initial block of data to be used in the first release of the new TNM software. Little time was available to address the limitations of the method so data was collected using the algorithm used by Glegg & Yoon in the original study [2]. Although the data collected concurred with that collected by Glegg & Yoon and, in controlled studies, measured the height of a known source with reasonable accuracy over most of the frequency band of interest, it was apparent that there were problems at low frequencies (less than 500 Hz) where the method was significantly overestimating the source height and at high frequencies (above 3 kHz) where there was a large increase in the standard deviation of the data. It also became clear that the method was significantly overestimating the height of sources below 1m. All the data collected before 3/13/96 was measured using this method and therefore contains these errors.

Between January and March 1996 efforts were made to address these problems and resulted in the modification of the algorithm to include the new microphone selection criteria discussed in section 2.4.2. Interrupted flow data (accelerating vehicles) was then collected using this new algorithm and in June 1996 more tests were performed in a hemi-anechoic chamber to evaluate the performance of a taller array which was then used to collect all the data from that point on. The results of these tests proved conclusively that the old method was producing large overestimation's of the source heights particularly for low sources and low frequencies. The old data is presented in the form of averaged plots and the spectra are usable, however only the more accurate data collected with the new algorithm and array is used to determine any trends or conclusions about vehicle source heights.

The data will therefore be divided into 4 groups which will be discussed in the following sections;

4.2. Data collected before March 1996. (With the original algorithm.)

4.3. Experimental test data using loud speakers. (For comparison of each method.)

4.4. Data collected after July 1996. (With the modified algorithm and taller array.)

4.5. Accelerating vehicle data collected between March and July 1996. (With the modified algorithm.)

All the LabView programs and data files are included with this report on diskette. The data filenames and format will be discussed in section 4.6.

A total of 2500 individual vehicle pass-byes were measured from 16 different sites in Florida. The vehicles are classified at the time of measurement into the following 10 vehicle types;

0 - Compact Autos
1 - Standard Autos
2 - Medium trucks (2-Axles, 6 Wheels)
3 - 3-Axle Heavy trucks
4 - 4-Axle Heavy trucks
5 - 5-Axle Heavy trucks (Standard 18 Wheelers)
6 - 6-or-more-Axle Heavy trucks
7 - motorcycles
8 - 2-Axle Buses
9 - 3-Axle Buses

The data was then averaged according to vehicle class and site type. The site types are classified by the following parameters:

1 - Pavement Type. (Asphalt or Concrete.)
2 - Vehicle Speed. (High > 72.4 kph, Low < 72.4 kph)
3 - Acceleration State. (Cruising or Distance from Standing Start)
4 - Road Grade. (Level or Percent Incline.)

Where sufficient data allows each vehicle class/site type combination is separated into the following 5 speed ranges;

1 - < 56.3 kph
2 - 56.3 - 72.4 kph
3 - 72.4 - 88.5 kph
4 - 88.5 - 104.6 kph
5 - > 104.6 kph

4.1.1. Data Collection Sites; Data was collected at the following 16 sites in Florida;

1 - Route 710, Beeline Highway, West Palm Beach FL.
2.- Loxahachee Road, Parkland FL
3 - Highway 27, Broward County, FL
4 - Hillsboro Blvd., Parkland FL.
5 - Highway 441, Gainesville FL.
6 - I-75, Gainesville FL.
7 - Route 19, Georgia-Florida Parkway, Jefferson County, FL
8 - S.R. 155, Tallahassee FL.
9 - I-10, Jefferson County, FL
10.- Jog Road, West Palm Beach FL
11.- A1A, Highland Beach FL
12.- Blount Road, Pompano Beach FL
13.- Parkside Road, Parkland FL
14.- Hillsboro Blvd., Pompano Beach FL
15.- Sawgrass Expressway, Broward County, FL
16.- North Dixie Hwy, Boca Raton, FL

Sites 1,2 and 3 are high speed level asphalt roads.
Sites 4,10,11,12,13, 14 and 16 are low speed level asphalt roads.
Sites 5,6,7 and 8 are graded asphalt roadways.
Site 9 is a high speed level concrete road.
Site 15 is a toll booth exit with accelerating vehicle.

4.2. Data Collected Before March 1996.

This data is contained in the files named 'OLDCRUIS', 'OLDCONC' and 'OLDGRADE'. It was collected using the Lowest Microphone Pair Selection Criteria outlined in section 2.4.1.

4.2.1. 'OLDCRUIS' Data; This data includes all measurements taken on level asphalt roadways where the vehicles were traveling at constant cruising speed. Figure 4.1 shows averaged measured spectra and source heights for vehicle types 0 to 4 and figure 4.2 shows the same for types 5 to 9. These curves show clearly the dominance of tire noise between 500 and 2000 Hz where all the vehicles have source heights below 1m. A general increase in source height is also apparent as the size of the vehicle increases. The differences become more obvious above 2000 Hz where it is thought that wind driven by the vehicle pass-bye itself is producing some phase scattering. This effect also increases as the size of the vehicle increases and is less apparent for smaller more aerodynamic vehicle types. At the other end of the spectrum below 1000 Hz there is an increase in the source heights of all vehicles and a general convergence of the data. Some of this increase is due to the influence of aerodynamic noise from higher noise sources such as wing mirrors and further contributions from higher engine and exhaust stacks. However the main cause of this increase and convergence is the overestimation of low sources that is produced using the lowest microphone pair selection criteria discussed in section 2.4.2. No further analysis of this data will be presented here since the new data presented in sections 4.4 and 4.5 is shown, in section 4.3, to be more accurate and will thus be used to determine any relationships between source height and speed, pavement type and vehicle acceleration.

4.2.2. 'OLDCONC' & 'OLDGRADE' Data; The data file 'OLDCONC' includes all the measurements taken on level concrete roadways where the vehicles were traveling at constant speed. Figure 4.3 shows the averaged data for the five different vehicle types measured at this site. 'OLDGRADE' contains all the data for measurements taken on graded asphalt roadways where the vehicles were traveling up an incline at approximately constant speed. The averaged data for these vehicles is plotted in figure 4.4 for vehicle types 0 through 4 and in figure 4.5 for vehicle types 5 through 9. Figures 4.6 through 4.8 show comparisons between asphalt, concrete and graded roadways for standard autos, medium trucks and 5-Axle heavy trucks respectively for the 88.5 - 104.6 kph speed range. In these plots there appears to be no difference in the measured source heights on the different road surfaces or grades. However no conclusions can be made from this data since it contains large errors due to the overestimation of the source heights produced with the lowest microphone pair selection criteria discussed in section 2.4.2.

4.3. Experimental Test Data Using Loud Speakers.

After the collection of the first set of data described in section 4.2, with the original algorithm developed by Glegg & Yoon [2] & [3], more time was available to assess the measured data. It was concluded that there was little confidence in the source height results below 500 Hz and it was suspected that the method was producing significant overestimates of the source heights. Further analysis led to the development of a different microphone pair selection criteria where the highest valid pair is used to calculate the source height as opposed to the lowest pair. This is described in more detail in section 2.4.2. To evaluate this change some experiments were conducted in a hemi-anechoic chamber using loud speakers, driven with white noise sources, positioned at known heights above the floor.

4.3.1. Single Source Experiments; A single loudspeaker, driven with amplified white noise covering the whole frequency range of interest, was positioned at heights of 0.5m, 1.0m and 1.5m in turn and the system was used to measure its source height first with the Lowest Microphone Pair Criteria and then with the Highest Pair Criteria. The results are displayed in figure 4.9. Here it can be seen clearly that the Highest Pair Criteria produces a much better estimate of the source height and that as the height of the source increases the difference between the two algorithm's estimates decreases. For low sources however errors in the order of 0.5m are common with the lowest pair criteria which are unacceptable. It can also be seen that as the height of the source increases the source size error increases producing some underestimation of the actual source height. When there is no microphone pair that is valid for a particular frequency the source height is returned as zero. Figure 4.9 shows very well how it is possible to measure higher source heights to much lower frequencies. A 0.5m high source can only be measured down to about 600 Hz as can be seen in figure 4.9(b) but a 1.5m high source is measurable down to about 250 Hz as shown in figure 4.9(d). This effect is due to the limits imposed on the valid D_m regions for each microphone pair and the low frequency cut-offs concur well with the theoretical predictions shown in figure 2.2.

4.3.2. Experiments with Two Sources; Having established that the highest microphone pair selection criteria gave the best source height predictions, tests were then conducted with two loudspeakers at different heights above the floor using just this criteria. Each source was driven with a separate white noise signal and the individually measured spectra at the ground-level microphone were used to calculate the equivalent point source position using equation 2.11. Figure 4.10 shows an example of the result obtained for sources positioned at 0.45m and 1.4m. In this example the measured equivalent source height slightly underestimates the calculated result but is within the expected 15% maximum error. It should be noted here also that the calculated equivalent source height is not exact since the individual source strengths may have changed when the amplifier was loaded with both sources.

In a further test the white noise drive signal for a source at 0.5m was high-pass filtered at 1500 Hz and the signal for a 1.5m source was low-pass filtered at 1500 Hz. The equivalent point source height in this case is simply a step function that changes from 1.5m below 1500 Hz to 0.5m above 1500 Hz. Measured spectra and source heights for each speaker alone and for the combination of both speakers are shown in figure 4.11. In this figure it can be seen that when the 0.5m source is measured on its own the source height is measured correctly above 1000 Hz where the high-pass filter starts to cut on and is overestimated below this frequency where the signal to noise ratio is very low. Similarly the 1.5m source is measured correctly up to 1500 Hz where the measurement deteriorates because of the low-pass filter roll off. When both speakers are played together there is ample signal to noise across the whole frequency spectrum and the system measures the step function in the source height with a high degree of accuracy.

4.4. Data collected after July 1996.

From July 1996 onward all the data was collected using the new highest microphone pair algorithm and a taller array. The microphones in the array were now distributed between 0.02m and 1.61m which allowed for better measurement of low source heights at low frequencies. This data is contained in the files named 'NEWCRUIS', 'NEWCONC' and 'NEWGRADE'.

4.4.1. 'NEWCRUIS' Data; This data includes all measurements taken with the new algorithm on level asphalt roadways where the vehicles were traveling at constant cruising speed. Figure 4.12 shows averaged measured spectra and source heights for vehicle types 0 to 4 and figure 4.13 shows the same for types 5 to 9. With the new algorithm being better able to measure low sources to lower frequencies there are now more pronounced differences in source heights between vehicle types across the whole frequency band. Compared to the old data in figures 4.1 and 4.2 the new average source heights, in figures 4.12 and 4.13, are in general about 20-25 cm lower. This difference decreases at frequencies below about 500 Hz where the source heights rise to where the overestimate of the old algorithm is smaller.

Figures 4.14 through 4.23 show plots of the scatter of the data for each vehicle type. These scatter plots show that for small vehicles the relative distribution is <0.25m and for heavy trucks is <0.5m. Above 2000 Hz there is a little more scatter which may be resulting from the effects of wind generation as discussed. Figures 4.24 through 4.30 show the same data averaged over the five speed bands for the vehicle types with sufficient data. In these figures it can be seen that there are small changes in the source heights as vehicle speed increases. In general vehicles moving at higher speeds have slightly higher source heights which is contrary to what one would expect since tire noise increases with speed. However although there is as much as 10-12 dB difference in the spectrum levels of the slow and fast speed bands the differences in the source heights are generally <0.25m. This difference does increase for the larger trucks at low frequencies as can be seen in figure 4.29.

4.4.2. 'NEWCONC' Data; This data includes all measurements taken with the new algorithm on level concrete roadways where the vehicles were traveling at constant speed. Figure 4.31 & 4.32 show the averaged data for all the different vehicle types measured and figures 4.35 to 4.37 show comparisons between asphalt and concrete roadways with the new algorithm for standard autos, medium trucks and 5-Axle heavy trucks respectively for the 88.5 - 104.6 kph speed range. It can be seen in these figures that for standard autos and 5-axle trucks there appears to be more tire noise at low frequencies on the concrete roadways producing slightly lower source heights. These differences are again generally less than 0.25m at all but the lowest frequencies. For medium trucks this is not the case as the concrete roads show significantly higher source heights above 1000 Hz. This result is not intuitive and may be the result of the sparse data set for the concrete road case which is magnified by the large diversity of vehicle shapes and sizes that the term 'medium truck' encompasses.

4.4.3. 'NEWGRADE' Data; This data includes all measurements taken on Graded Asphalt roadways with the new algorithm where the vehicles were traveling up an incline at approximately constant speed. Figures 4.33 and 4.34 show the averaged data for all the different vehicle types and figures 4.35 through 4.37 show comparisons between level and graded roadways for standard autos, medium trucks and 5-Axle heavy trucks for the 88.5 - 104.6 kph speed range. It can be seen here that there are small differences between the source heights measured on level and graded roadways particularly at frequencies below about 800 Hz. This result would be intuitive if the source heights for accelerating vehicles were higher since this frequency range is where the additional engine related noises would contribute. However this is not the case and the cruising vehicles on level roadways have the higher source heights. At this time no explanation for this result has been found. These differences are again in general <0.25m which is small compared to the divergence of the whole data set.

4.5. Accelerating vehicle data collected between March & July 1996.

This section covers the first set of source height data collected using the new highest microphone pair algorithm. Difficulty was encountered in finding suitable sites to measure accelerating vehicles and the data presented here was collected at just one site. This site was adjacent to a toll booth at the entrance to the Sawgrass Expressway in Broward County, Florida. Here the vehicles stopped to pay the toll and then accelerated onto the expressway. Even at this site physical restraints meant it was only possible to take measurements at three ranges downstream from the toll booth. The measurement locations were at positions 30.48, 45.72 and 60.96 m from the point where the vehicles stopped to pay the toll. Two days of measurements were collected at each of the ranges and the data is divided into three files, one for each of these measurement positions. The data file names are; ACCEL100, ACCEL150 and ACCEL200. Figures 4.38 through 4.43 show average spectra and source heights for all the vehicle types at each of the three measurement positions. In these figures it is again clear that there are more distinct differences in the source heights between different vehicle types than was suggested with the old algorithm. Figures 4.44 through 4.46 show comparisons between the three ranges for standard autos, medium trucks and 5-axle heavy trucks respectively. In these figures it is now possible to see a slight decrease in the source height of each vehicle as its speed increases and tire noise becomes more dominant over the engine and associated sources. This effect is most noticeable in figure 4.44 for standard autos and this would be expected since the change in speed between the three ranges is more pronounced than with the heavier vehicle types. However the differences in the source heights measured at the three different ranges is again <0.25m for all frequencies except 250 Hz. Figure 4.47 shows a comparison between accelerating and cruising vehicles for the 0-56.3 kph speed range. Here it can be seen that in general the source heights of the accelerating vehicles are slightly higher than the cruising equivalent but that this difference is always <0.25m except in the 250 and 315 Hz 1/3rd octave frequency bands where the difference is closer to 0.5m. The differences observed here, between slow speed accelerating and cruising vehicles, are bigger than for all of the other parameter changes that were studied but still relatively small when compared to the overall deviation of the data.

4.6. Sub-Source Emission Spectra and Ratios.

In the propagation calculations in which these source height results will be used, there may be errors introduced because a distribution of sources is being modeled as a point source. In an effort to overcome this problem it was decided by the FHWA to split the total energy of the single equivalent source between two sub-sources and then perform propagation calculations for each sub-source individually before summing the results at the observer position. These two sub-sources were chosen at heights 0 & 3.66 m for heavy trucks and 0 & 1.52 m for all other vehicle types. This apportioning of the energy is done using the measured spectra at the ground level reference microphone and the measured source height. Using equations 2.16 of section 2.5 the total emission spectrum can be found from the auto-spectrum measured at the ground level reference microphone. The sub-source emission spectra can then be calculated from equations 2.13 and 2.14. Alternatively the ratio of the sub-source emission levels can be found independently of the total emission level using equation 2.15. Examples of the results of this procedure are shown in figures 4.48 to 4.50 for standard autos, medium trucks and 5-axle heavy trucks in the average level asphalt cruise condition. In these figures it can be seen that this process actually apportions most of the total energy to the ground level sub-source, especially for heavy trucks where the higher sub-source is chosen at 3.66 m. Concerns that this may actually lead to larger errors inspired a parallel study in the form of a Masters thesis topic that was conducted by Glynn [7] and this work is summarized in section 6. In figures 4.48 and 4.49 it can also be seen how this energy apportioning method breaks down below 315 Hz when the measured source height is just above 1.52 m and does not lie between the chosen heights of the two sub-sources as specified in equation 2.17.

4.7. Programs and Data Files Included on Diskette

There are 2 diskettes included with this report. One contains the LabView program files and the other the source height data files.

4.7.1. Diskette 1: Labview Programs; There are two main programs and 12 sub-programs included in one directory. These must all be downloaded into the same LabView directory for the programs to run properly. All the files are listed below;

SOURCE-HEIGHT.VI
MICROPHONE CALIBRATION.VI
Set Variables.svi
Acquire.svi
Calculated Parameters.svi
Calc fft Averages.svi
Calc Dm Parameters.svi
DmTrim.svi
Calc SHHighest.svi
Calc Avg 1/3 Oct Source Heights.svi
Spectrum Integration.svi
Select Vehicle Type.svi
Write Data to File.svi
Global Variables.svi

4.7.2. Diskette 2: Source Height Data Files; All 9 data files discussed in section 4.5 are included in ASCII format so that they may be loaded into any spreadsheet program. The file names and their corresponding number of events are;

OLDCRUIS	702	Events
OLDCONC	102	Events
OLDGRADE	378	Events
ACCEL100	164	Events
ACCEL150	143	Events
ACCEL200	456	Events
NEWCRUIS	225	Events
NEWCONC	109	Events
NEWGRADE	170	Events

In each file the data for each pass-by event is stored on a separate line. Each file therefore contains a matrix with 67 columns. The data in each column is as follows;

Column 1:	Site Number	(1 through 14 see section 4.1.1)
Column 2:	Event Number	(at site in column 1))
Column 3:	Vehicle Type	(0 through 9 see section 4.1)
Column 4:	Vehicle Speed	(mph)
Column 5:	Road Grade	(%)

Column 6:	Pavement Type	(0=asphalt, 1=concrete)
Column 7:	Overall Level	(dBA 200-10,000 Hz)
Columns 8-27	1/3 Octave Band Levels	(dBA of ground level Mic.)
Columns 28-47	Source Heights	(meters, for each 1/3 octave)
Columns 48-67	Sub-Source Ratio	(r in equation 2.15)

4.8. Conclusions

A total of 2500 individual vehicle pass-byes were measured from 16 different sites around Florida. The first 1182 vehicle source heights were calculated with the original algorithm used by Glegg & Yoon [1]. This algorithm was shown to produce unacceptable overestimates of the actual source heights of known sources. This overestimate is particularly severe for sources below 1m and frequencies below about 1 kHz. These results should therefore not be used in any source height regression curves. The spectra from this data is quite acceptable and may be used, along with the rest of the data to show relationships between source level, speed, pavement type and vehicle acceleration state.

The remaining 1318 source heights were calculated using a modified version of the original algorithm. This approach uses a different criteria for selecting the pair of microphones, at a particular frequency, from which to calculate the equivalent source height. Controlled tests using loud-speaker sources showed this method to be more accurate across the whole frequency spectrum producing greater confidence in the measured vehicle source height data down to about 250 Hz. This new vehicle data showed lower source heights across the whole frequency range and more significant differences between vehicle types, especially below 1000 Hz. The data also showed some relationship between source height and vehicle speed, pavement type and acceleration state. These differences in source heights for a given vehicle type were shown to be relatively small across the whole data set and in most cases were less than 0.25m. Only at the extreme low frequencies were the maximum changes in the order of 0.5m. Regression of this whole data set to include all the possible parameters would be possible but quite cumbersome and computationally intensive. The changes produced in the overall level at a distant receiver by moving the source up or down by 20cm or so would be small and therefore not worth the extra computational resources.

Apportioning of this single equivalent source between two sub-sources is shown in section 6 to produce underestimates of propagation losses to the order of 1 or 2 dB. This error is significantly more than that produced by a $\pm$ 25 cm error in the source height. It is suggested therefore that the vehicle source heights that should be used in the TNM software should be the average of all the data collected with the new algorithm. and that only the differences between vehicle types be included. The results of this average are shown in figures 4.51 and 4.52. These curves can then be used to define the source heights for the ten vehicle types to an accuracy of approximately $\pm$ 25cm for all roadway conditions without the need for regression curves to account for the small changes that occur with speed, pavement type, road grade or acceleration state.

5. A MATCHED FIELD PROCESSING COMPARISON

A study was conducted by Joseph Armstrong [6], as a Masters Thesis topic, where a matched field processing method was developed to obtain the vehicle source height, from the same time series data, for comparison with the results presented in section 4. This study originated from the need to improve the low frequency response of the current algorithm which was believed to be overestimating the source heights because of noise contamination. However the changes made to the original array and algorithm discussed in section 2.4 improved the low frequency response considerably and the matched field process was unable to significantly better that result. The study does however serve as a valuable means of confirming the results obtained with the turn-key system. The results presented in this section match those presented in section 4 very well giving validation of the results down to 200 Hz.

5.1. The Matched Field Process

The matched field method uses a least mean square error function to match the measured data to a theoretical model of the sound field. The measured sound field is characterized by the frequency response function, defined as;

$$H(x_m, \omega) = \frac{C_m}{C_0} \tag{5.1}$$

where C_m is the cross spectral density between the m^{th} microphone in the array and the ground level reference microphone at x_0. C_0 is the autospectral density of the reference microphone. The theoretical model is calculated using Green's function for a point source above a reflecting plane and is given by;

$$H_T(\bar{y}_T, \bar{x}_m, \omega) = \frac{\left[\dfrac{\exp(jk(r_+ - r_0))}{r_+ r_0} + \gamma^* \dfrac{\exp(jk(r_- - r_0))}{r_- r_0}\right]}{\left[\dfrac{1+\gamma^*}{r_0^2}\right]} \tag{5.2}$$

The theoretical frequency response function is calculated for a set of discrete source locations $\overline{y}_T$ and these are compared to the measured functions given in equation 5.1. To allow for a source height that changes with frequency, the matching process is performed over consecutive 200 Hz bands over which the source height is assumed to be constant. An error function given by;

$$E(y_T, x_m, \omega_b) = \frac{1}{B}\sum_{b=1}^{B}\left|H(x_m, \omega_b) - H_T(y_T, x_m, \omega_b)\right|^2 \tag{5.3}$$

is calculated where B represents the number of points in the matching bandwidth and $\omega_b = \omega_0 + b\Delta\omega$. The theoretical point source height for which this function is a minimum is assumed to be the equivalent source height for that frequency band.

5.2. Evaluation Using Loud-Speaker Sources.

The matched field processing algorithm was tested using loud-speakers in a hemi-anechoic chamber. Two speakers were used, one at 1.44 m and the other at 0.48 m above the hard floor. Each speaker was driven with a separate amplified white noise source. The matched field algorithm was then used to calculate the height of the speakers using data recorded with the same microphone array as the turn-key system. A frequency resolution of 50 Hz and a matching bandwidth of 200 Hz were used for analysis of the data. The test was first performed using each speaker in turn and then with both speakers running simultaneously. When the speakers were run individually the algorithm calculated their physical height to within 5 cm down to about 200 Hz. When both speakers were run simultaneously the measured source height concurred, to within 10 cm down to 200Hz, with the equivalent source height calculated using the individual spectra and speaker heights as described in section 2.5.

5.3. Vehicle Source Heights Using Matched Field Processing.

When the roadside measurements were made with the turn-key system the time series data was stored for a few sparse examples. This allowed for the same data to be used to calculate the vehicle source heights with the original algorithm described in section 2 and then with the matched field process. Figures 5.1 through 5.3 show comparisons, of the results obtained with the two independent methods, for one example each of a standard auto, a medium truck and a 5-axle heavy truck. It can be seen in these figures that the two methods produce very similar results. The matched field results show more undulation because they are calculated every 200 Hz whereas the turn-key system computes the average source height over each 1/3rd octave.

5.4. Matched Field Processing Conclusions.

The matched field processing algorithm was used to accurately measure the height of loud speakers in controlled tests down to frequencies less than 200 Hz. There had been some question as to the validity of the vehicle source heights measured with the turn-key system at frequencies below 500 Hz but the matched field results calculated with the same time series data produced very similar source heights. The matched field method therefore produced a considerable increase in the level of confidence with the turn-key system data. Further improvement of the matched field method could be made if the record length of the measured vehicle pass-by data could be increased allowing for increased frequency resolution. The implications of this on other error sources such as Doppler errors and horizontal source distribution would need to be investigated further before this could be implemented.

6. AN INVESTIGATION OF THE EFFECTS OF MEASURED NOISE SOURCE HEIGHTS ON BARRIER INSERTION LOSS PREDICTIONS IN TNM.

The measured data collected in this study produces single equivalent source heights from a distribution of sources around that height. Since some of the real sources in the distribution are actually above this height there was concern that moving the energy of these sources down to the equivalent source height would produce overestimates of barrier insertion losses. It was this concern that led to the apportioning of the total energy at the measured source height, between two sub-sources (see section 2.5) whose propagation could be treated individually and results summed at the observer position. A study was conducted by Glynn [7], as a Masters thesis topic, in which the effects on the barrier insertion loss calculations of modeling a distribution of sources as a single equivalent source and then as two sub-sources were investigated. He concluded that on average the two sub-source approach is less accurate than the single equivalent source approximation but since it produces an underestimate of the barrier insertion loss conservative barrier heights would be designed from this result.

6.1. Propagation Without a Barrier.

In order to calculate the insertion loss of a noise barrier it is first necessary to develop a propagation model to deal with general propagation without the barrier. This is done by coherently adding the direct and ground reflected fields at an observer position. The reflected field is modified using a spherical reflection coefficient which is a function of the plane wave reflection coefficient, the ground wave, the acoustic impedance and the complex wave number of the ground. The ground model used to determine the acoustic impedance and the complex wavenumber is taken from Delany & Bazley [8]. Using this spherical reflection coefficient for a particular ground type, the total acoustic field at an arbitrary observer position was obtained for two vertical source distributions representative of a typical car and truck. These distributions contained tire, engine, exhaust and aerodynamic noise sources whose spectra were artificially shaped using a function similar to a Skewed-Wright distribution. The turn-key algorithm was then used to compute the single equivalent source height and strength of the distribution and then the same propagation calculations were performed for this source. When the acoustic fields were compared for the distributed and equivalent source cases the results correlated very well for both distributions, especially when the observer was in the far field. The single equivalent source was then apportioned between two sub-sources at 0 & 1.52 m for the car and 0 & 3.66 m for the truck, as in section 2.5. Again the total field at the same observer position was calculated using the propagation model. Comparison with the distributed source result showed a good match at low frequencies but at frequencies where ground interference occurs there is a significant mismatch. For the case of hard ground the two sub-source result coincided with the envelope of the distributed and single equivalent source cases. Over soft ground the two sub-source case showed large discrepancies in the mid to high frequency range where ground interference comes into play. This is enhanced by the fact that the majority of the energy is concentrated at the lower sub-source particularly in the case of the heavy truck.

6.2. Propagation Over & Around a Barrier.

For propagation over and around a noise barrier Glynn used a model that calculates the contribution of eight diffraction paths. Four diffracted paths are due to the horizontal edge of the barrier and the other four account for the vertical sides of the barrier. Glynn used a model proposed by Jonasson [9] that includes the screening of the barrier and the ground effects in the computation of the barrier attenuation. For diffraction paths that include a ground reflection the diffraction coefficient is multiplied by a spherical reflection coefficient. After each of the paths has been computed and modified with the appropriate reflection coefficient, a coherent summation is performed to obtain the total acoustic field at a point behind the barrier. In the TNM model the barrier attenuation is calculated in a similar manner. The Fresnel-Kirchhoff diffraction theory proposed by Bowman et al [10] was used to calculate the diffraction coefficients along with the same spherical reflection coefficients discussed in section 6.1. The barrier insertion loss was then calculated for the same uncorrelated source distributions as in the no barrier case for a typical car and truck. The calculation was first performed for the distributed sources whose paths were calculated individually and then added incoherently at the observer position behind the barrier. Next the vertical distribution was replaced with the single equivalent source and the diffracted field calculated in the same manner. Finally the single equivalent source was apportioned to two sub-sources as before and the field at the observer point behind the barrier was again calculated by summing the contributions from both sub-sources. The results for the two simplified source models were compared to the truly distributed case for four different barrier configurations and two ground covers, one hard and one soft. The results indicate that on average the single equivalent source will under-estimate the barrier insertion loss producing an overestimate of the total overall dBA level of no more than 2.75 dBA for a car and 3.75 dBA for a truck. On the other hand, with the two sub-source model the insertion loss is always under-estimated resulting in an over-estimation of the overall levels at the observer of 3.6 dBA for a car and 4.5 dBA for a truck. Glynn concluded from this analysis that on average the two sub-source concept is less accurate than the single equivalent source model and will underestimate the barrier attenuation leading to more conservative barrier height designs.

7. SUMMARY

A turn-key data acquisition and reduction algorithm was developed and implemented in collecting vehicle spectra and source height data for a total of 2500 individual vehicle pass-byes from 16 sites around Florida. The first 1182 of these were collected with the same method as developed by Glegg & Yoon [1]. In controlled laboratory experiments it was shown that this initial data included significant over-estimations of the actual source height for low sources at low frequencies. By modifying the algorithm slightly to include an alternative microphone pair selection criteria this problem was resolved and the remaining 1318 pass-byes were recorded using the new algorithm. The four main conclusions that can be drawn from this study are;

(1.) The single equivalent noise source height of all vehicles is generally less than 1m at frequencies above 500 Hz because of the dominance of tire noise. Below 500 Hz source heights rise depending on vehicle type to a maximum of about 2m for heavy trucks as engine, exhaust and aerodynamic noise sources become more significant.

(2.) The dependence of vehicle source height on speed, pavement type, road grade and acceleration state is relatively small when compared with the deviation of the whole data set. Regression of this data base to account for these factors is therefore not recommended and it is suggested that the source heights calculated from the average of all the new data be used in the TNM model so that only the differences between vehicle types are included.

(3.) The source height data collected with this system was verified by calculations using an alternative more computationally intensive matched field processing algorithm. The matched field process produced very similar source height results from the same time series data as recorded with the turn-key system reinforcing the confidence in the data down to a frequency of 250 Hz.

(4.) The single equivalent source height model for a distribution of sources is more accurate than the two sub-source model when used in barrier attenuation calculations.

8. ACKNOWLEDGMENTS

The author would like to acknowledge Mr. Win Lindeman and the Florida Department of Transportation who sponsored the bulk of this work and Mr. Gregg Fleming and the Federal Highway Administration for their support of the initial system development. Their respective grants were;

FDOT HPR Study 0709, Contract B-9077
FHWA Request # DTRS57-94-Q-AT200-80200, DSR # 93179.

Thanks are also extended to Joseph Armstrong and Charles Glynn for their help in collecting the field data and to Dr. Stewart A.L. Glegg for his guidance throughout this project and help in the preparation of this report.

9. REFERENCES

[1] "Determination of Noise Source Height of Vehicles on Florida Roads and Highways." S.A.L. Glegg and J.R. Yoon, June 1989, *FDOT report No. FHWA/FL/DOT/MO-89-382*

[2] "Determination of Noise Source Heights, Part I: the Measurement of Equivalent Acoustic Source Height Above a Reflecting Surface." S.A.L. Glegg and J.R. Yoon, 1990, *Journal of Sound and Vibration* **143**, 19-37.

[3] "Determination of Noise Source Heights, Part II: Measurement of the Equivalent Source Height of Highway Vehicles." S.A.L. Glegg and J.R. Yoon, 1990, *Journal of Sound and Vibration* **143**, 39-50.

[4] "Binaural Source Location." R. Kinns, 1976, *Journal of Sound and Vibration* 44, 275-289.

[5] "Evaluation of Vehicle Sub-Source Spectra for Noise Barrier Design" R. K. Coulson, January 1994, *report for VNTSC order no. DTRS57-93-P-81631.*

[6] "Improved Estimate of Measured Source Height on Moving Vehicles for Frequencies Below 500 Hz." J. Armstrong, 1996, *Masters Thesis*, Florida Atlantic University

[7] "Investigating the Effect of Measured Noise Source Heights on the Predicted Insertion Loss of Noise Barriers in the New TNM Software." C. D. Glynn, 1996, *Masters Thesis*, Florida Atlantic University

[8] "Acoustic Properties of Fibrous Absorbent Materials." M.E. Delany & E.N. Bazley, 1970, *Applied Acoustics Volume 3*, 105-116.

[9] "Sound Reduction by Barriers on the Ground." H.G. Jonasson, 1972, *Journal of Sound & Vibration*, **22**, 113-126.

[10] "Electromagnetic and Acoustic Scattering by Simple Shapes." J.J. Bowman et al., *North Holland Publishing Company-Amsterdam.*

10. FIGURES

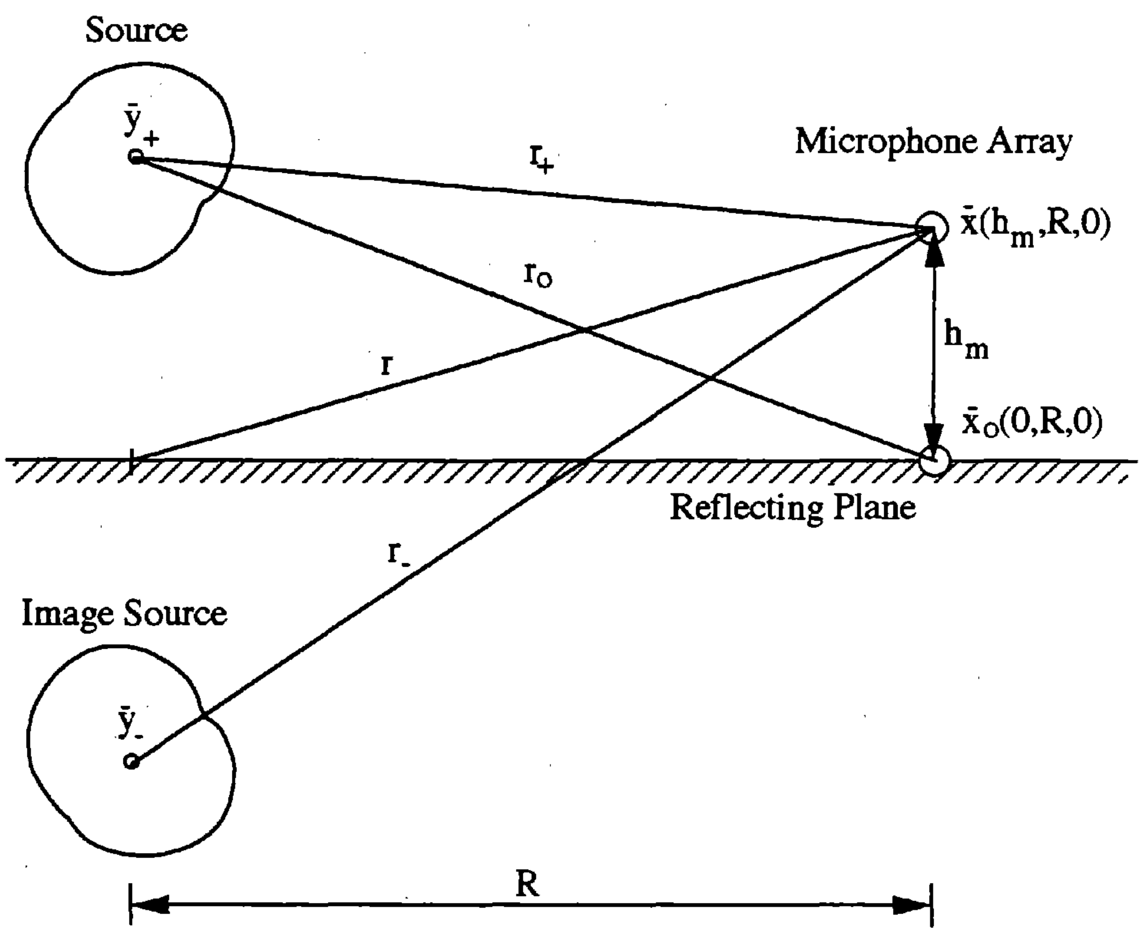

Figure 2.1: Source & Microphone Geometrical Notation

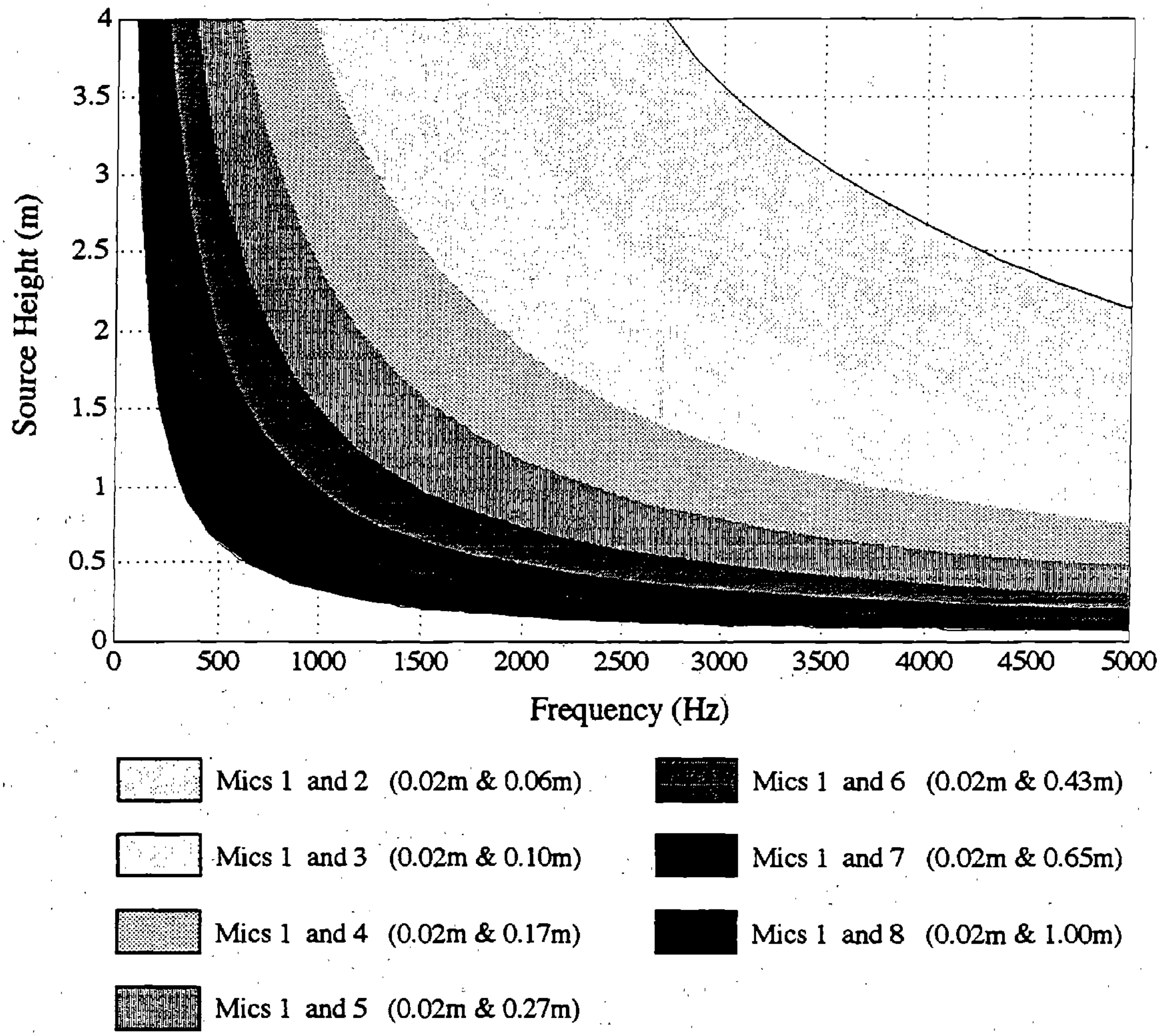

Figure 2.2: The Equivalent Source Heights which may be Measured at each Frequency for each Microphone Pair in the Array while Satisfying Equation 2.10

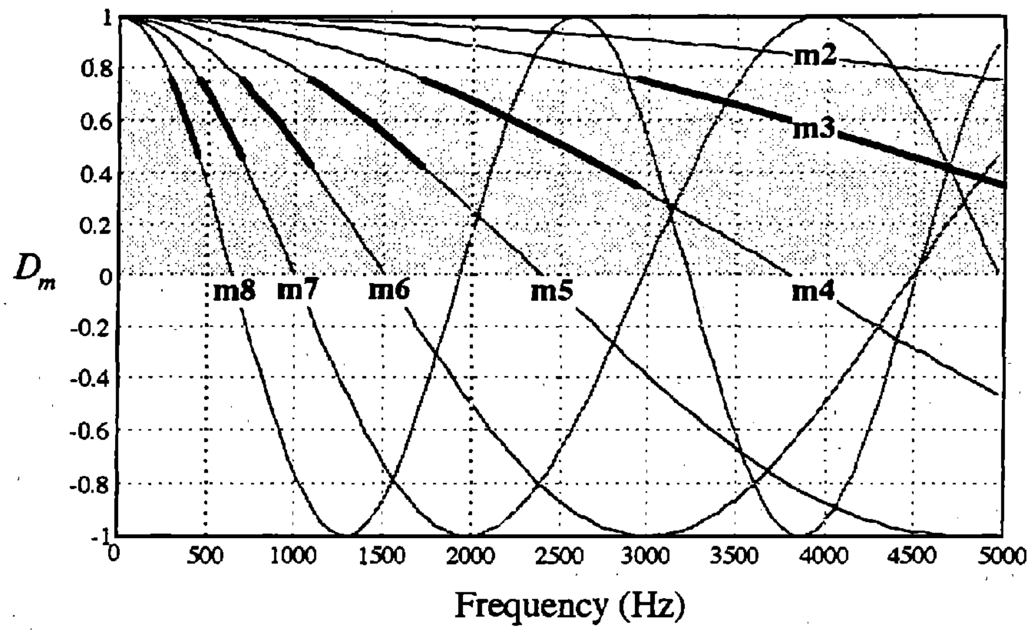

2.3(a) Lowest Pair Criteria

D_m Region Defined by Equation 2.10

Microphone #	m1	m2	m3	m4	m5	m6	m7	m8
Height (m)	0.02	0.07	0.10	0.17	0.27	0.43	0.65	1.00

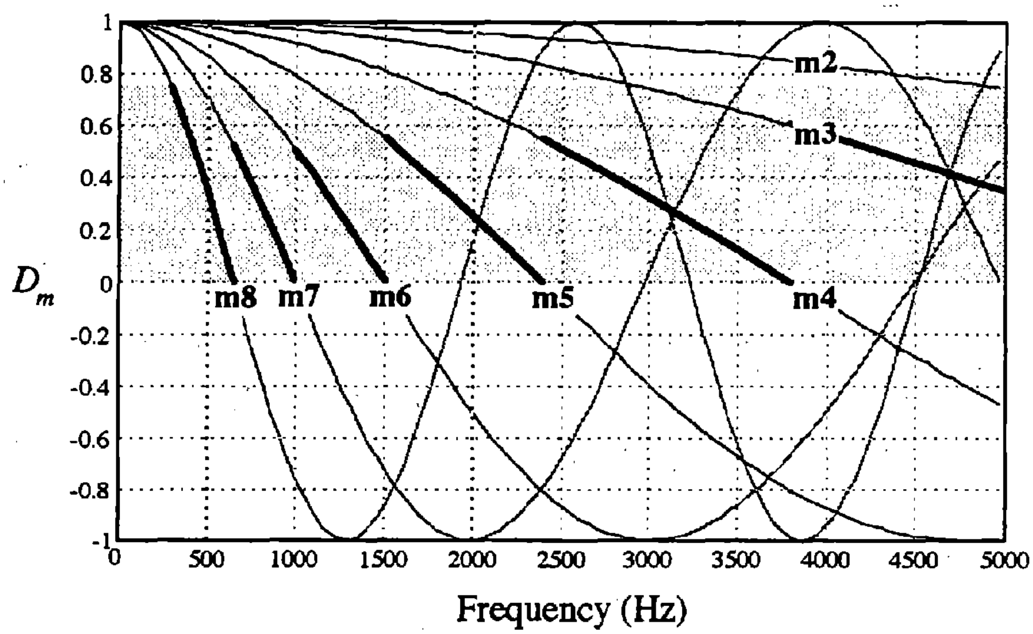

2.3(b) Highest Pair Criteria

Figure 2.3 : Theoretical D_m versus Frequency for each Microphone in the Array. Darker Solid Lines Show the Sections Used to Calculate the Source Height for;
(a) The Lowest Pair Selection Criteria
(b) The Highest Pair Selection Criteria.

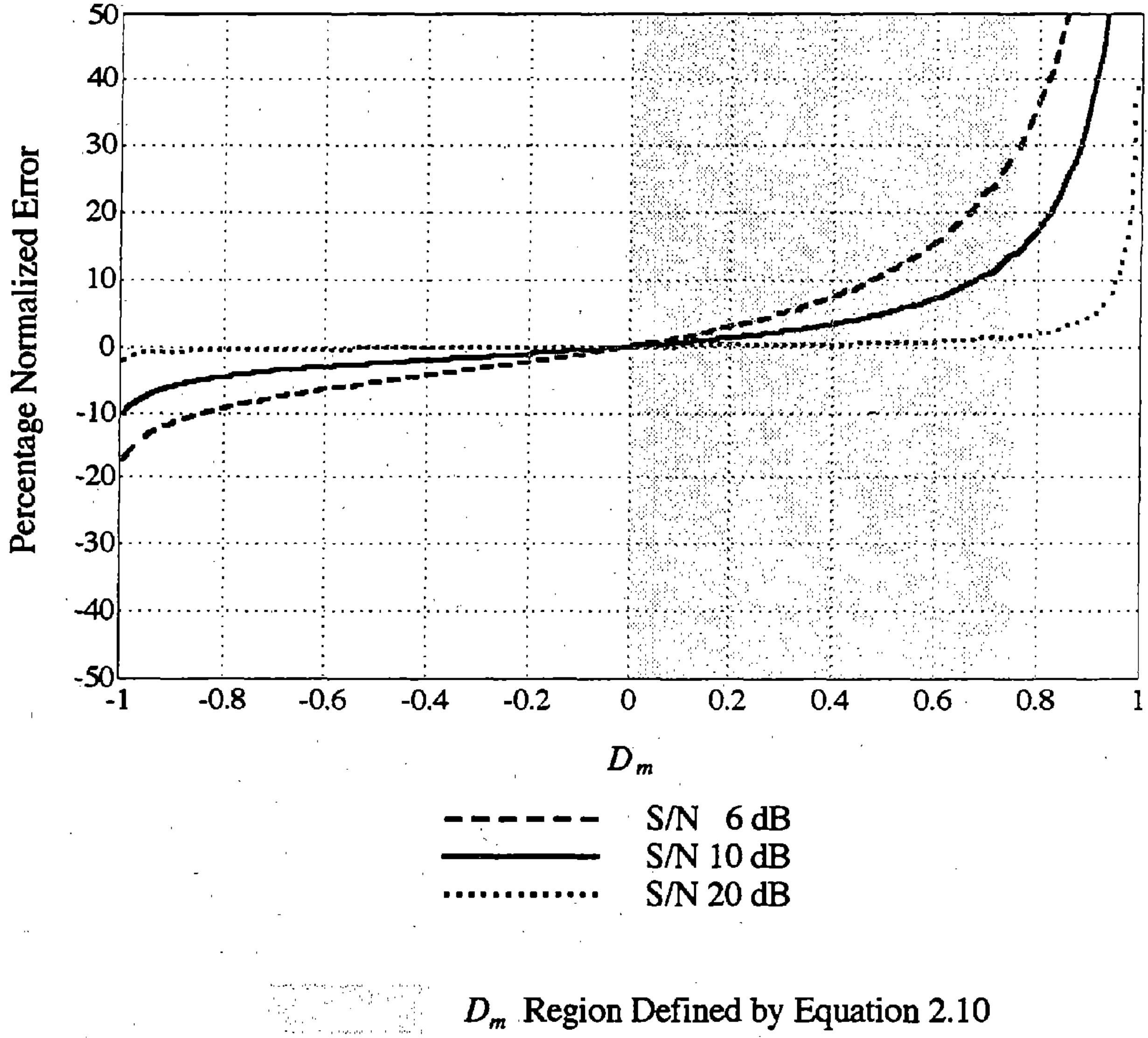

Figure 2.4 : Normalized Error of Source Height Measurement versus D_m for Different Signal to Noise Ratios

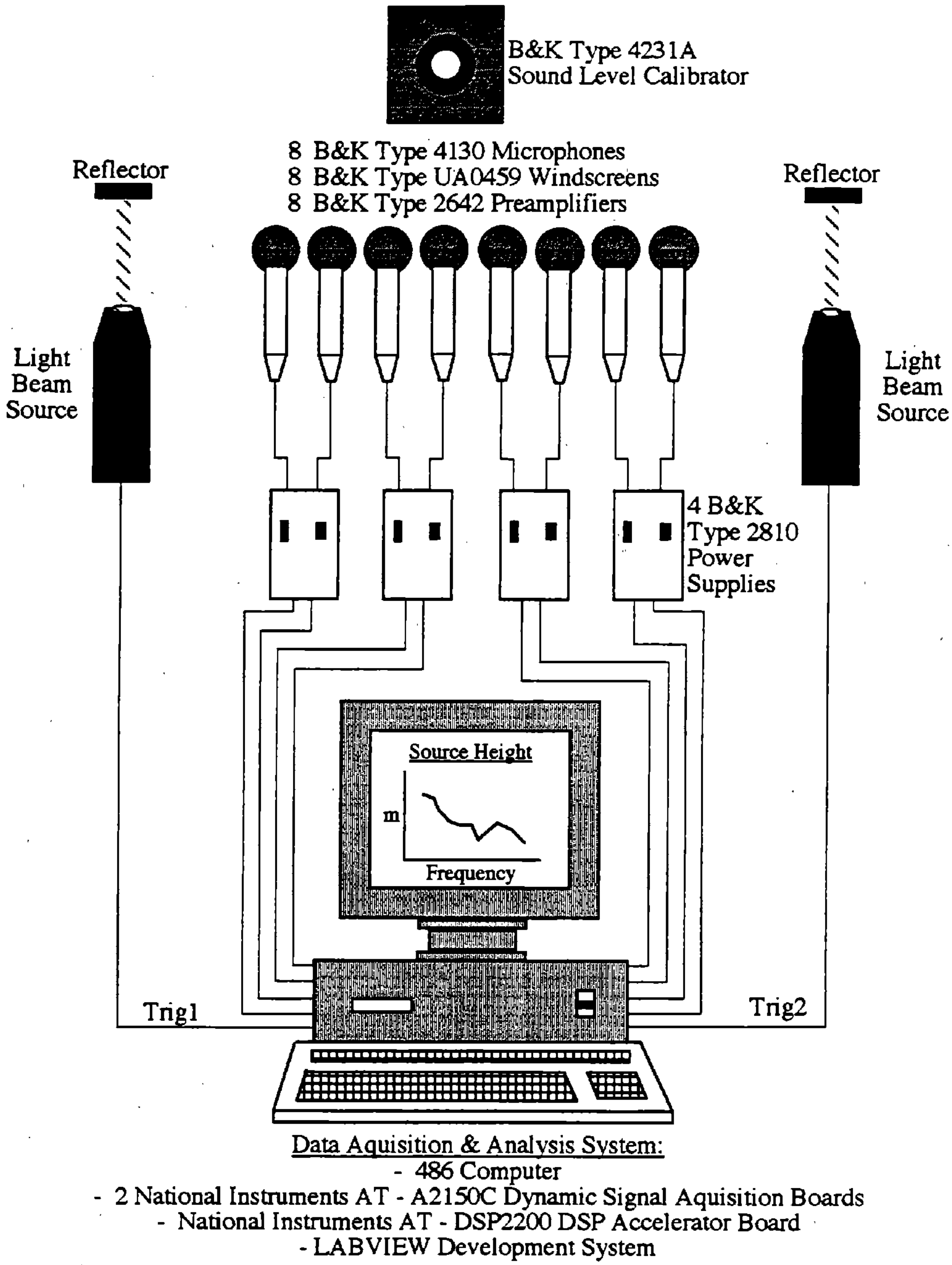

Figure 3.1: Source Height Measuring Equipment for Turn-Key Acquisition System.

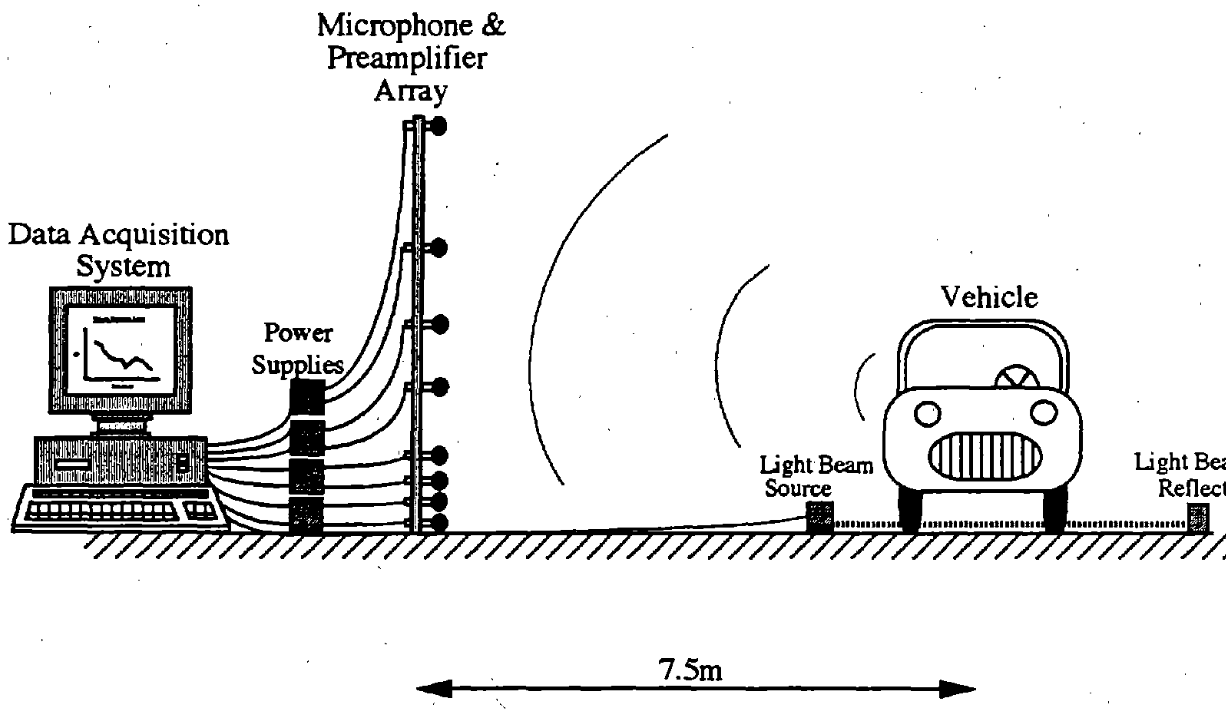

Figure 3.2: The Measuring Equipment Setup

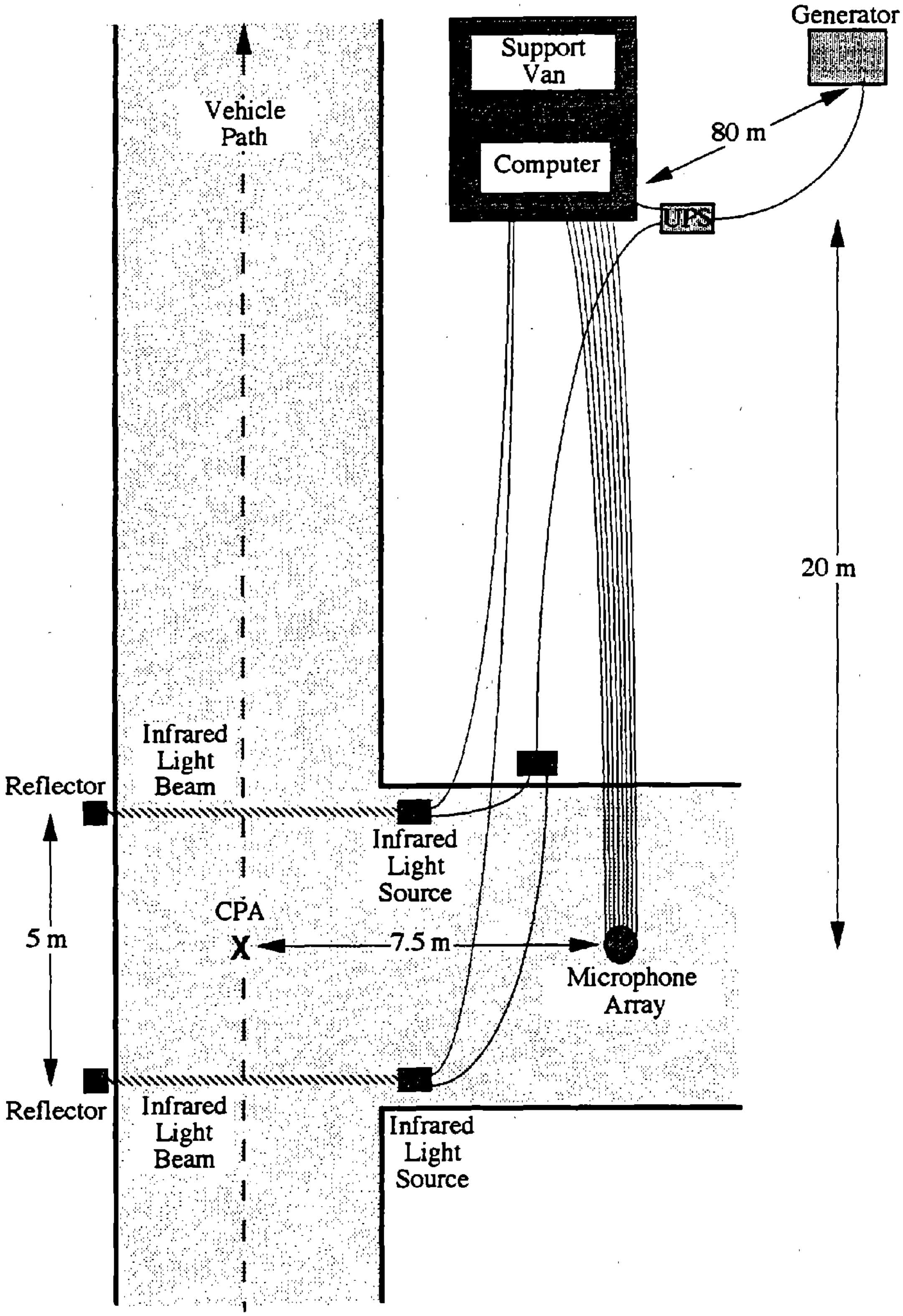

Figure 3.3: Plan View of Test Site Setup

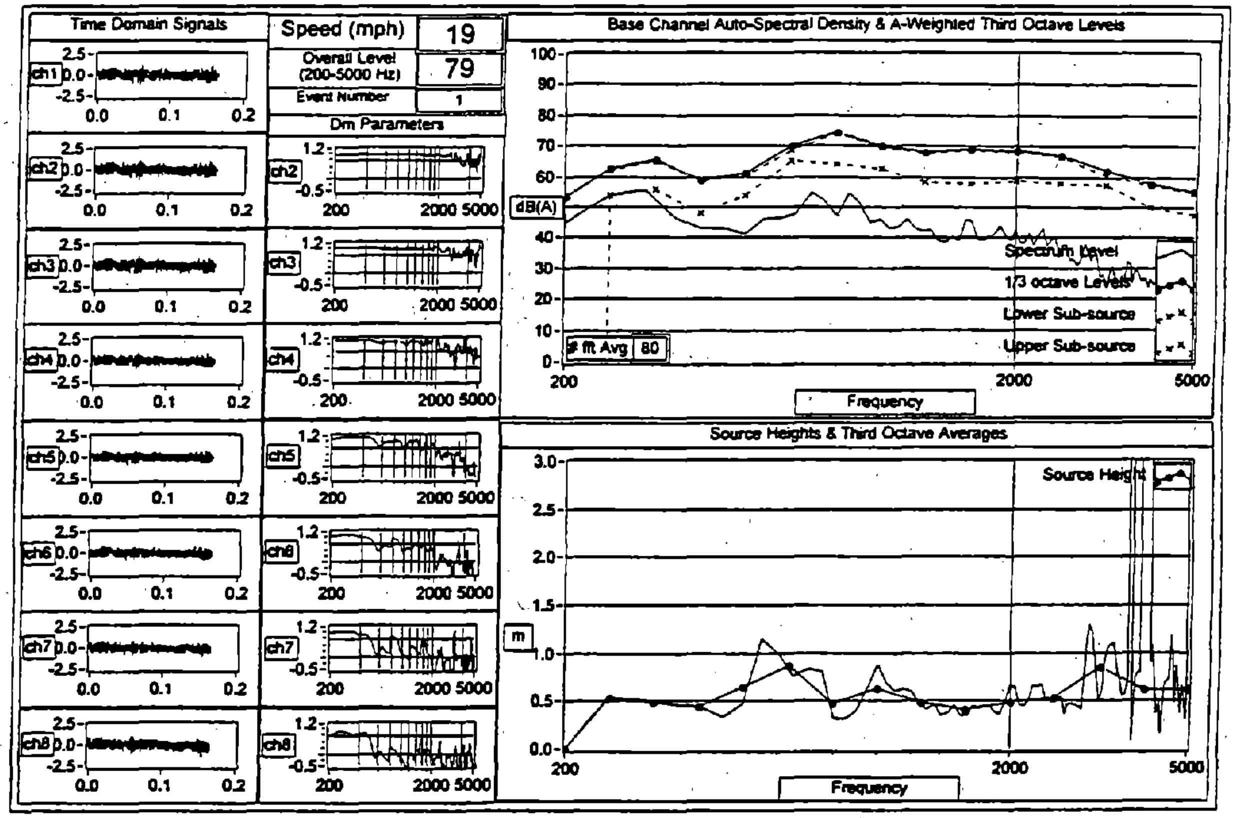

Figure 3.4: 'SOURCE HEIGHT.VI' Main Window

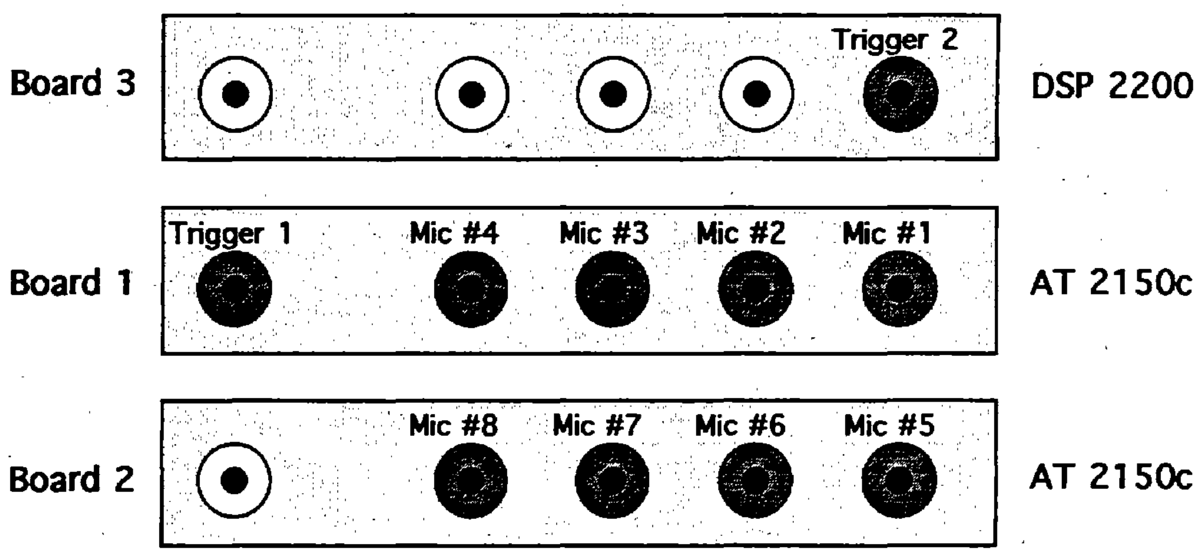

Figure 3.5: Acquisition Boards, Terminals & Input Signals

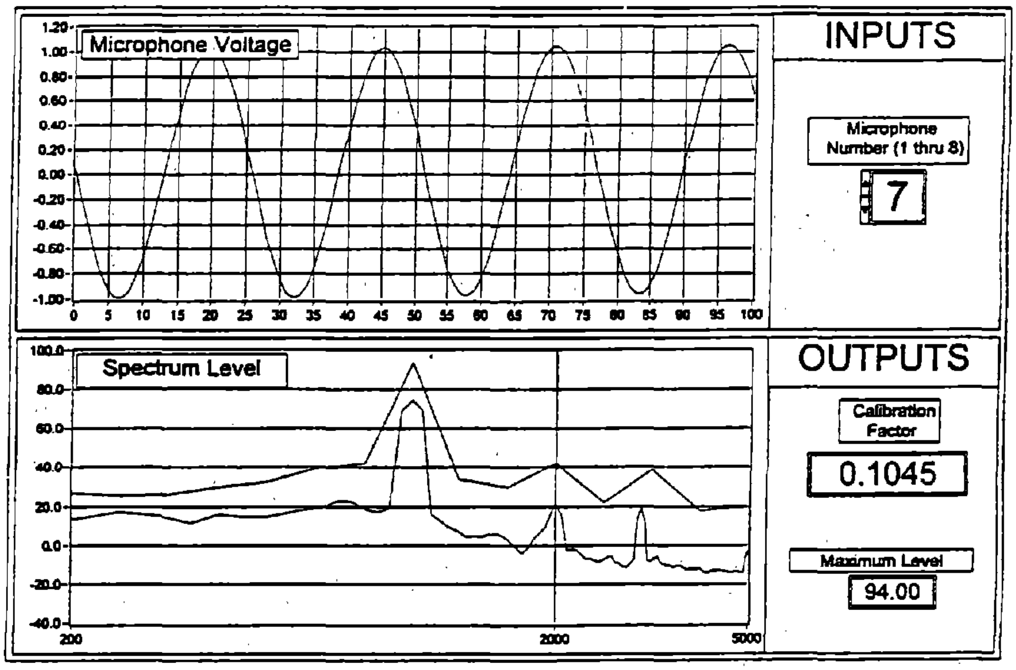

Figure 3.6: 'MICROPHONE CALIBRATION.VI' Window

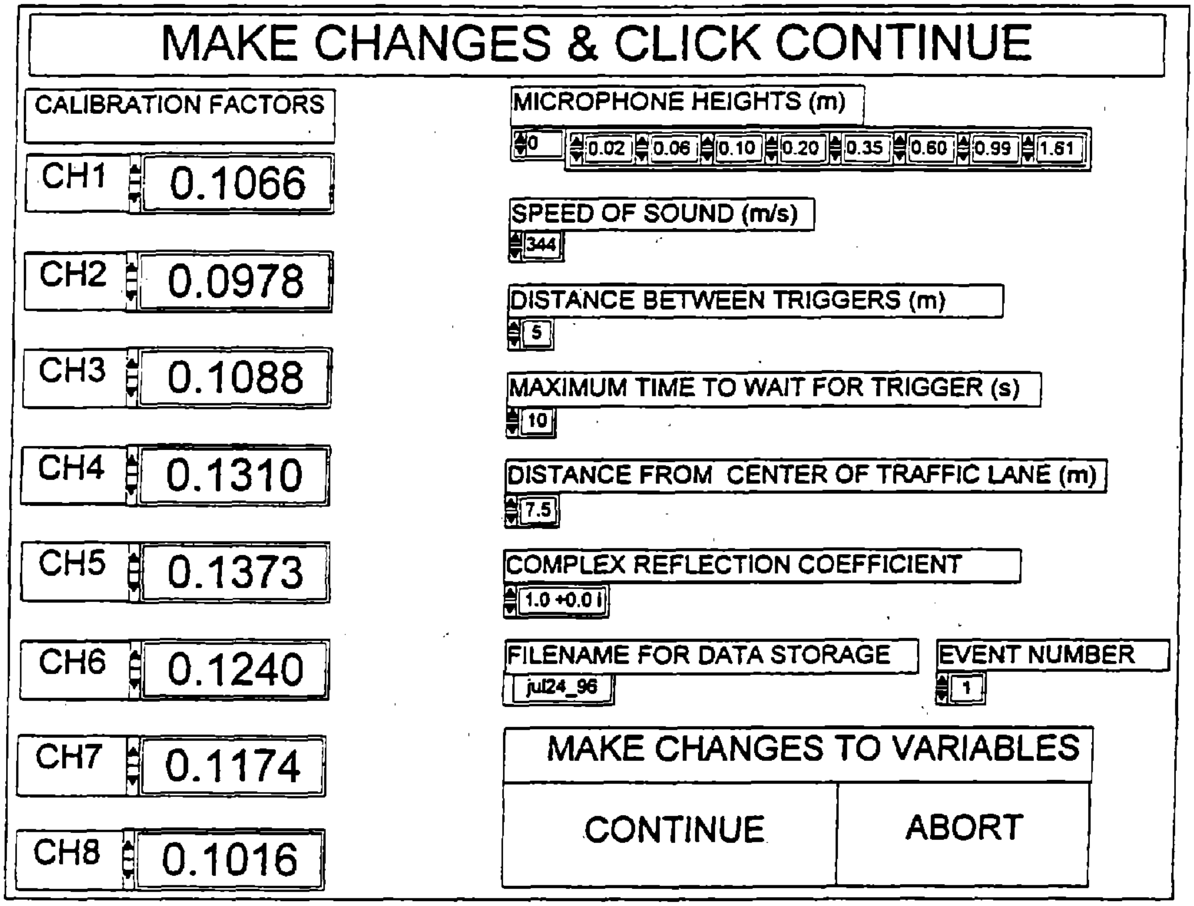

Figure 3.7: 'SOURCE HEIGHT.VI' Input Window

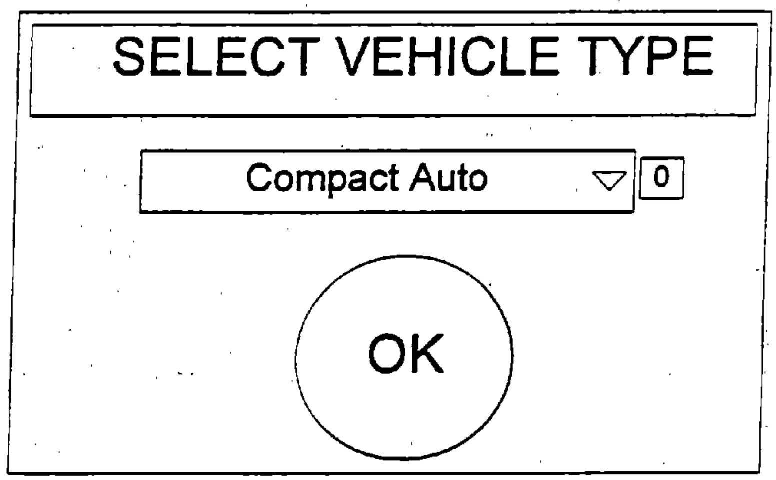

Figure 3.8: 'SOURCE HEIGHT.VI' Select Vehicle Type Window

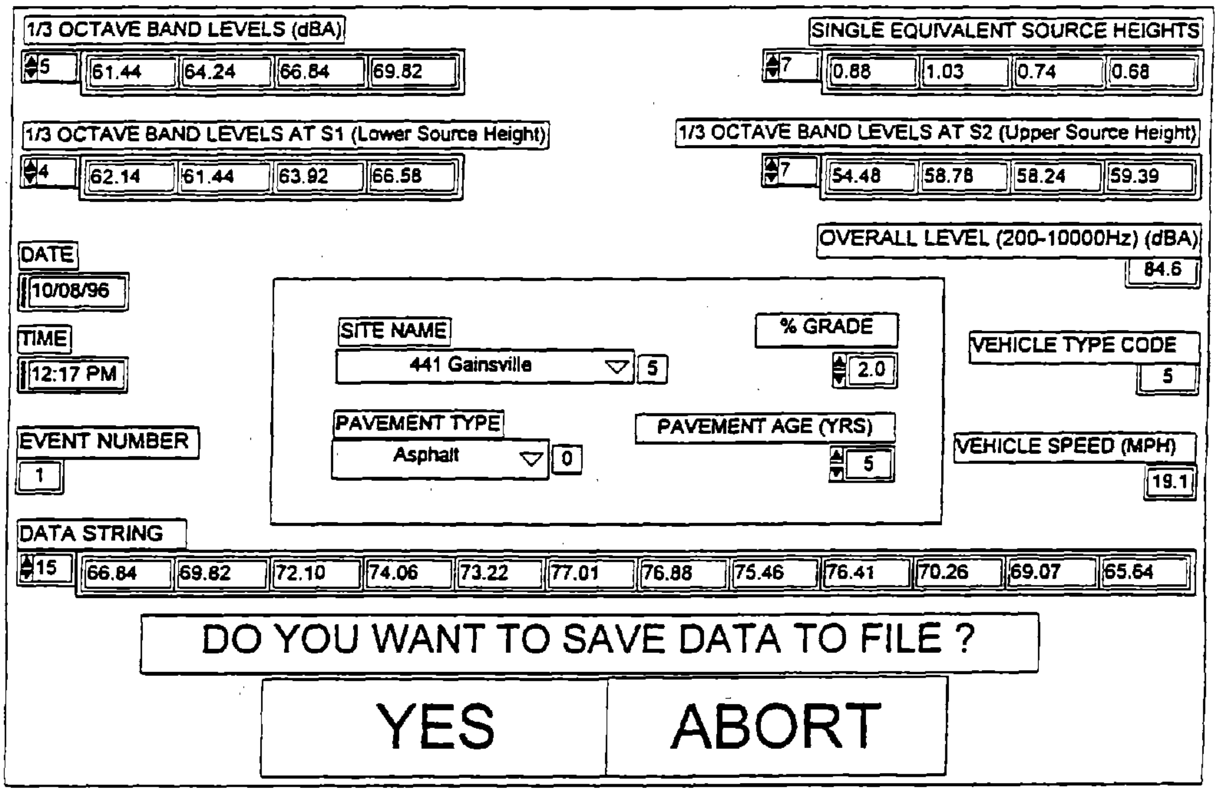

Figure 3.9: 'SOURCE HEIGHT.VI' Save Data to File Window

Figure 4.1: Averaged Spectra & Source Heights for Vehicle Types 0 to 4 Cruising on Level Asphalt Roadways. (Using the Lowest Microphone Pair Criteria)

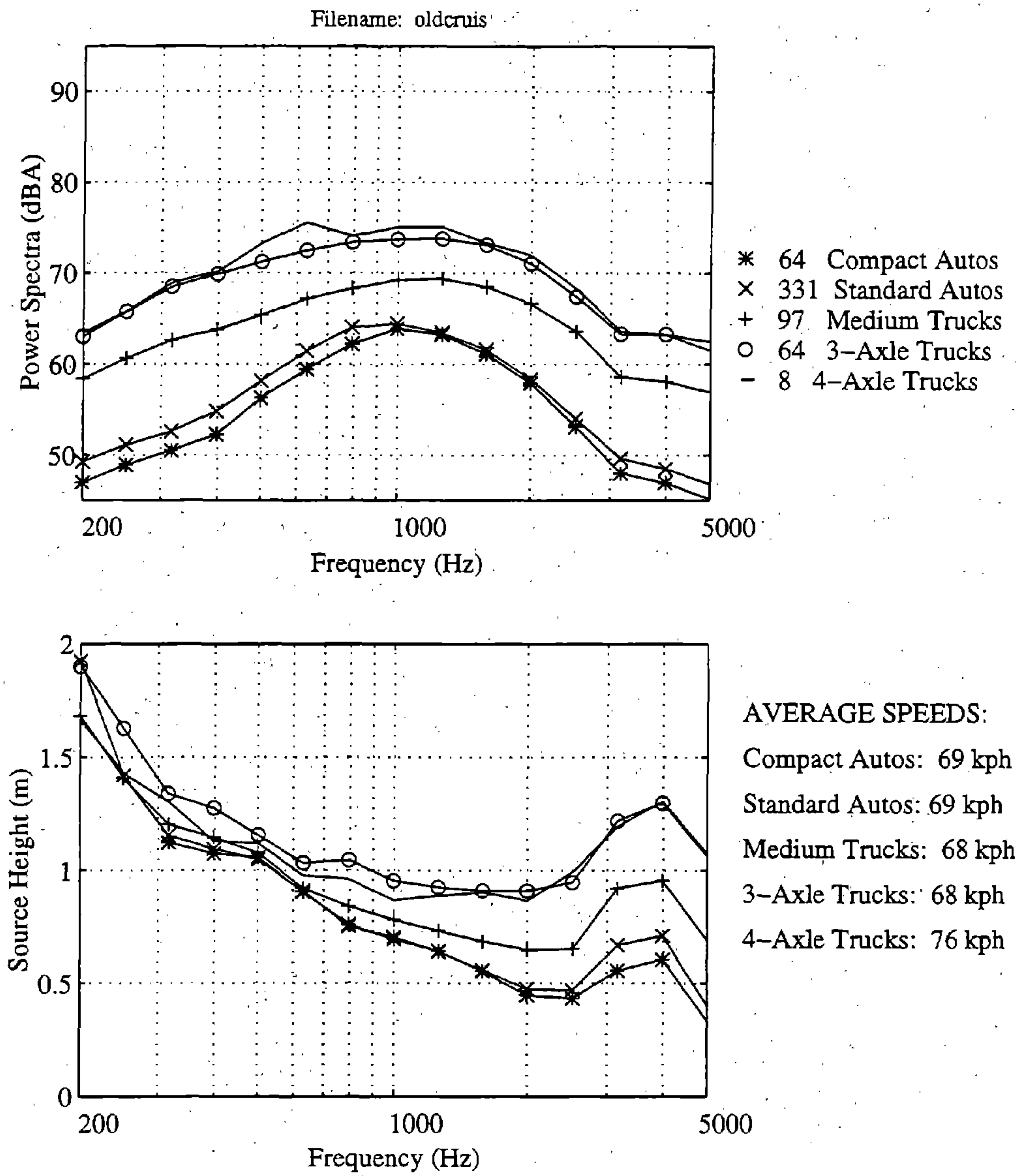

Figure 4.2: Averaged Spectra & Source Heights for Vehicle Types 5 to 8 Cruising on Level Asphalt Roadways. (Using the Lowest Microphone Pair Criteria)

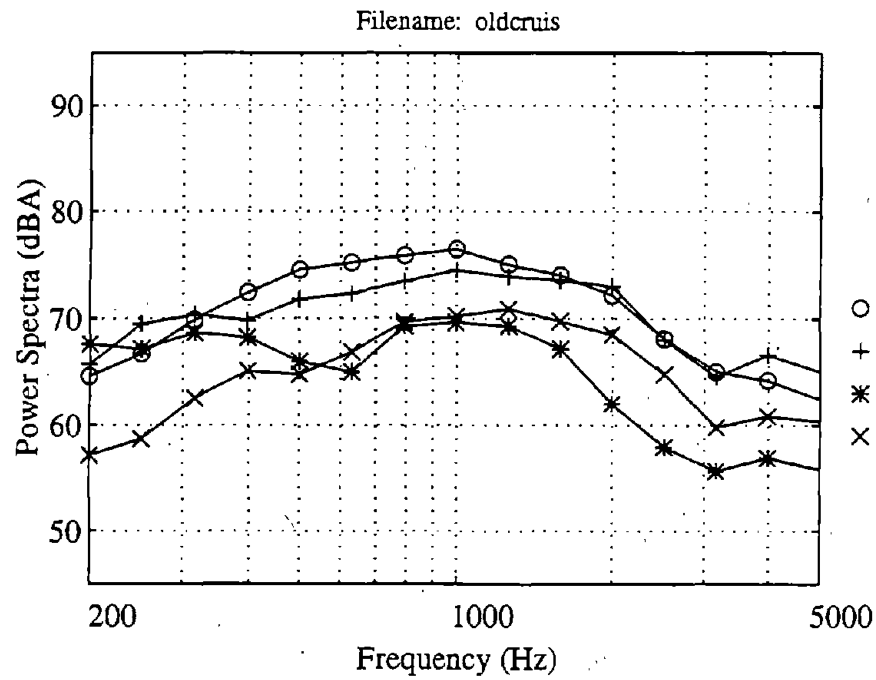

○ 123 5-Axle Trucks
\+ 4 6-Axle Trucks
✱ 2 Motorcycles
× 9 2-Axle Buses

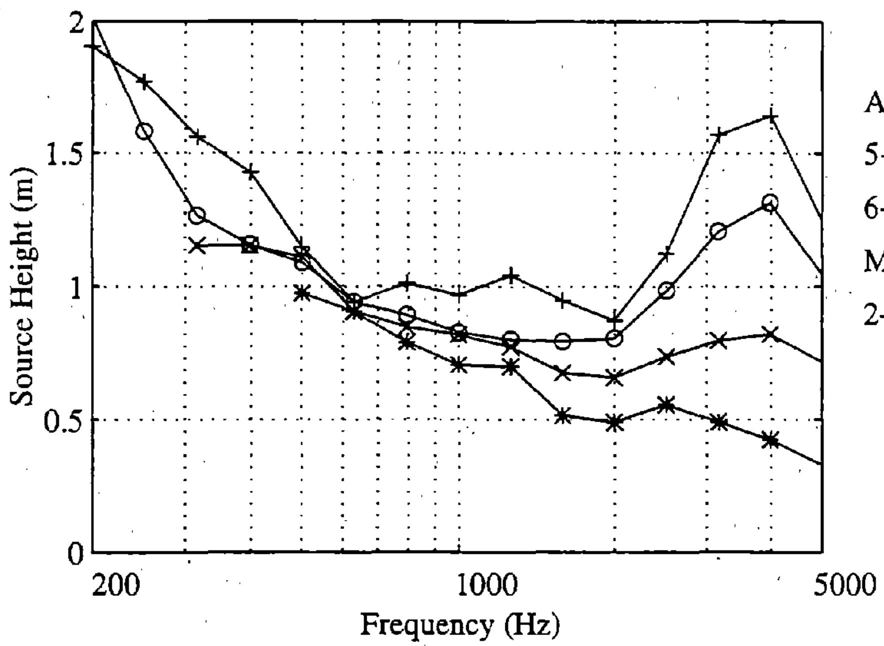

AVERAGE SPEEDS:
5-Axle Trucks: 90 kph
6-Axle Trucks: 66 kph
Motorcycles: 95 kph
2-Axle Buses: 71 kph

Figure 4.3: Averaged Spectra & Source Heights for all Measured Vehicle Types Cruising on Level Concrete Roadways.
(Using the Lowest Microphone Pair Criteria)

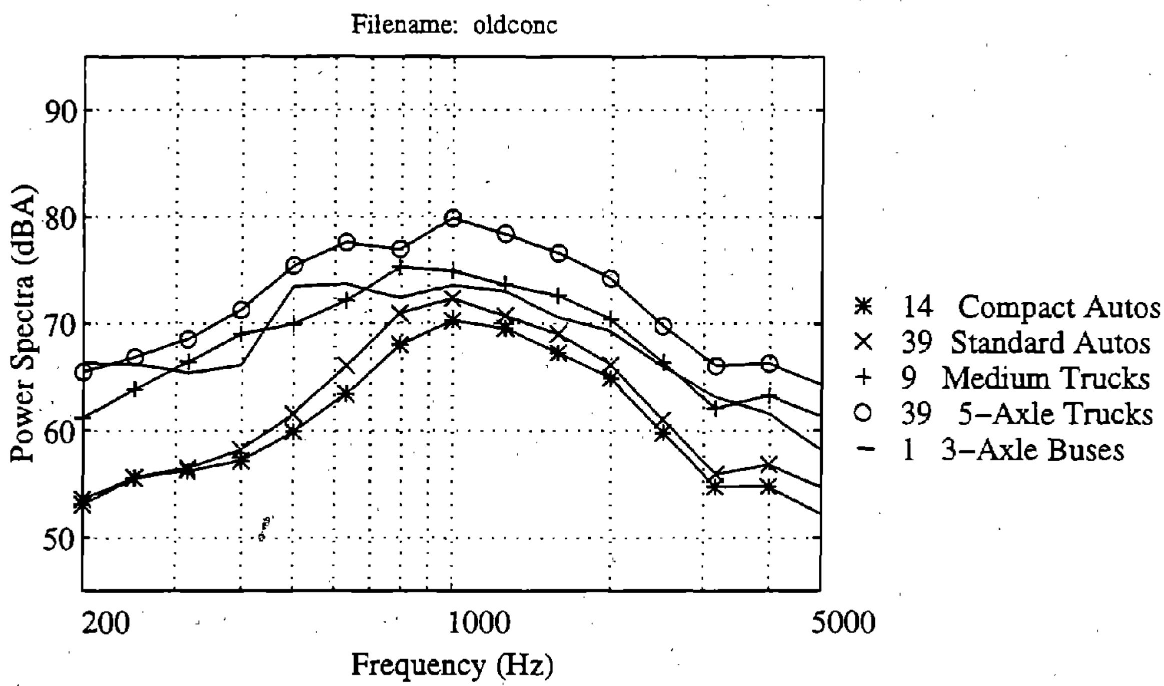

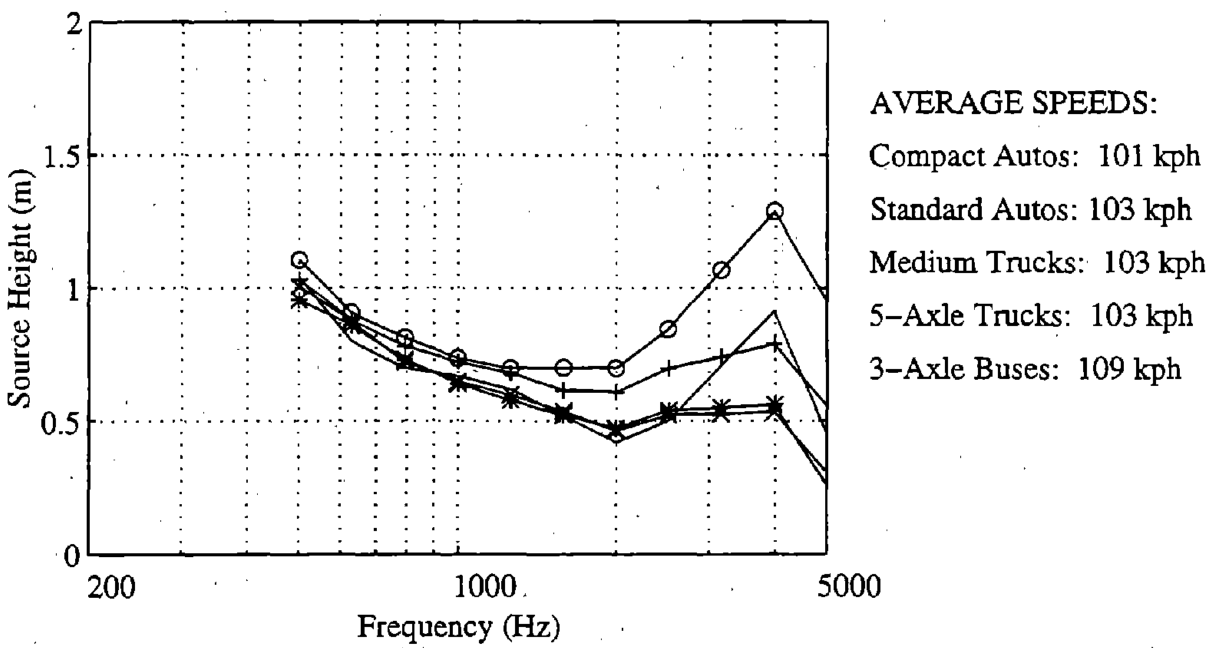

Figure 4.4: Averaged Spectra & Source Heights for Vehicle Types 0 to 3 Climbing Graded Asphalt Roadways. (Using the Lowest Microphone Pair Criteria)

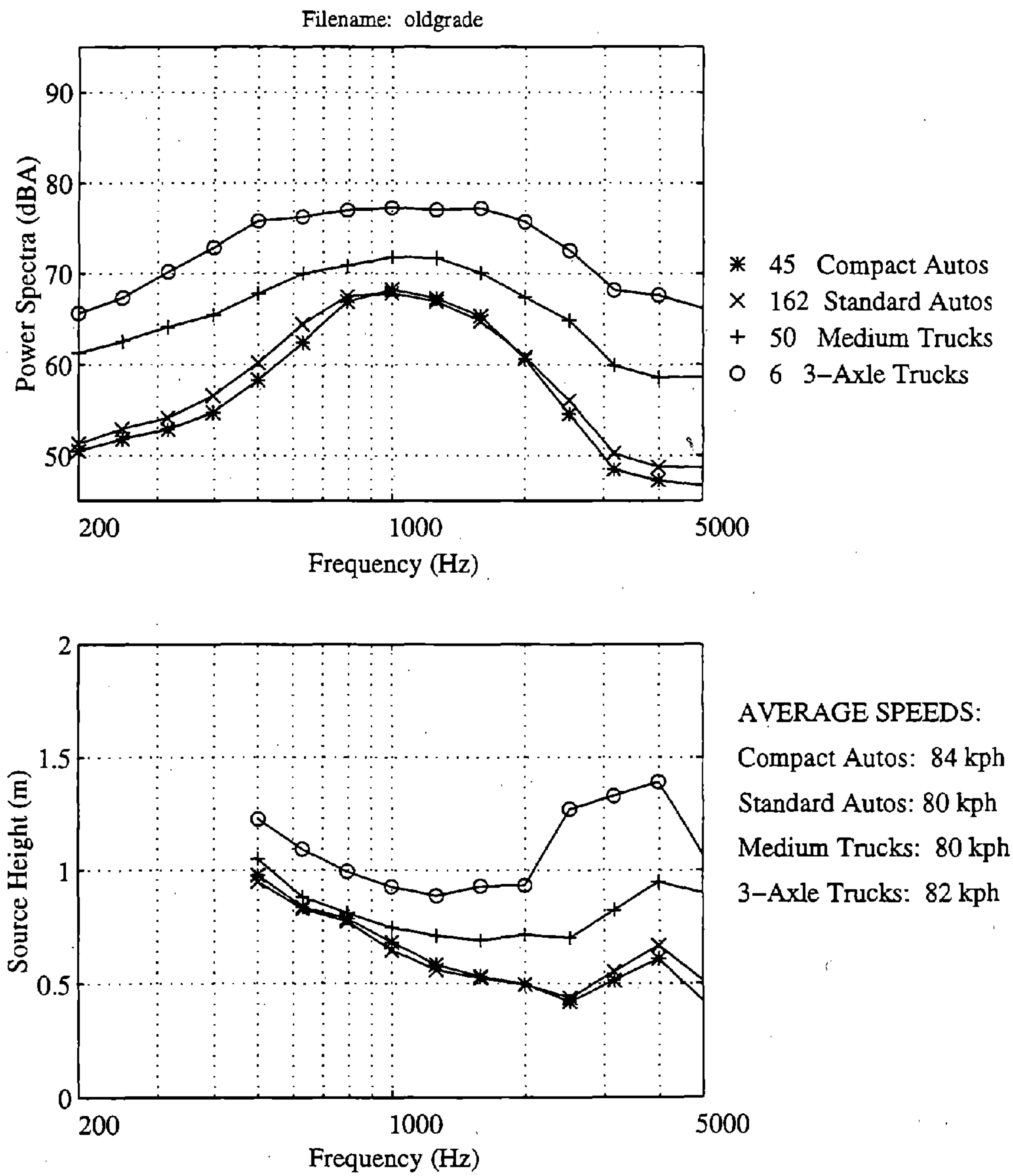

Figure 4.5: Averaged Spectra & Source Heights for Vehicle Types 5 to 9 Climbing Graded Asphalt Roadways.
(Using the Lowest Microphone Pair Criteria)

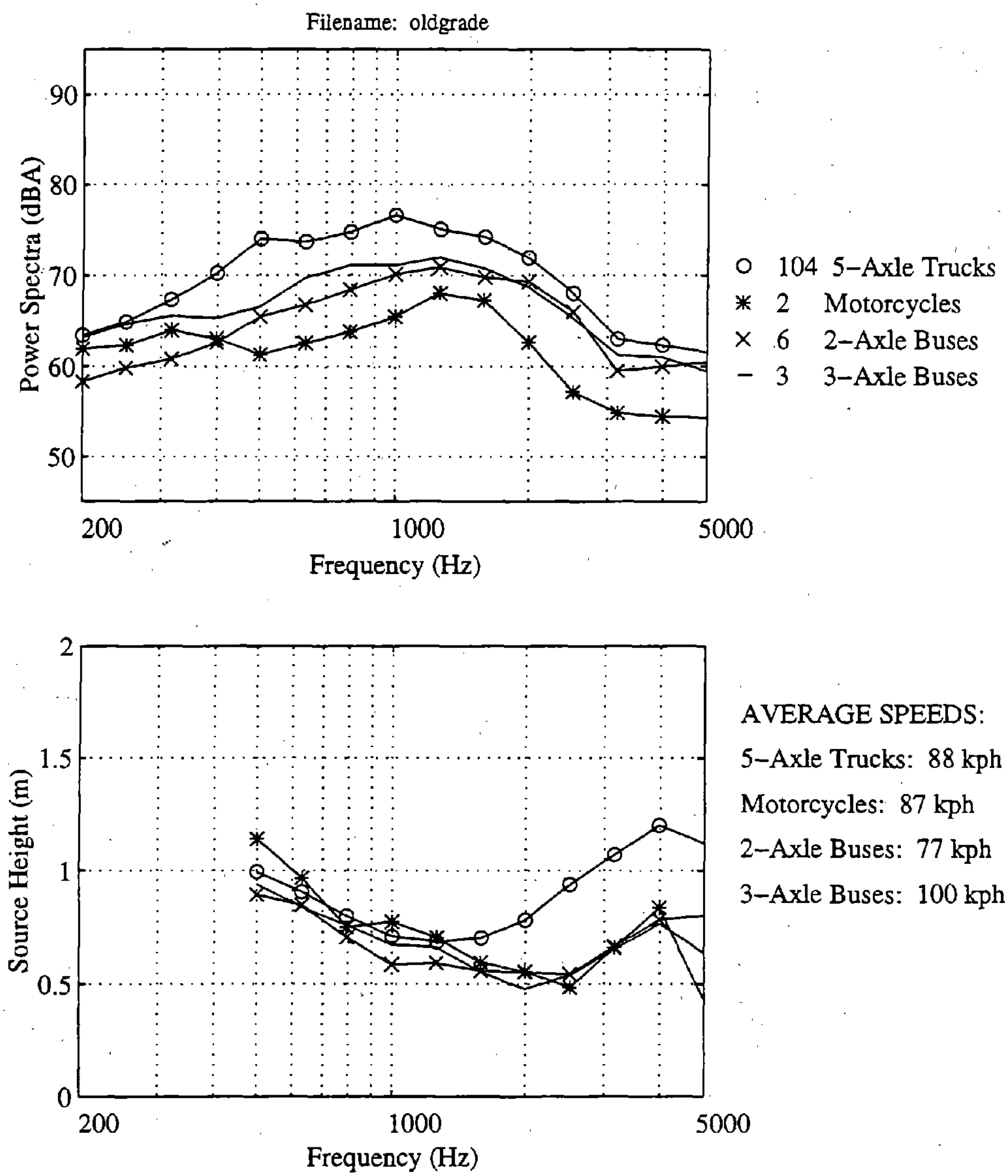

Figure 4.6: Comparison of Averaged Spectra & Source Heights for Standard Autos on Level Asphalt, Level Concrete and Graded Asphalt Roadways, for the 89-105 kph Speed Range. (Using the Lowest Microphone Pair Criteria)

Vehicle Type 1: STANDARD AUTOS

Speed Range 89–105 kph

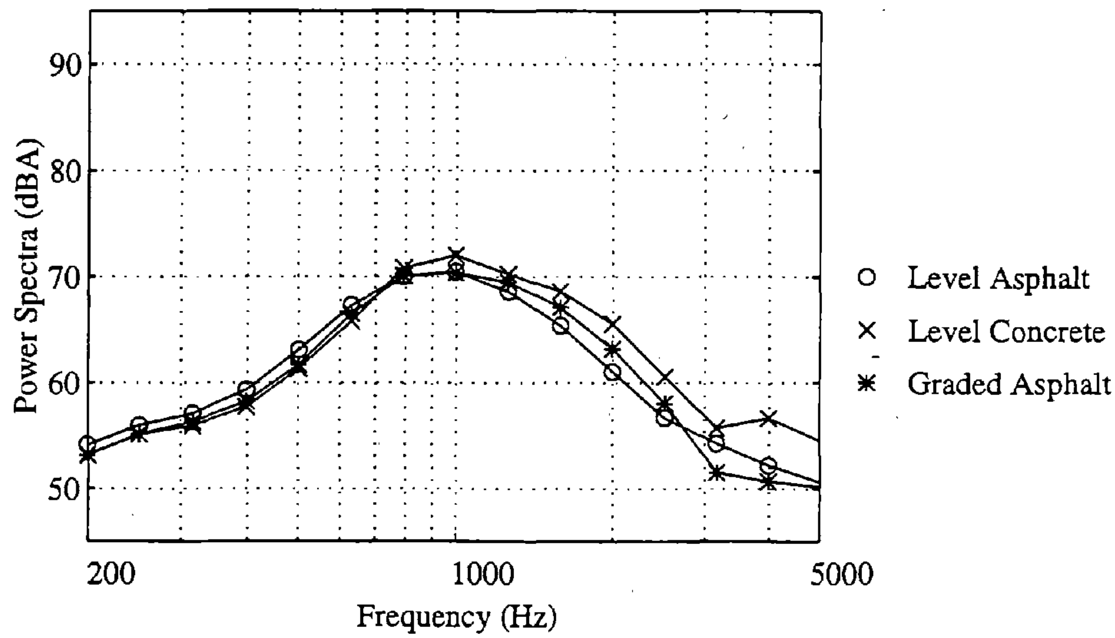

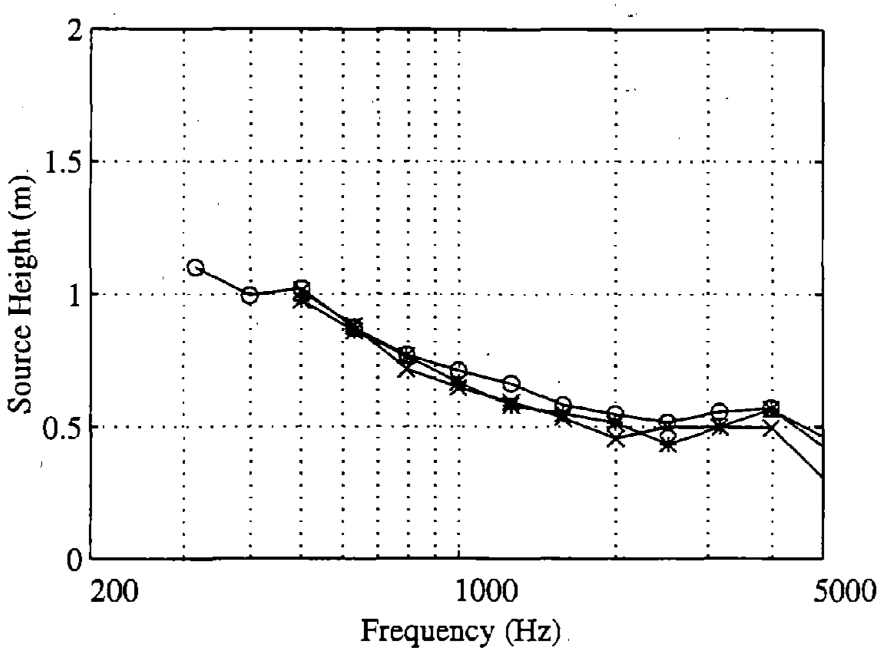

Figure 4.7: Comparison of Averaged Spectra & Source Heights for Medium Trucks on Level Asphalt, Level Concrete and Graded Asphalt Roadways, for the 89-105 kph Speed Range. (Using the Lowest Microphone Pair Criteria)

Vehicle Type 2: MEDIUM TRUCKS

Speed Range 89–105 kph

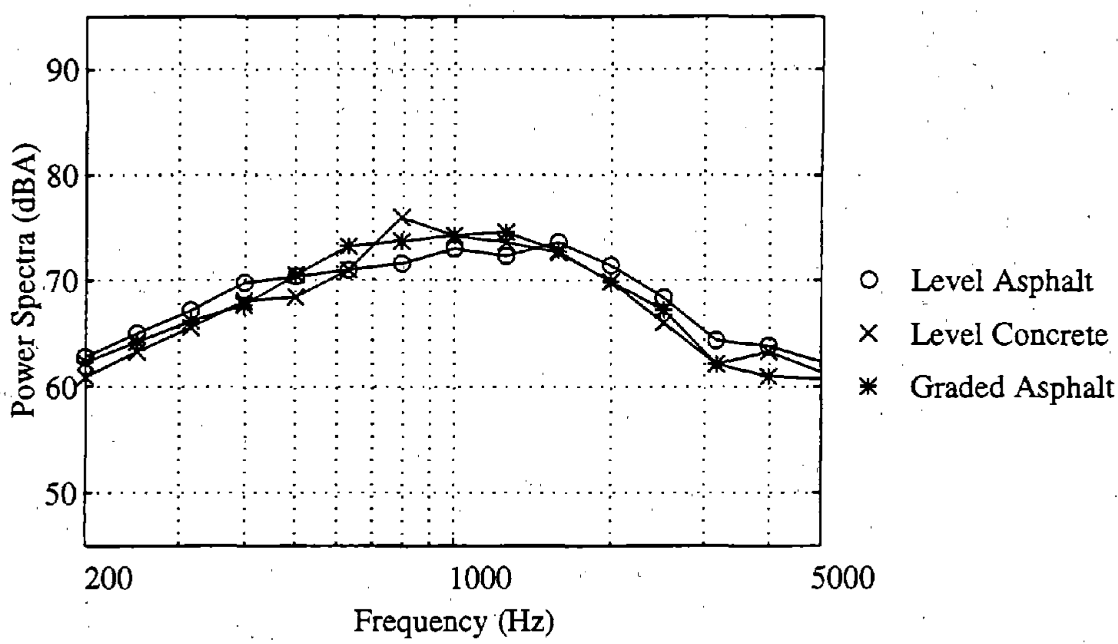

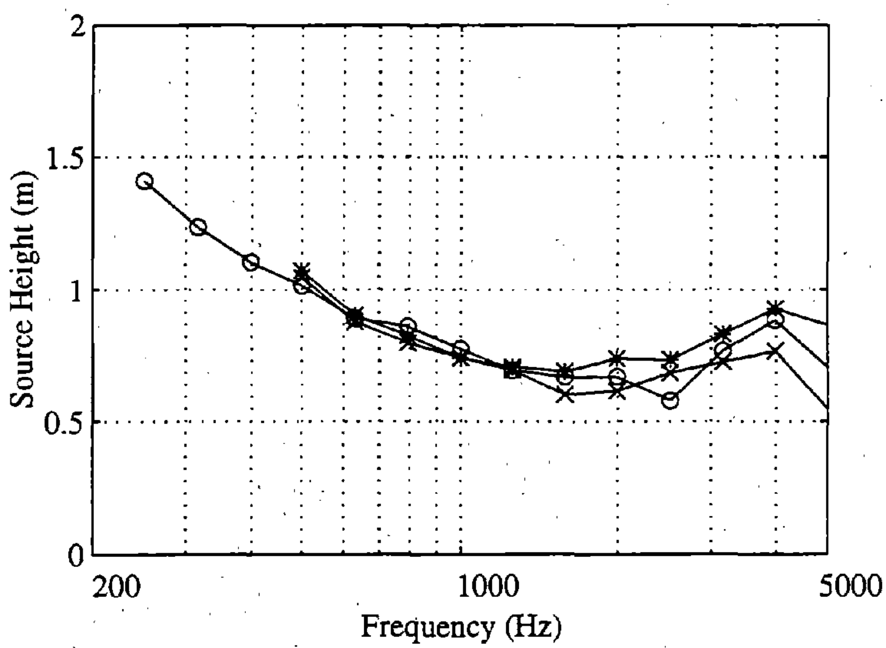

Figure 4.8: Comparison of Averaged Spectra & Source Heights for 5-Axle Heavy Trucks on Level Asphalt, Level Concrete and Graded Asphalt Roadways, for the 89-105 kph Speed Range. (Using the Lowest Microphone Pair Criteria)

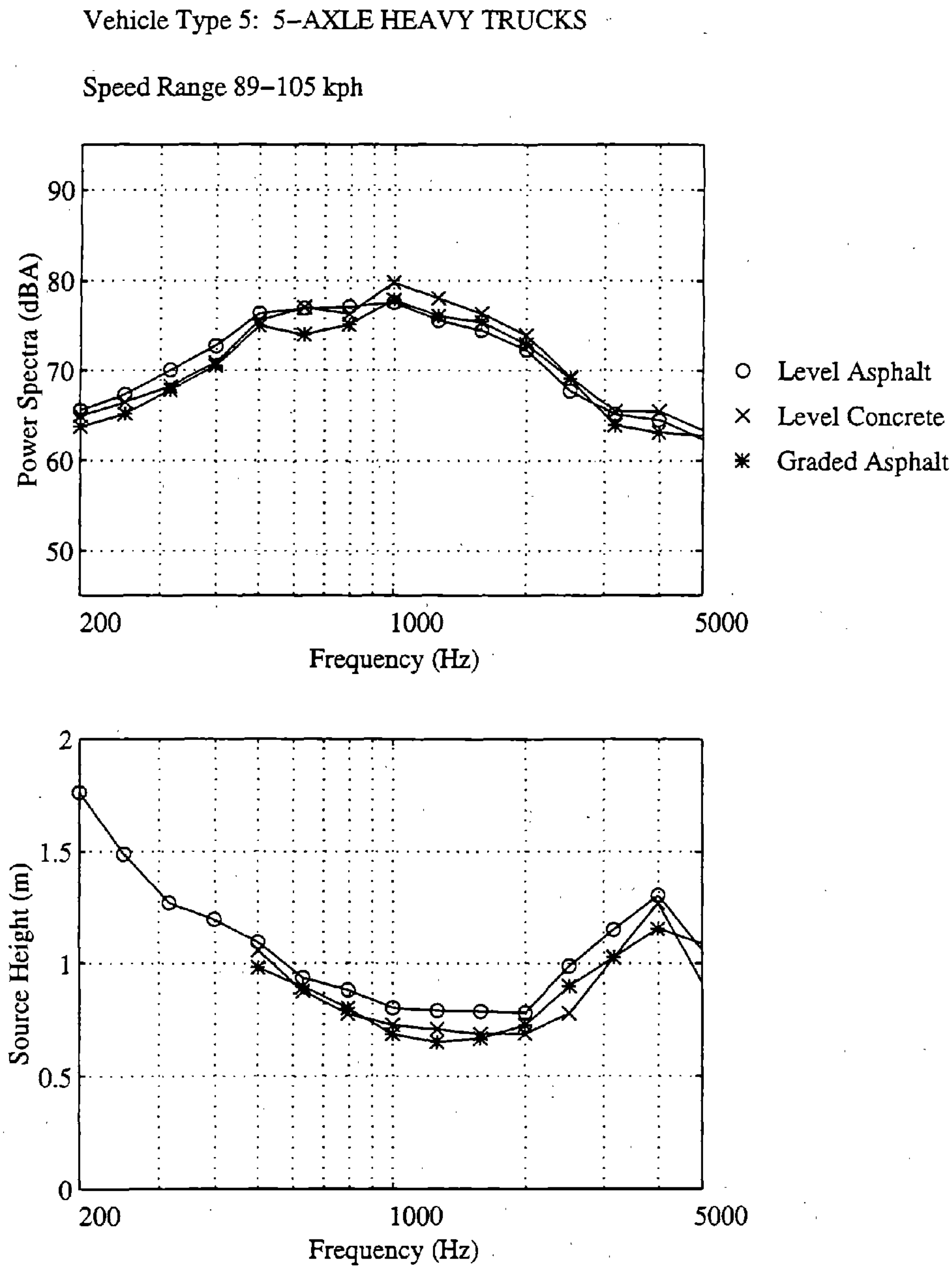

Figure 4.9: Comparison of Single Loudspeaker Test Results
Using Each Microphone Selection Criteria.
(a) Speaker Spectrum.
(b) For Speaker @ Height 0.5 m.
(c) For Speaker @ Height 1.0 m.
(d) For Speaker @ Height 1.5 m.

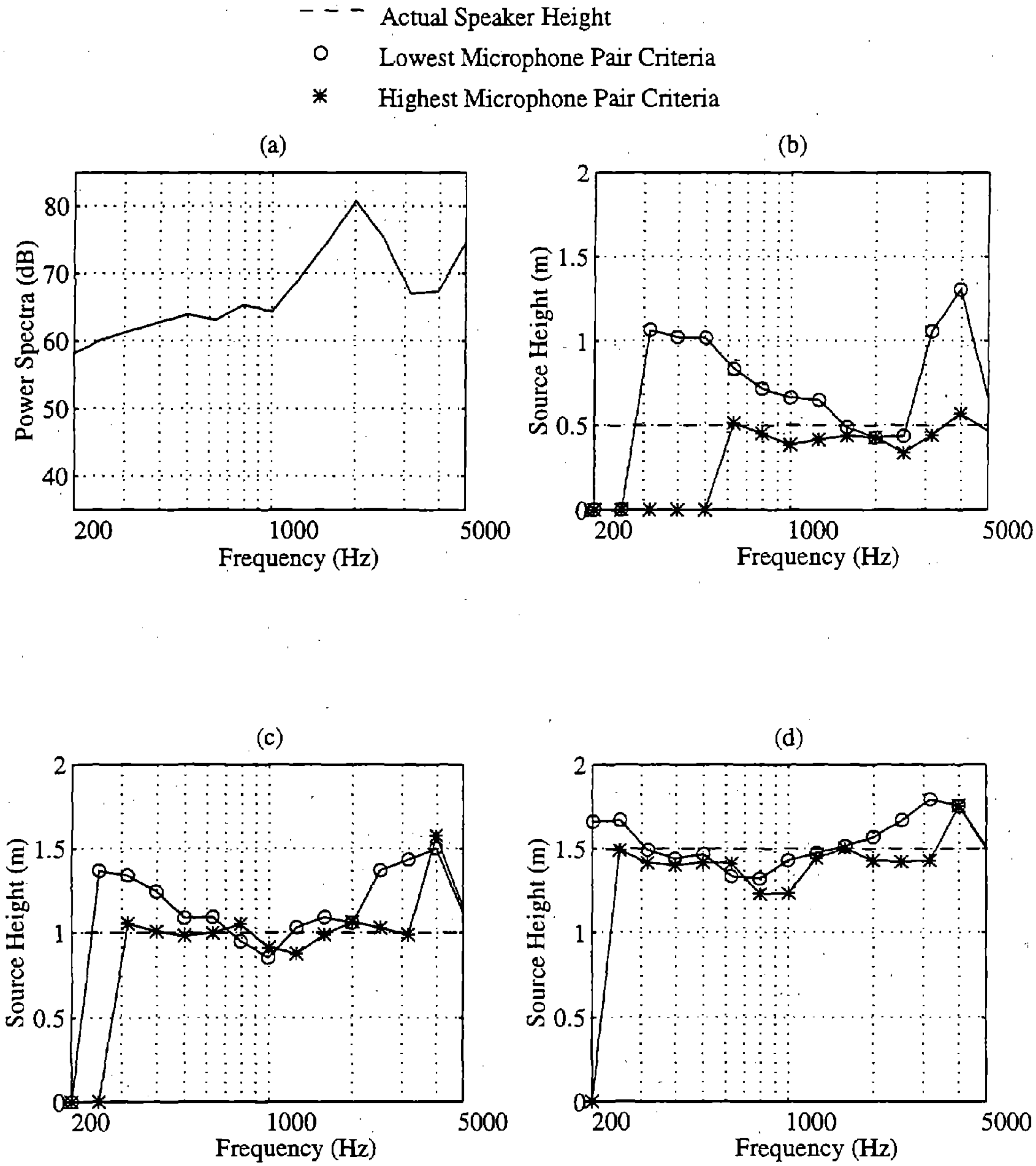

Figure 4.10: Comparison of Measured and Calculated Source Heights for Two Loudspeakers with the Same Spectra Placed at 0.45 m & 1.4 m. (Using the Highest Microphone Pair Criteria)

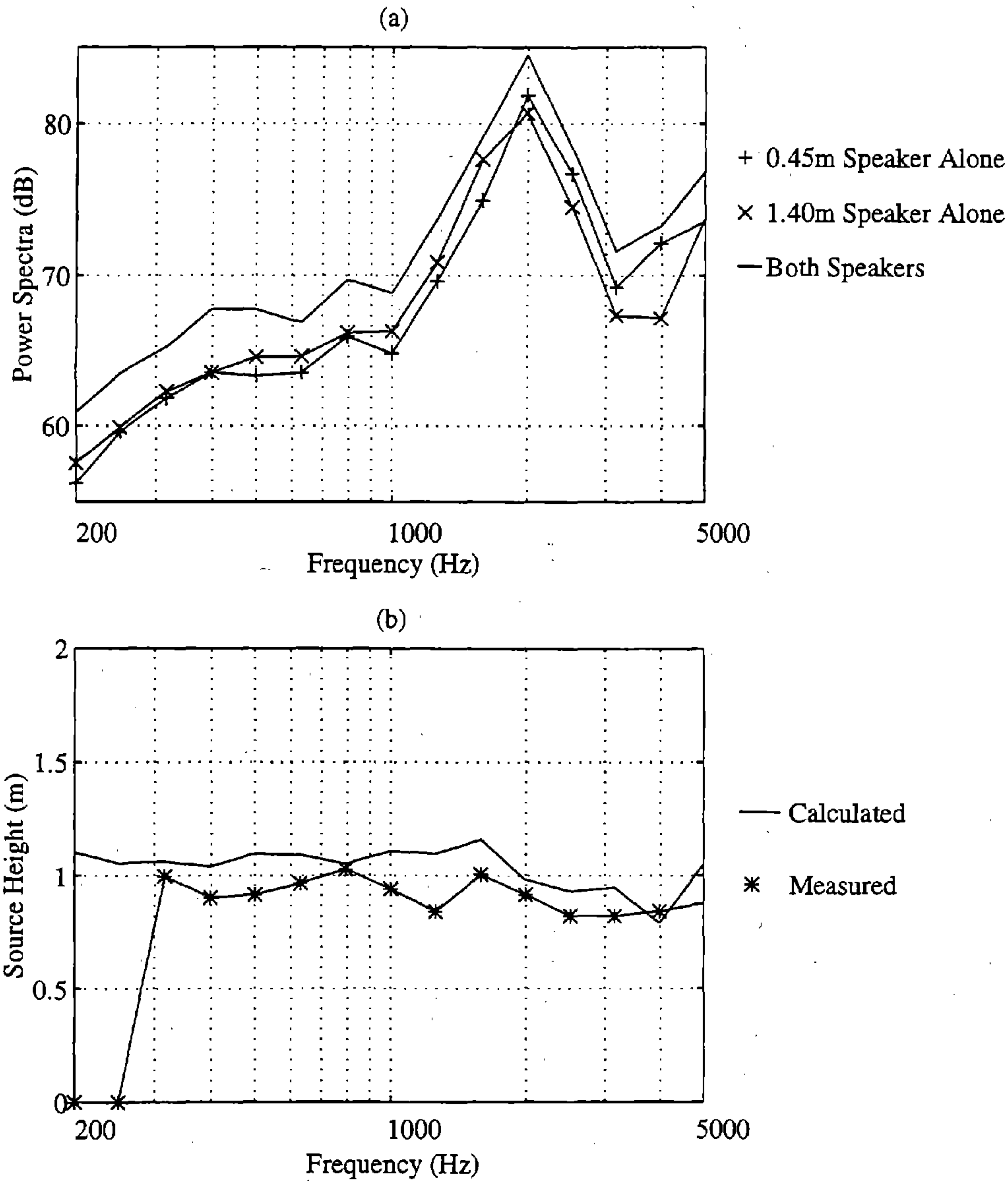

Figure 4.11: Measured Spectra & Source Heights for Two Loudspeakers with Different Spectra Placed at 0.45 m & 1.4 m.
(Using the Highest Microphone Pair Criteria)

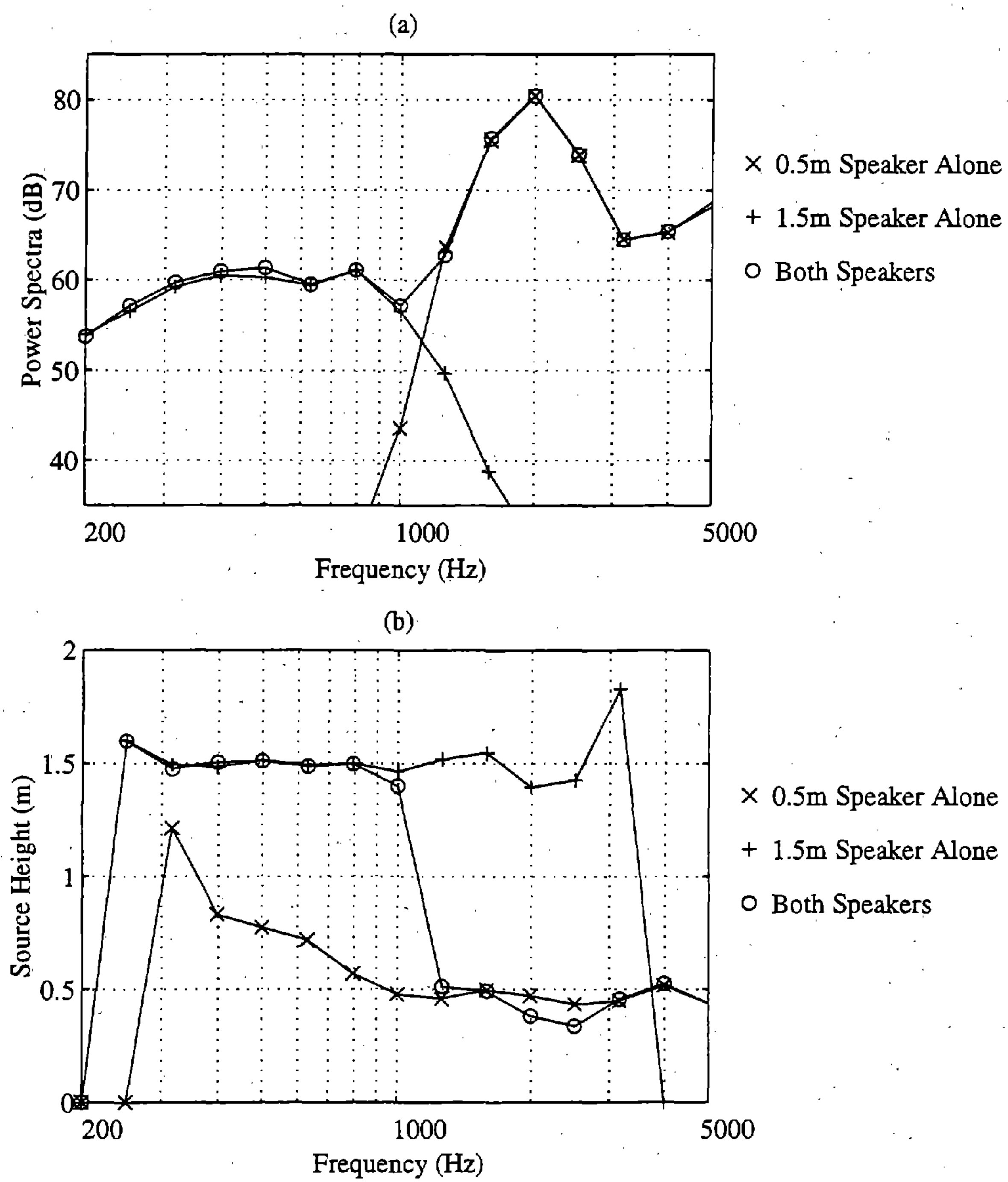

Figure 4.12: Averaged Spectra & Source Heights for Vehicle Types 0 to 4 Cruising on Level Asphalt Roadways.
(Using the Highest Microphone Pair Criteria)

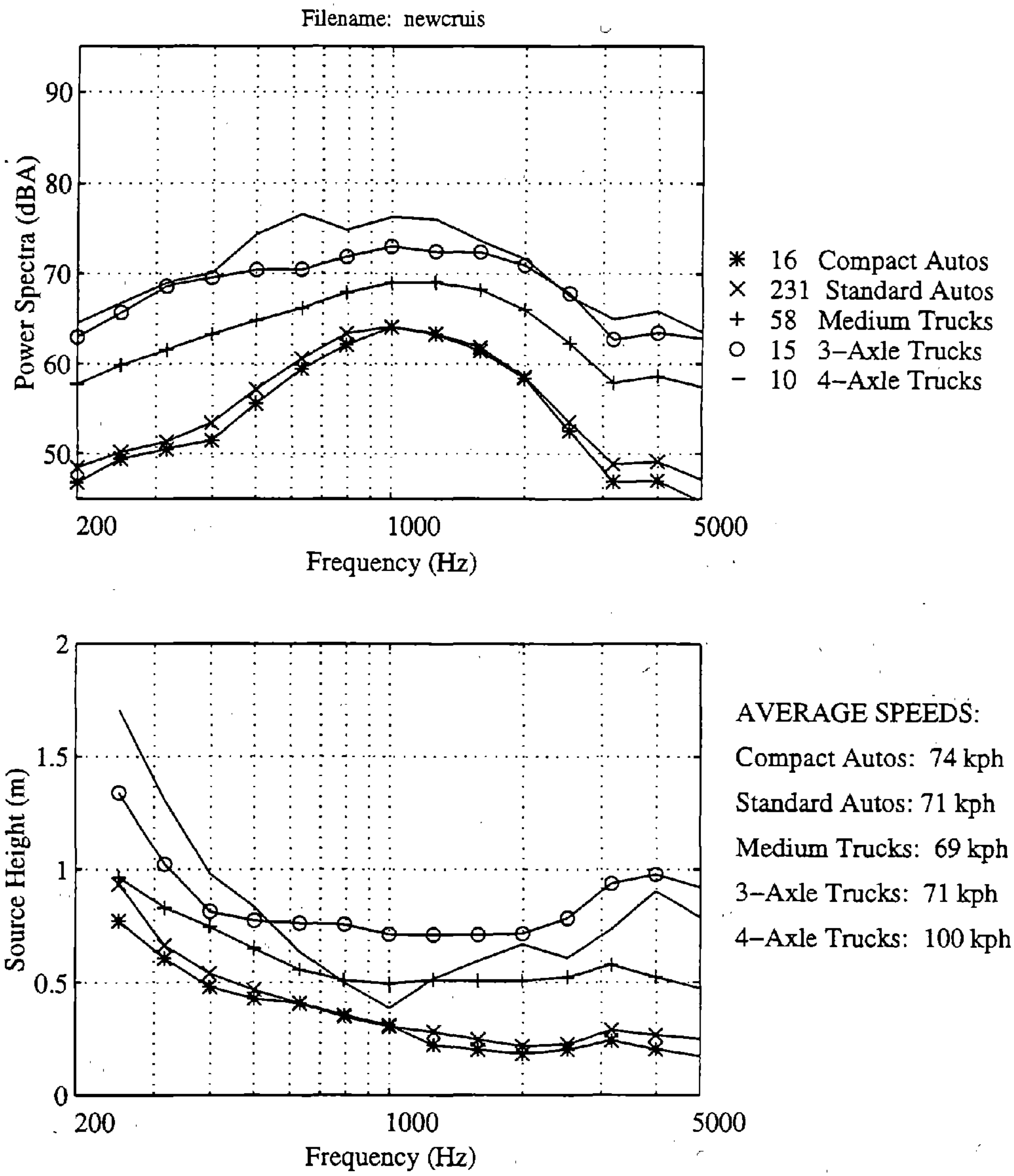

Figure 4.13: Averaged Spectra & Source Heights for Vehicle Types 5 to 9 Cruising on Level Asphalt Roadways. (Using the Highest Microphone Pair Criteria)

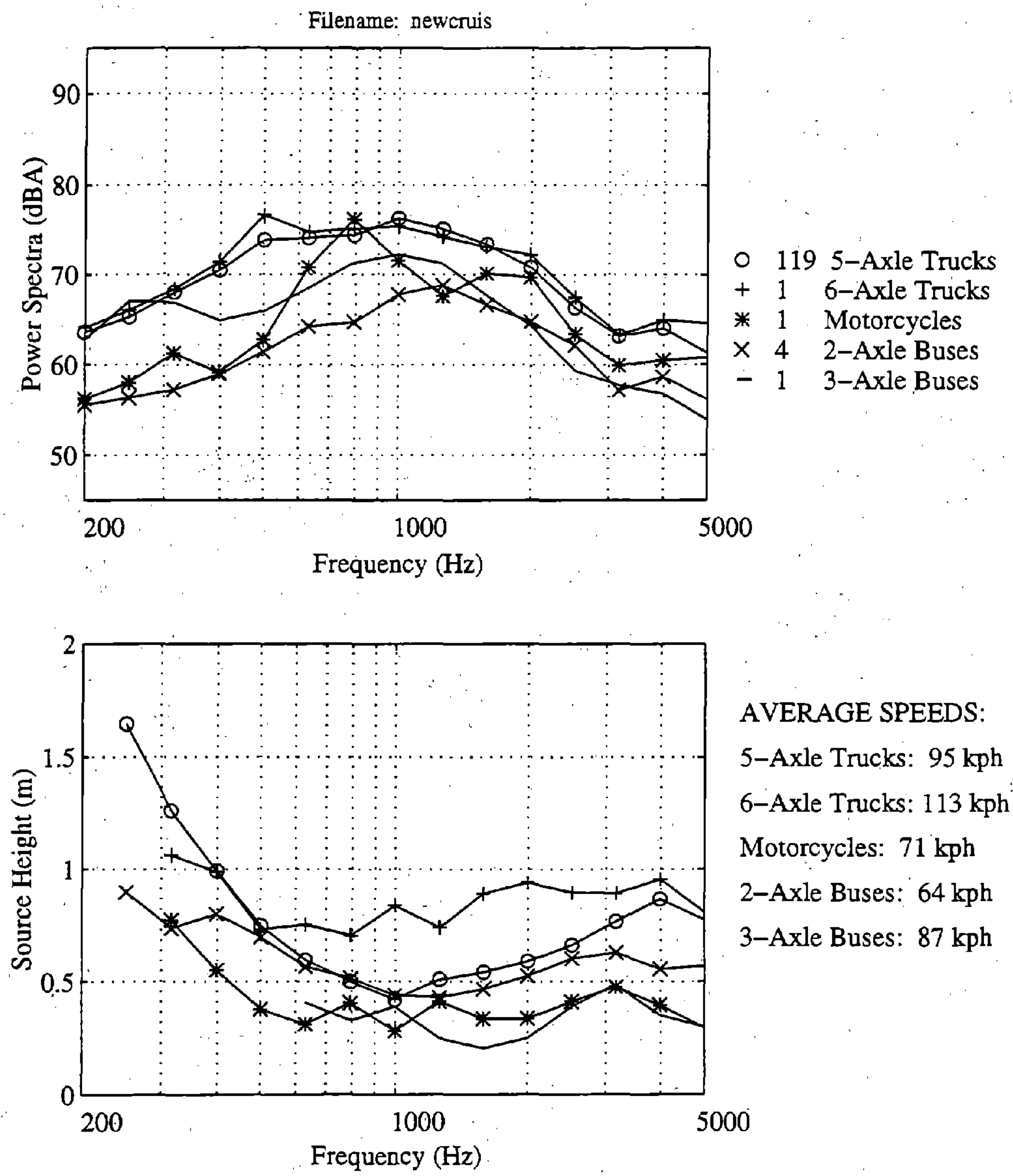

Figure 4.14: Scatter Plots of all Measured Spectra & Source Heights for Vehicle Type 0 Cruising on Level Asphalt Roadways. (Using the Highest Microphone Pair Criteria)

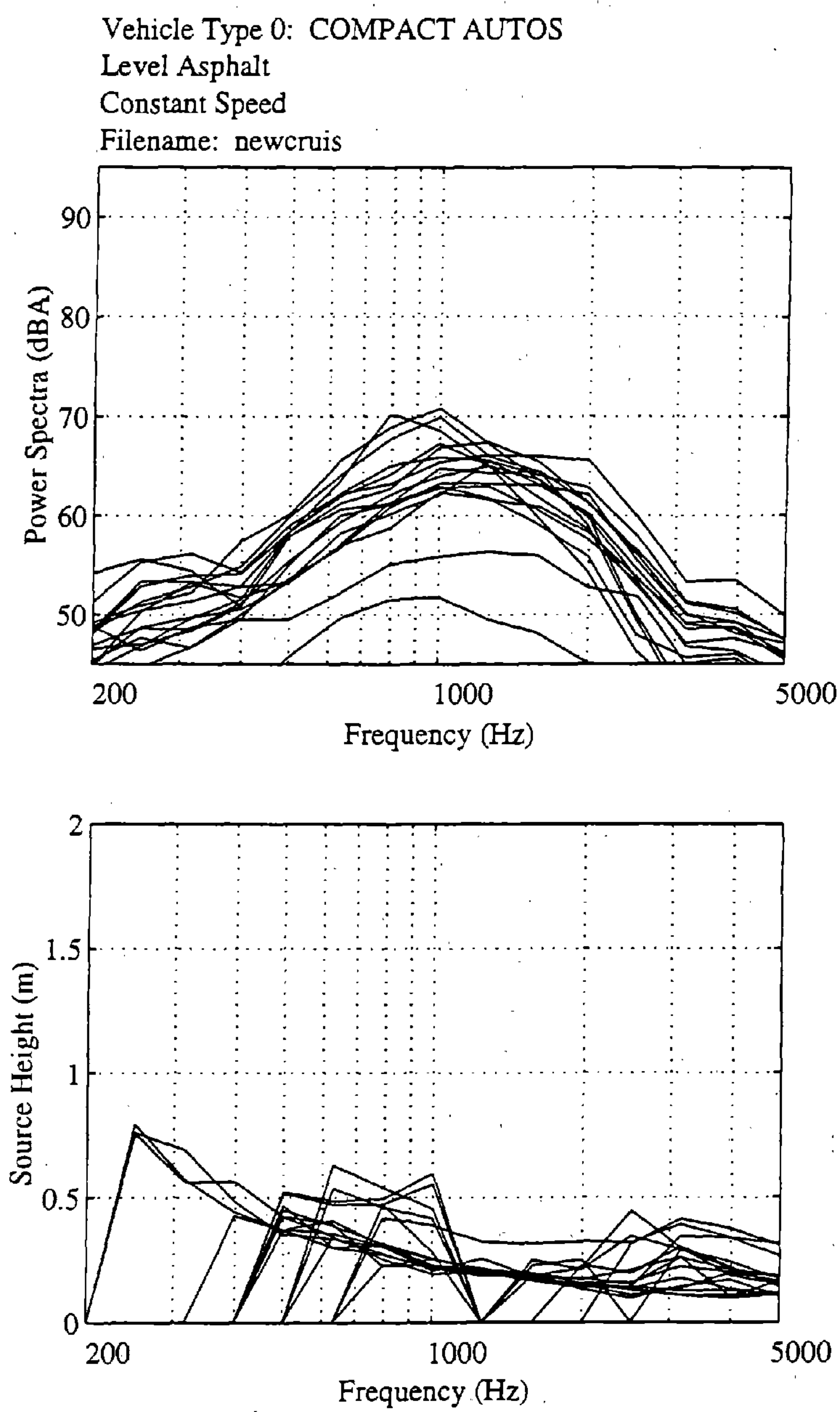

Figure 4.15: Scatter Plots of all Measured Spectra & Source Heights for Vehicle Type 1 Cruising on Level Asphalt Roadways.
(Using the Highest Microphone Pair Criteria)

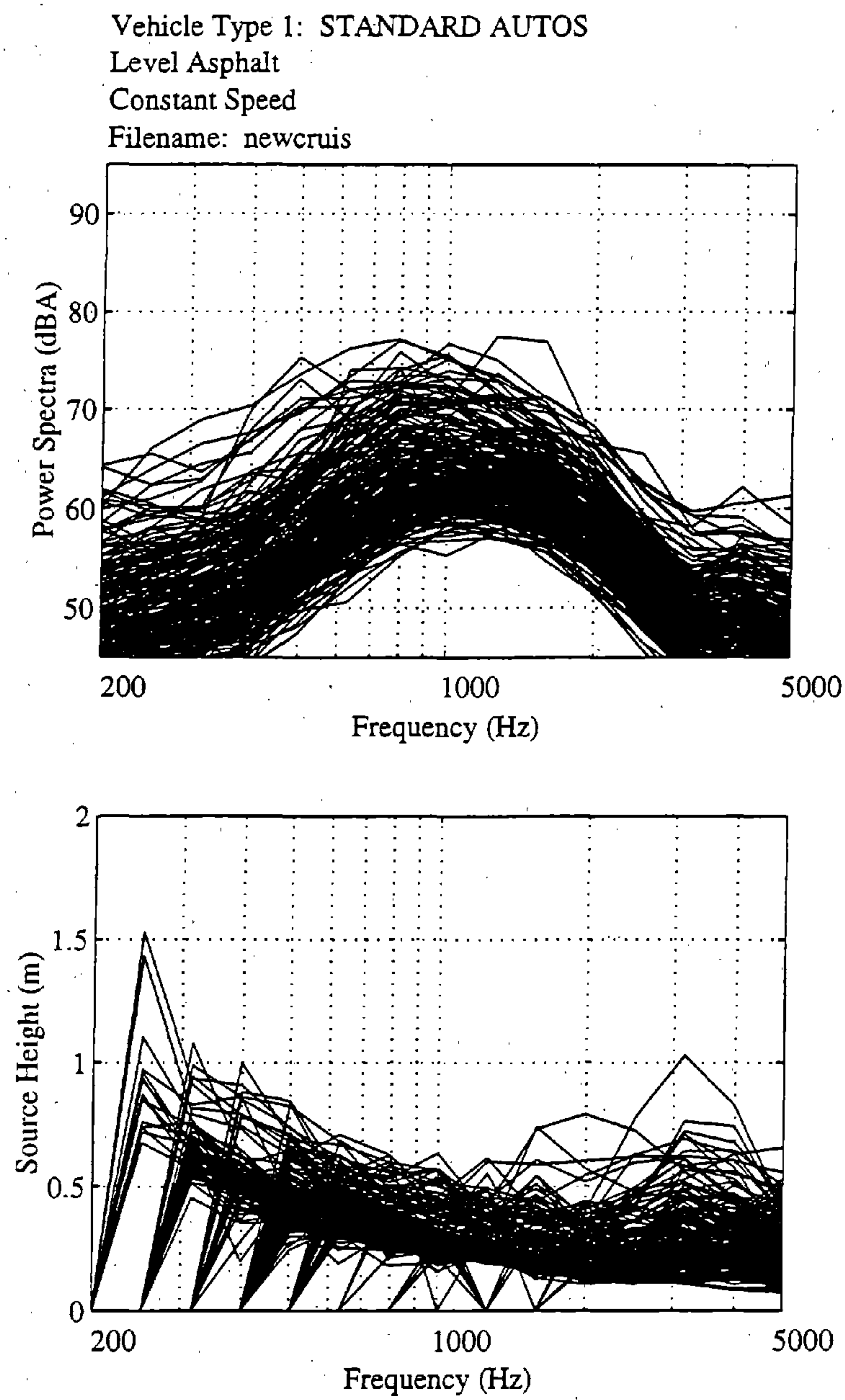

Figure 4.16: Scatter Plots of all Measured Spectra & Source Heights for Vehicle Type 2 Cruising on Level Asphalt Roadways. (Using the Highest Microphone Pair Criteria)

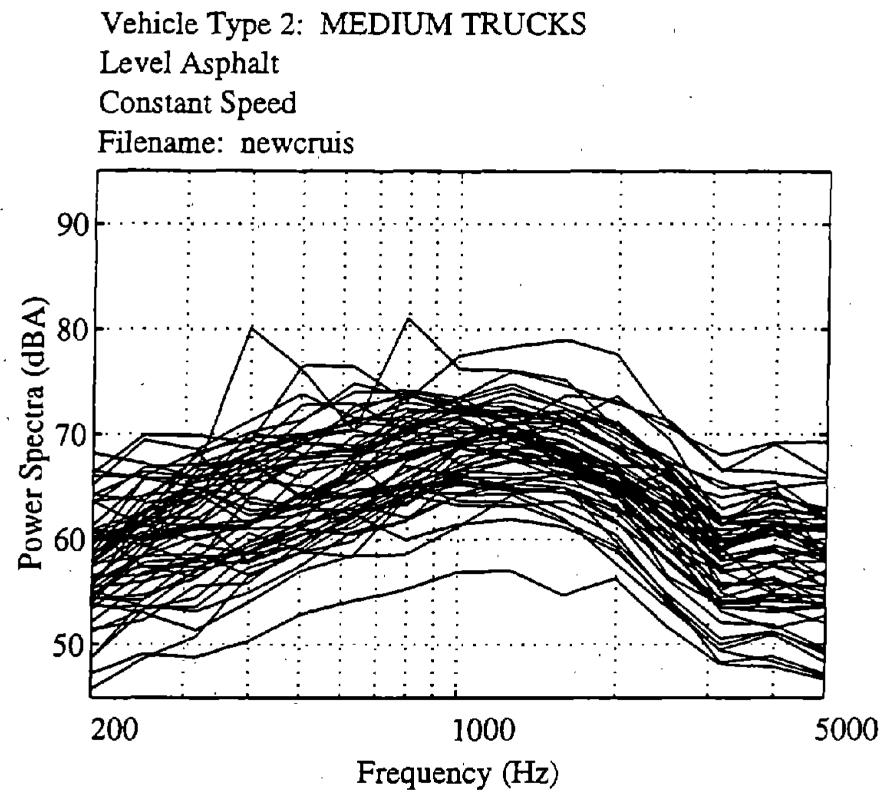

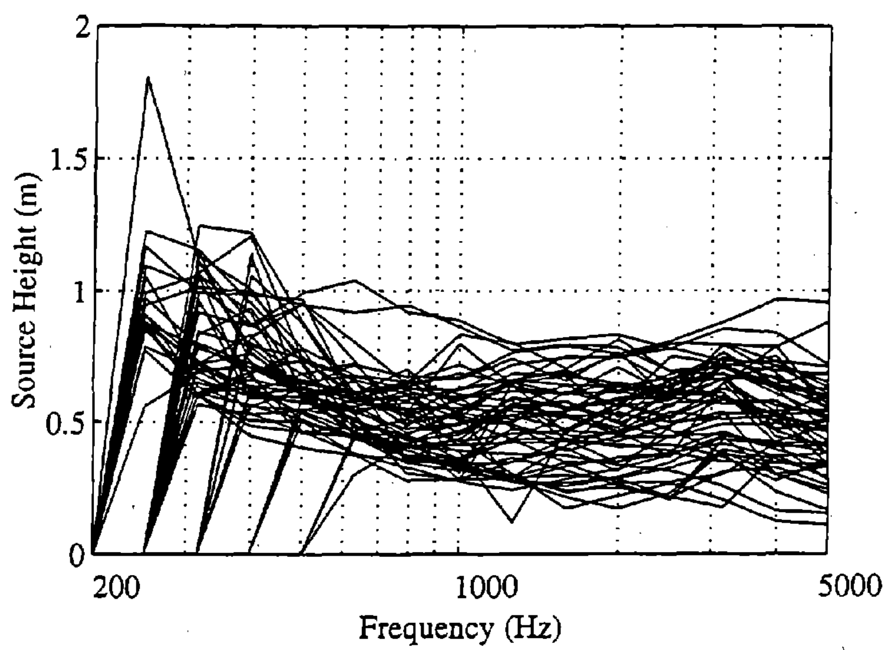

Figure 4.17: Scatter Plots of all Measured Spectra & Source Heights for Vehicle Type 3 Cruising on Level Asphalt Roadways. (Using the Highest Microphone Pair Criteria)

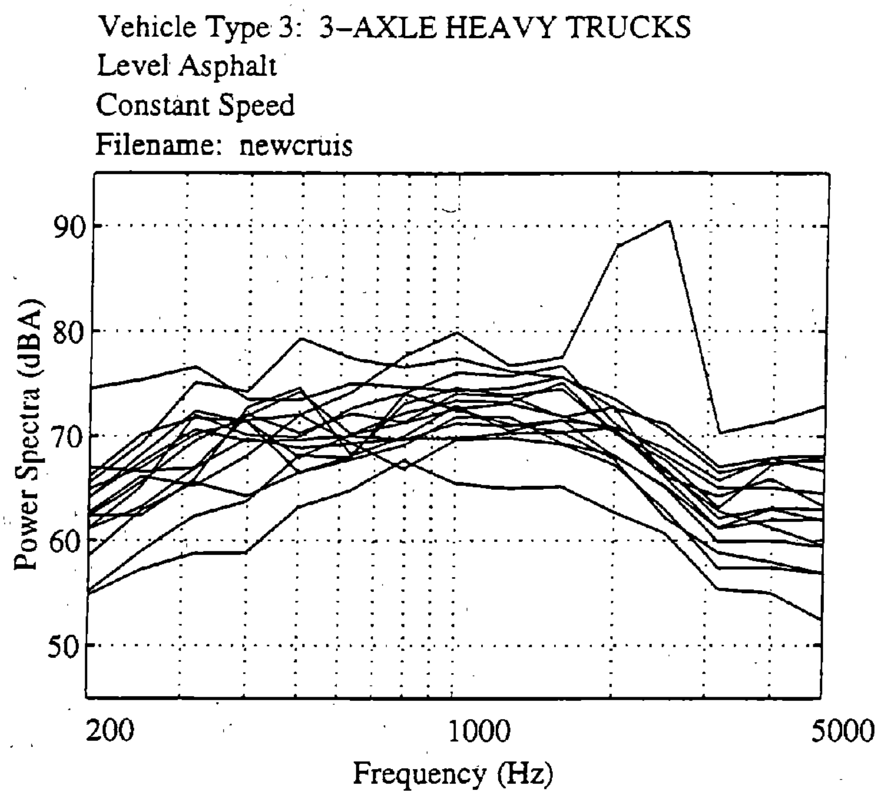

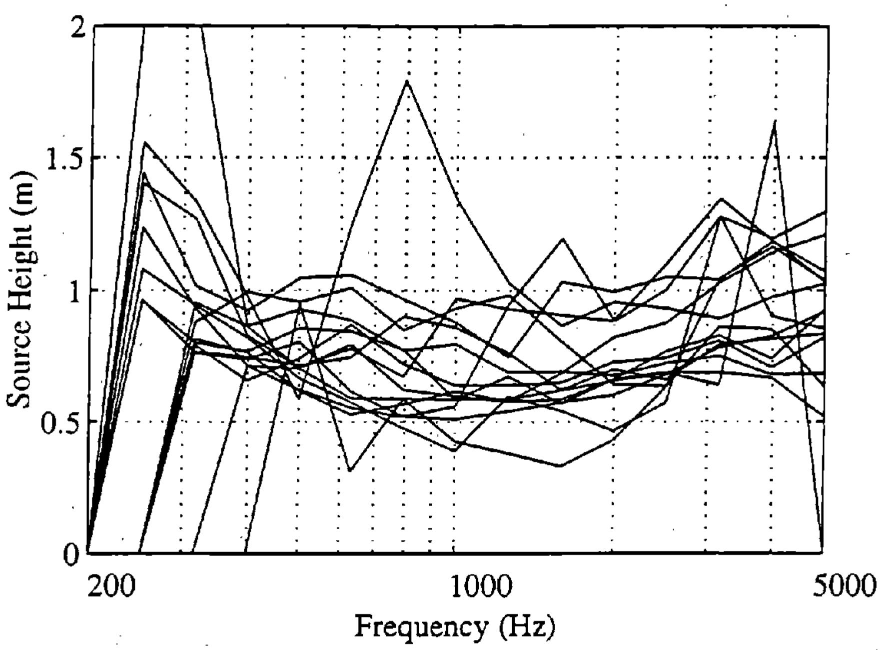

Figure 4.18: Scatter Plots of all Measured Spectra & Source Heights for Vehicle Type 4 Cruising on Level Asphalt Roadways. (Using the Highest Microphone Pair Criteria)

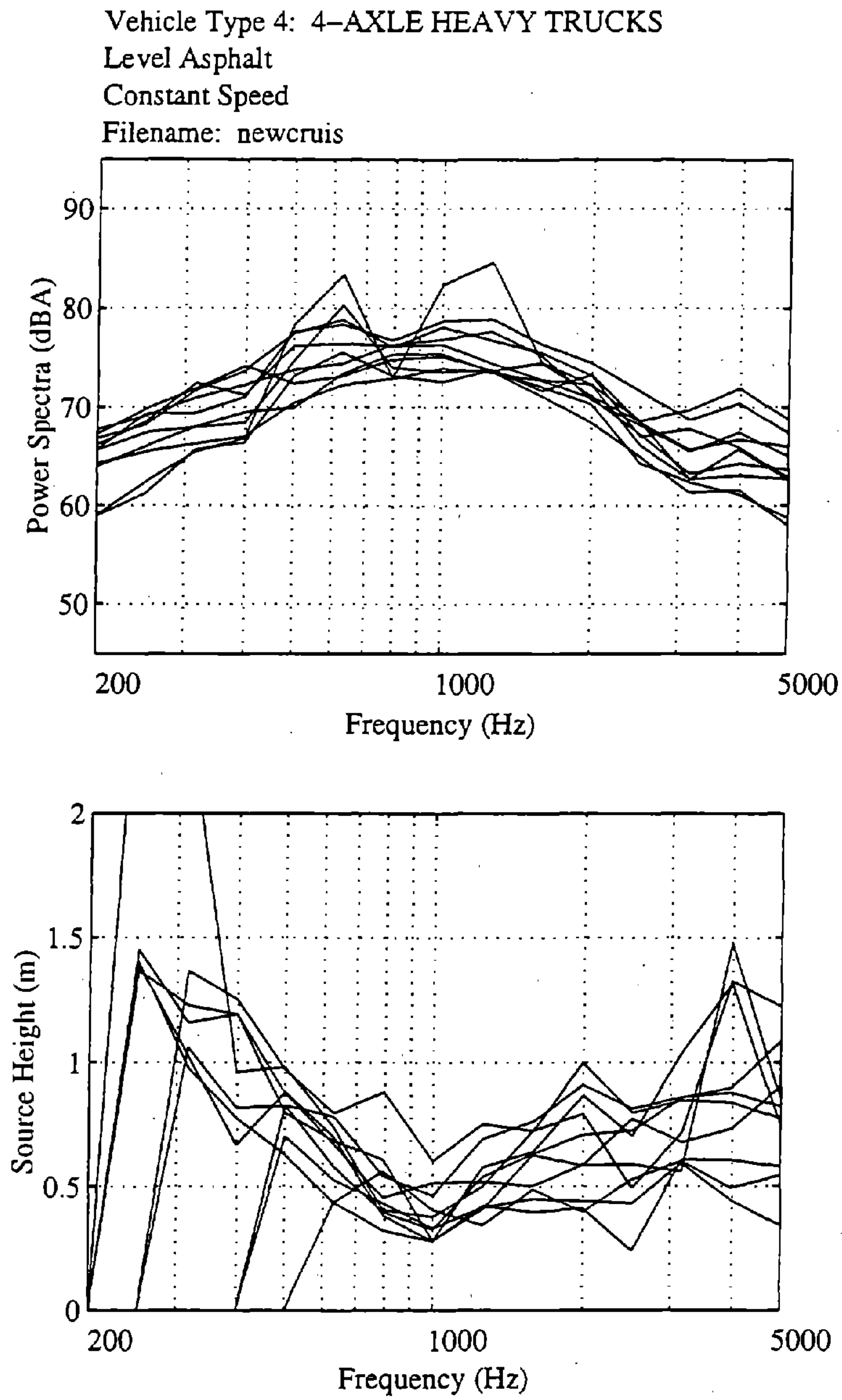

Figure 4.19: Scatter Plots of all Measured Spectra & Source Heights for Vehicle Type 5 Cruising on Level Asphalt Roadways.
(Using the Highest Microphone Pair Criteria)

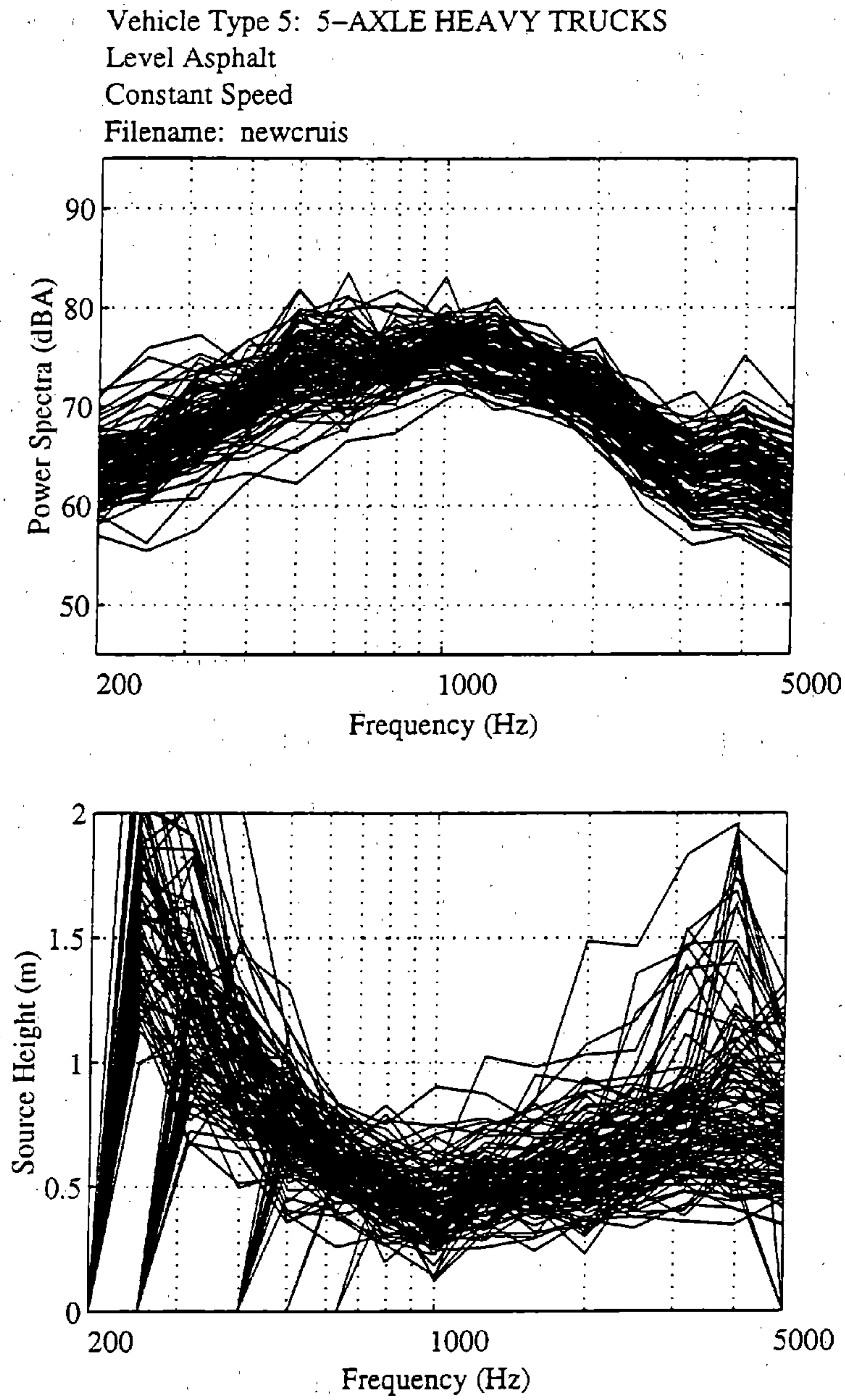

Figure 4.20: Scatter Plots of all Measured Spectra & Source Heights for Vehicle Type 6 Cruising on Level Asphalt Roadways. (Using the Highest Microphone Pair Criteria)

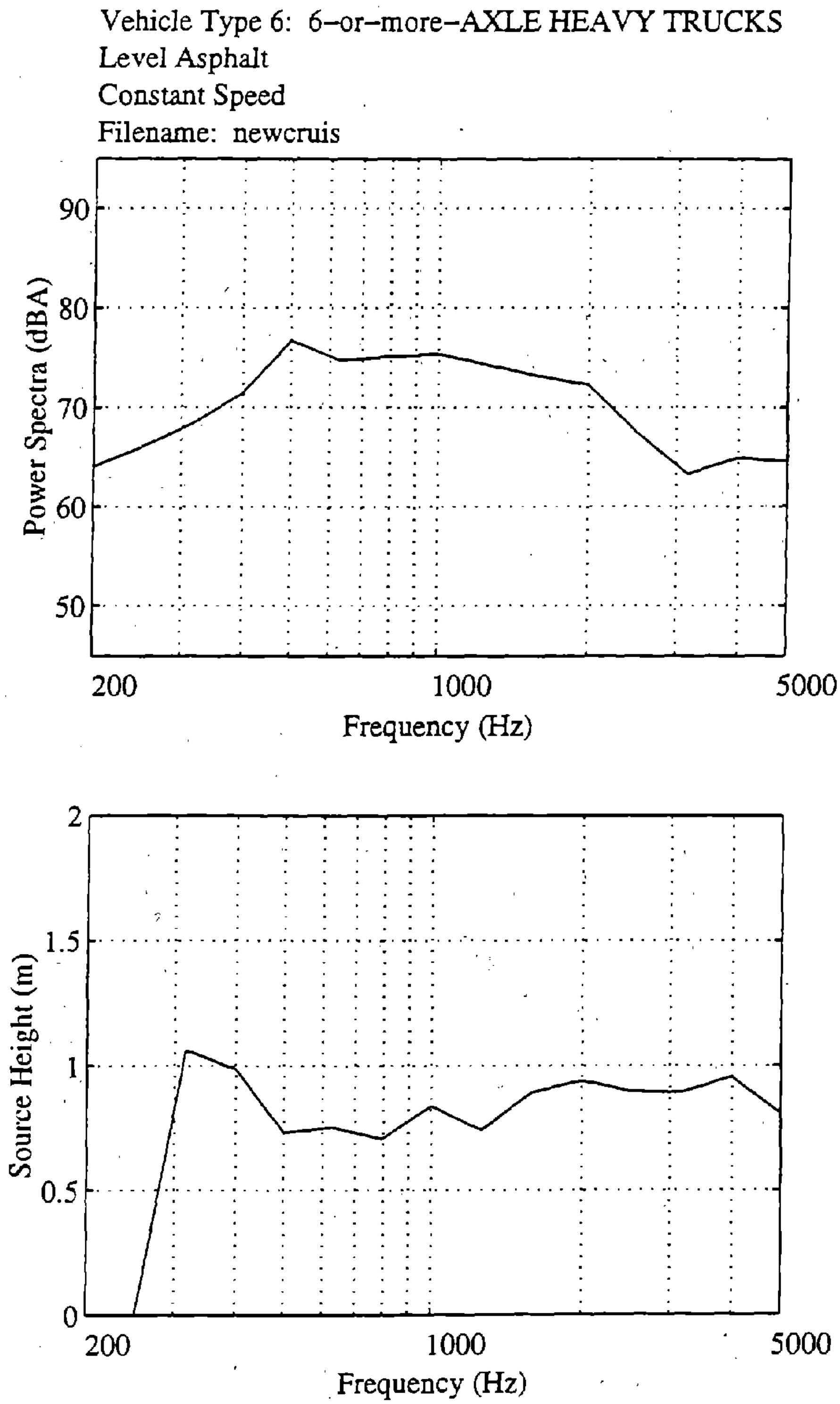

Figure 4.21: Scatter Plots of all Measured Spectra & Source Heights for Vehicle Type 7 Cruising on Level Asphalt Roadways. (Using the Highest Microphone Pair Criteria)

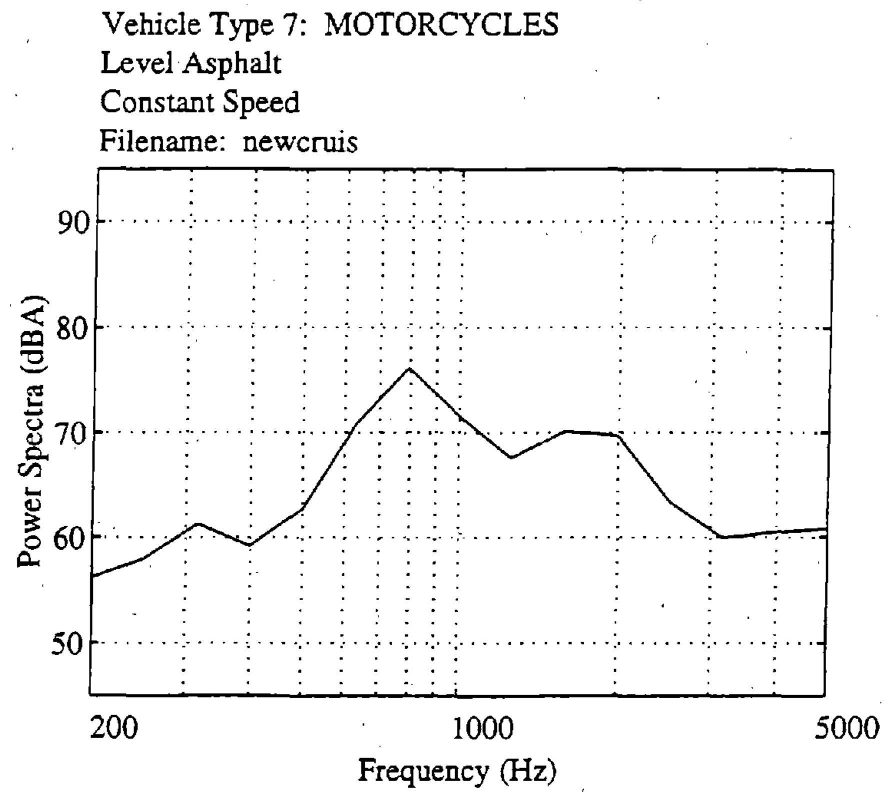

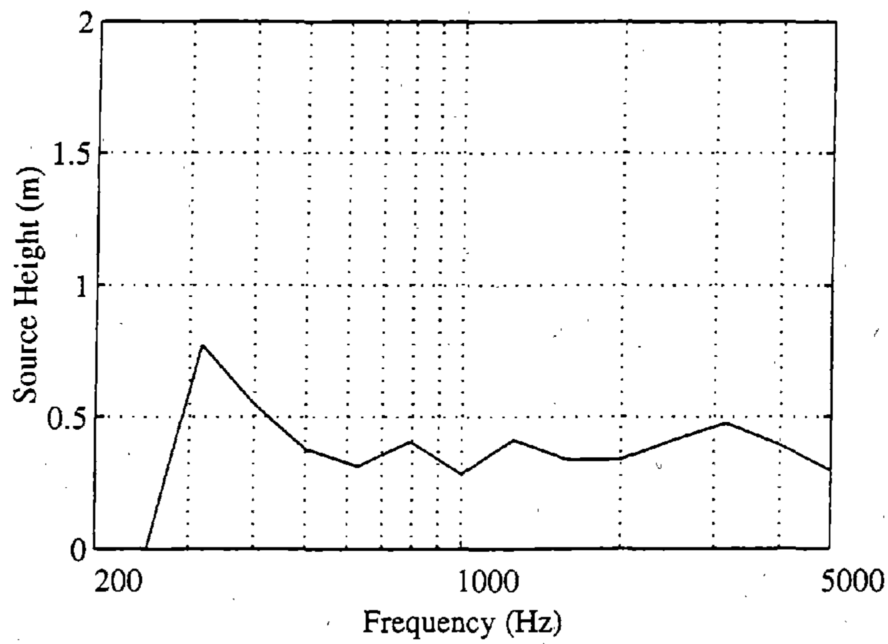

Figure 4.22: Scatter Plots of all Measured Spectra & Source Heights for Vehicle Type 8 Cruising on Level Asphalt Roadways.
(Using the Highest Microphone Pair Criteria)

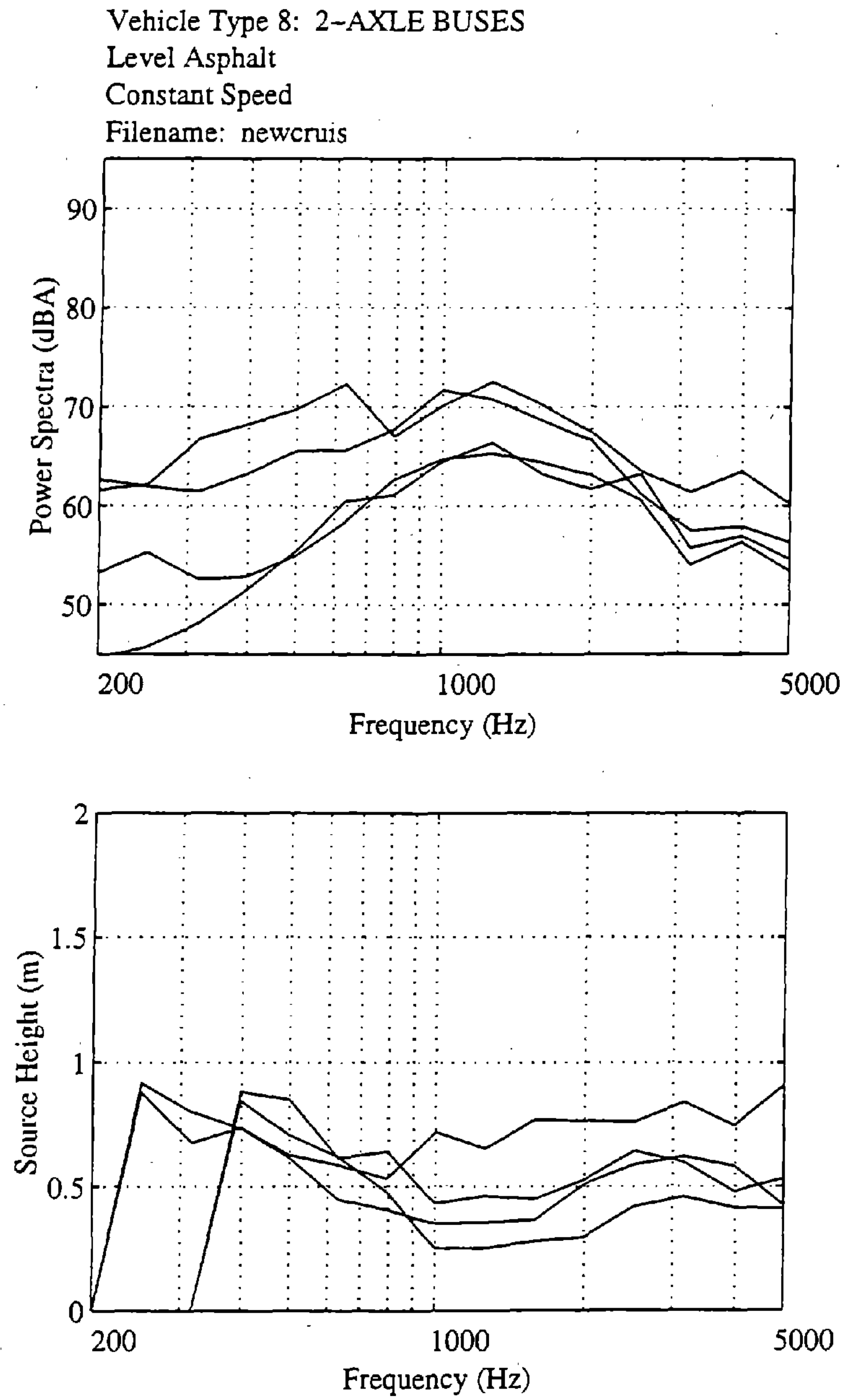

Figure 4.23: Scatter Plots of all Measured Spectra & Source Heights for Vehicle Type 9 Cruising on Level Asphalt Roadways. (Using the Highest Microphone Pair Criteria)

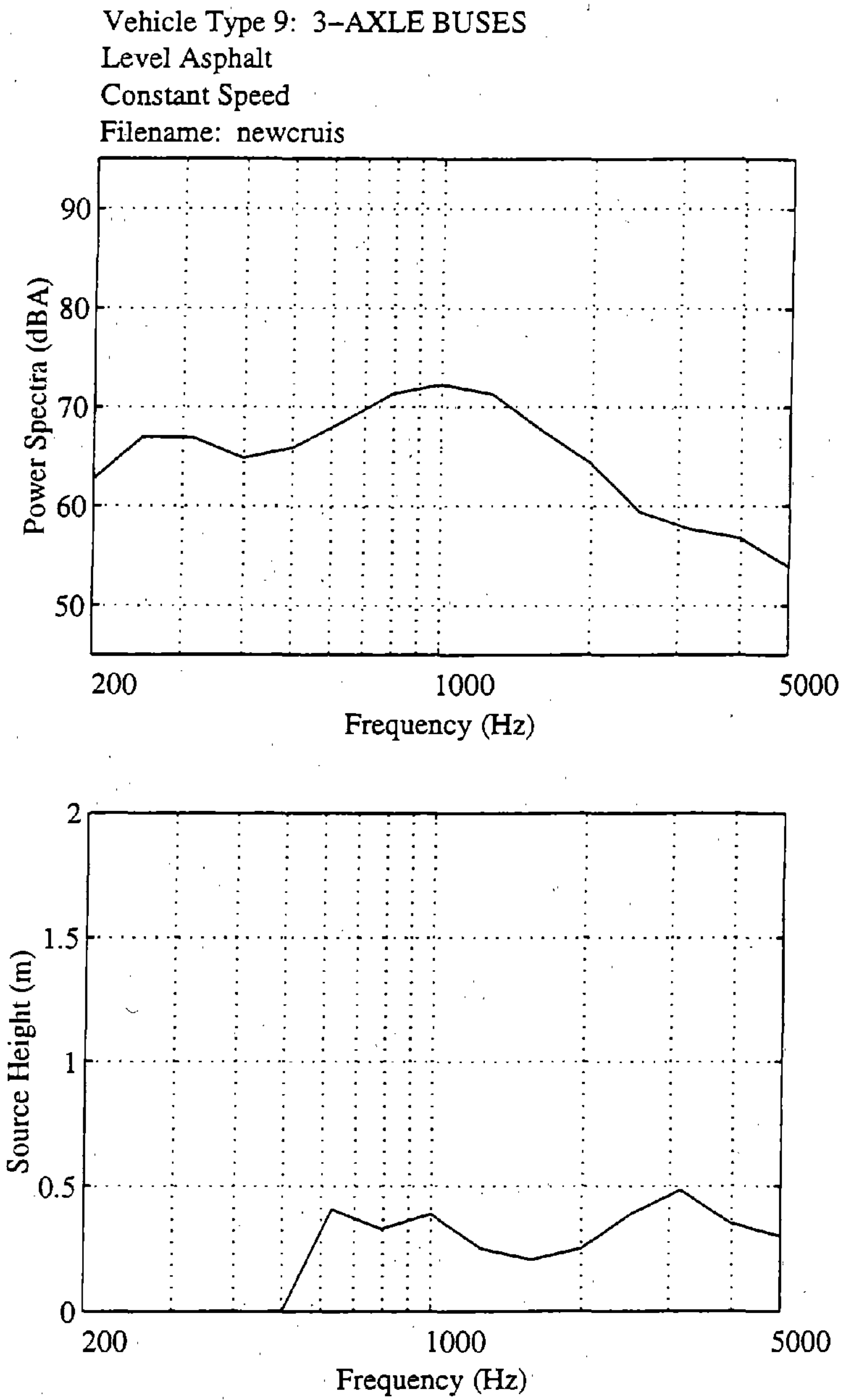

Figure 4.24: Averaged Spectra & Source Heights for Vehicle Type 0 Averaged over 6 Different Speed Bands Cruising on Level Asphalt Roadways. (Using the Highest Microphone Pair Criteria)

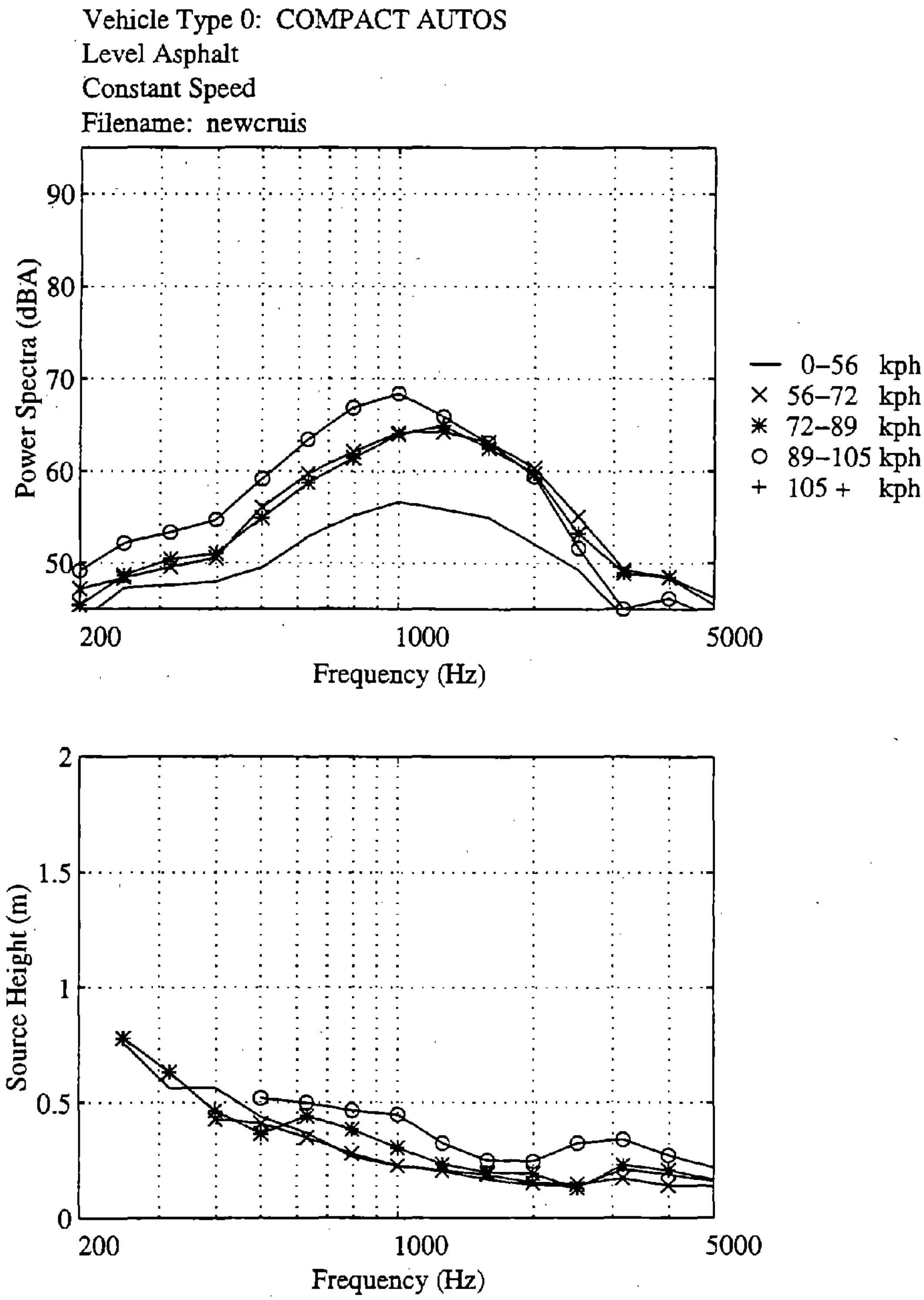

Figure 4.25: Averaged Spectra & Source Heights for Vehicle Type 1 Averaged over 6 Different Speed Bands Cruising on Level Asphalt Roadways. (Using the Highest Microphone Pair Criteria)

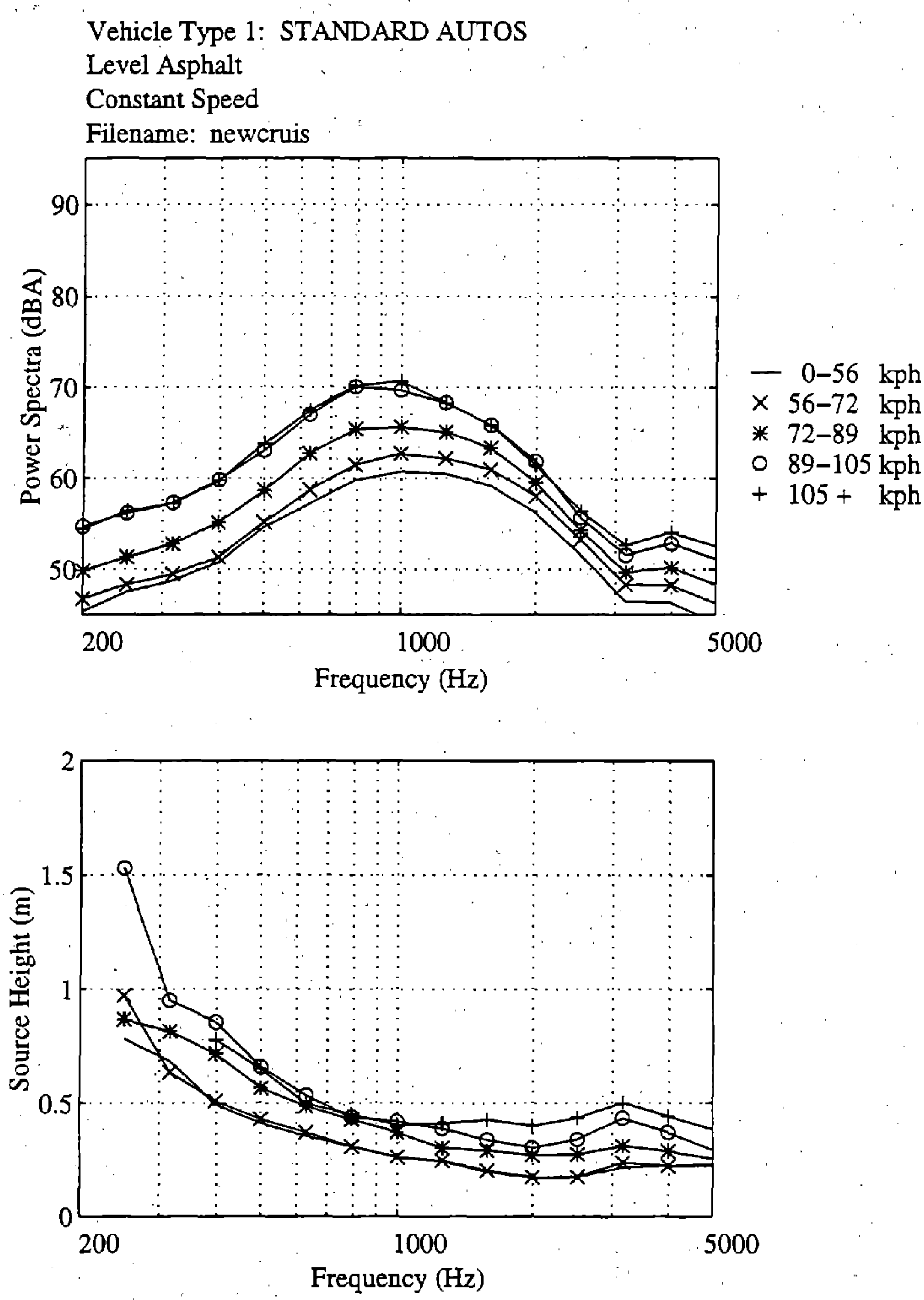

Figure 4.26: Averaged Spectra & Source Heights for Vehicle Type 2 Averaged over 6 Different Speed Bands Cruising on Level Asphalt Roadways. (Using the Highest Microphone Pair Criteria)

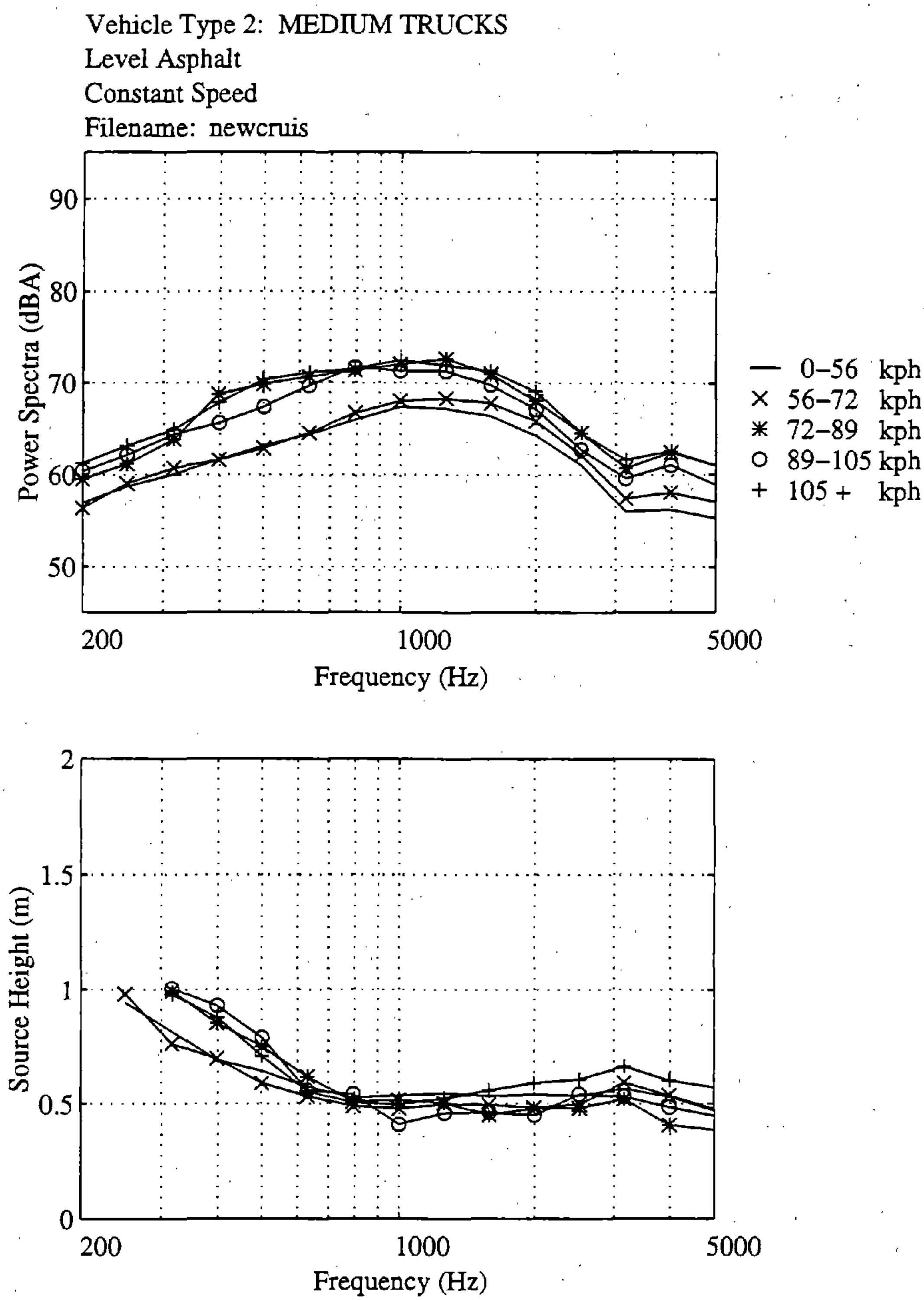

Figure 4.27: Averaged Spectra & Source Heights for Vehicle Type 3 Averaged over 6 Different Speed Bands Cruising on Level Asphalt Roadways. (Using the Highest Microphone Pair Criteria)

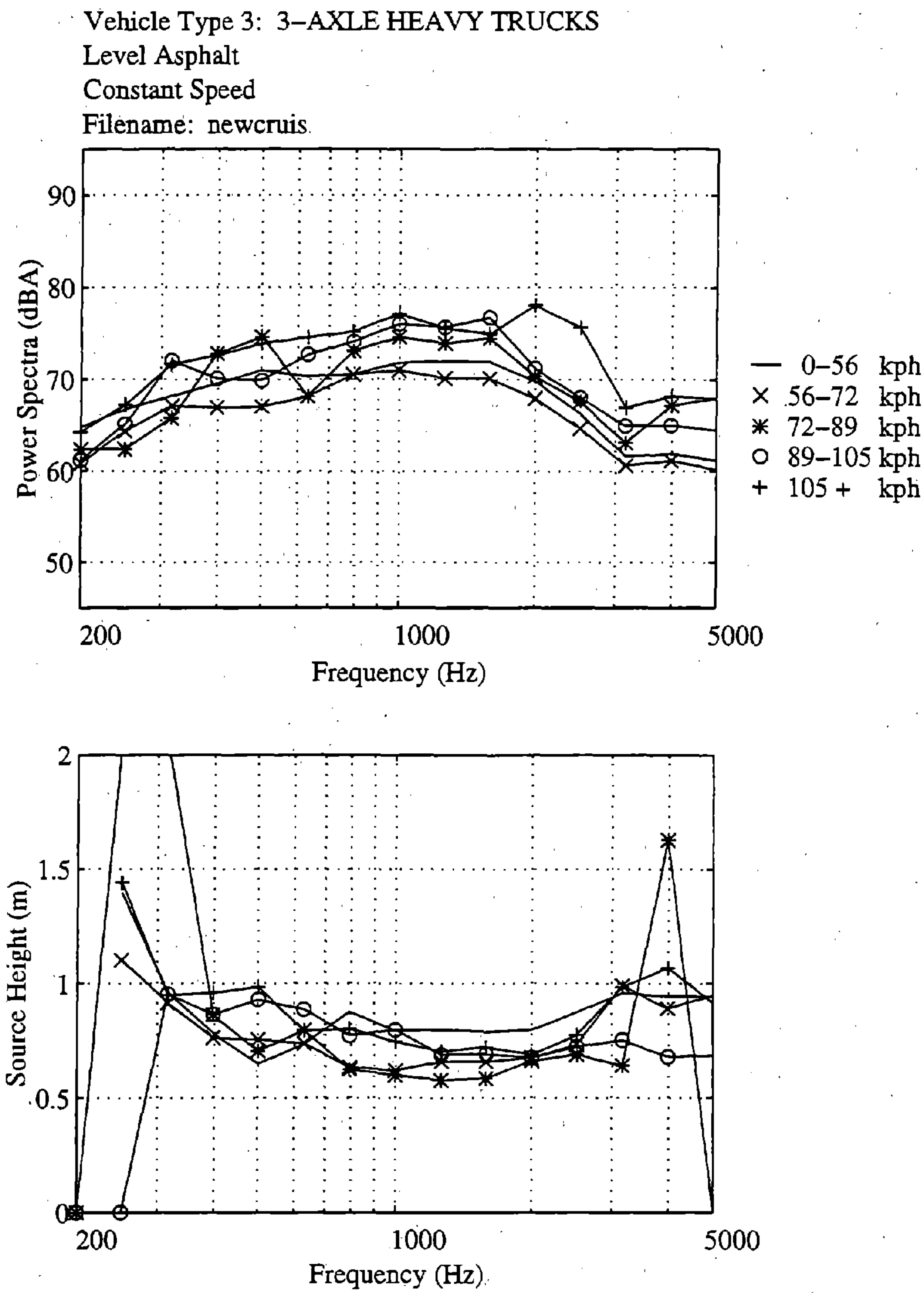

Figure 4.28: Averaged Spectra & Source Heights for Vehicle Type 4 Averaged over 6 Different Speed Bands Cruising on Level Asphalt Roadways. (Using the Highest Microphone Pair Criteria)

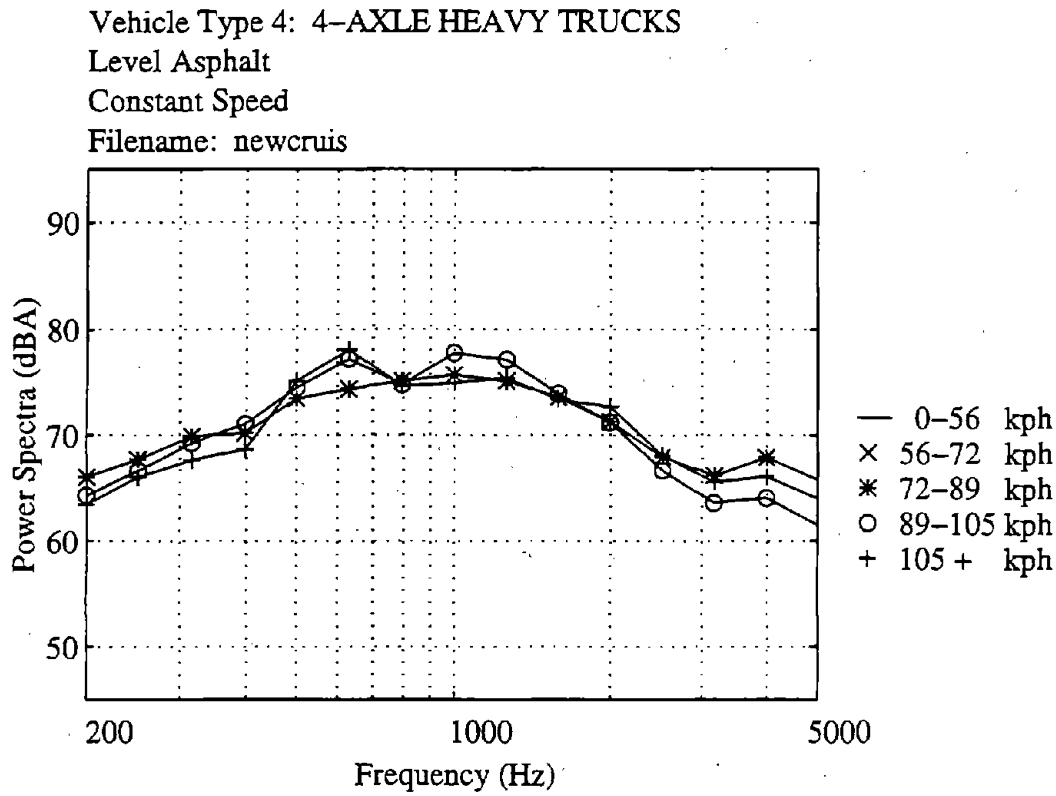

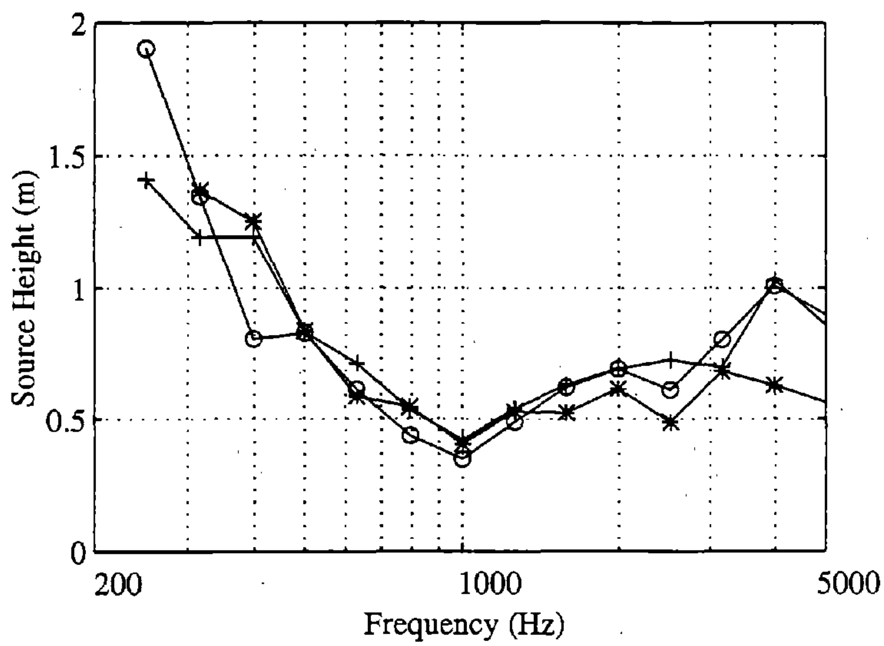

Figure 4.29: Averaged Spectra & Source Heights for Vehicle Type 5 Averaged over 6 Different Speed Bands Cruising on Level Asphalt Roadways. (Using the Highest Microphone Pair Criteria)

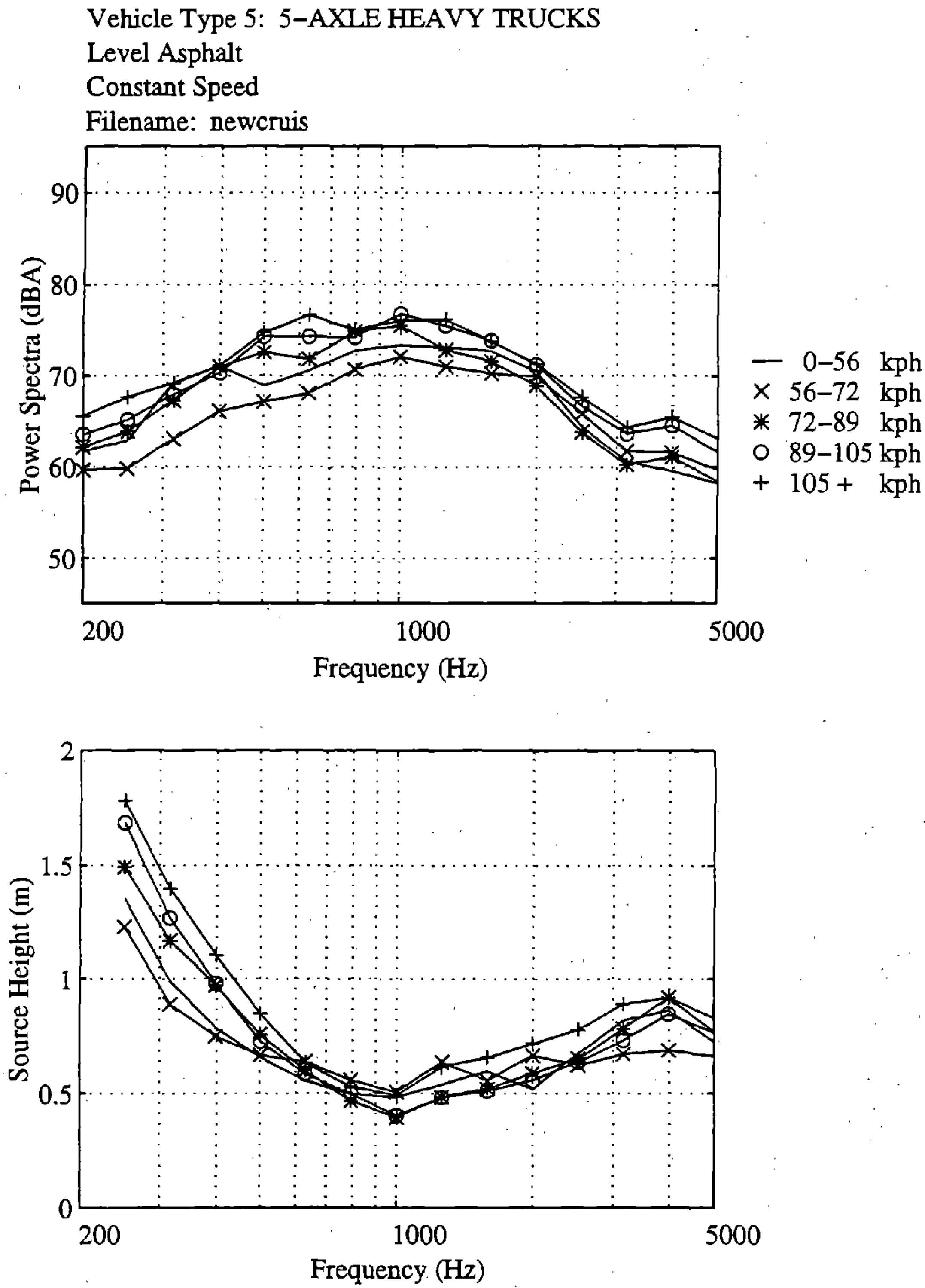

Figure 4.30: Averaged Spectra & Source Heights for Vehicle Type 8 Averaged over 6 Different Speed Bands Cruising on Level Asphalt Roadways. (Using the Highest Microphone Pair Criteria)

Vehicle Type 8: 2–AXLE BUSES
Level Asphalt
Constant Speed
Filename: newcruis

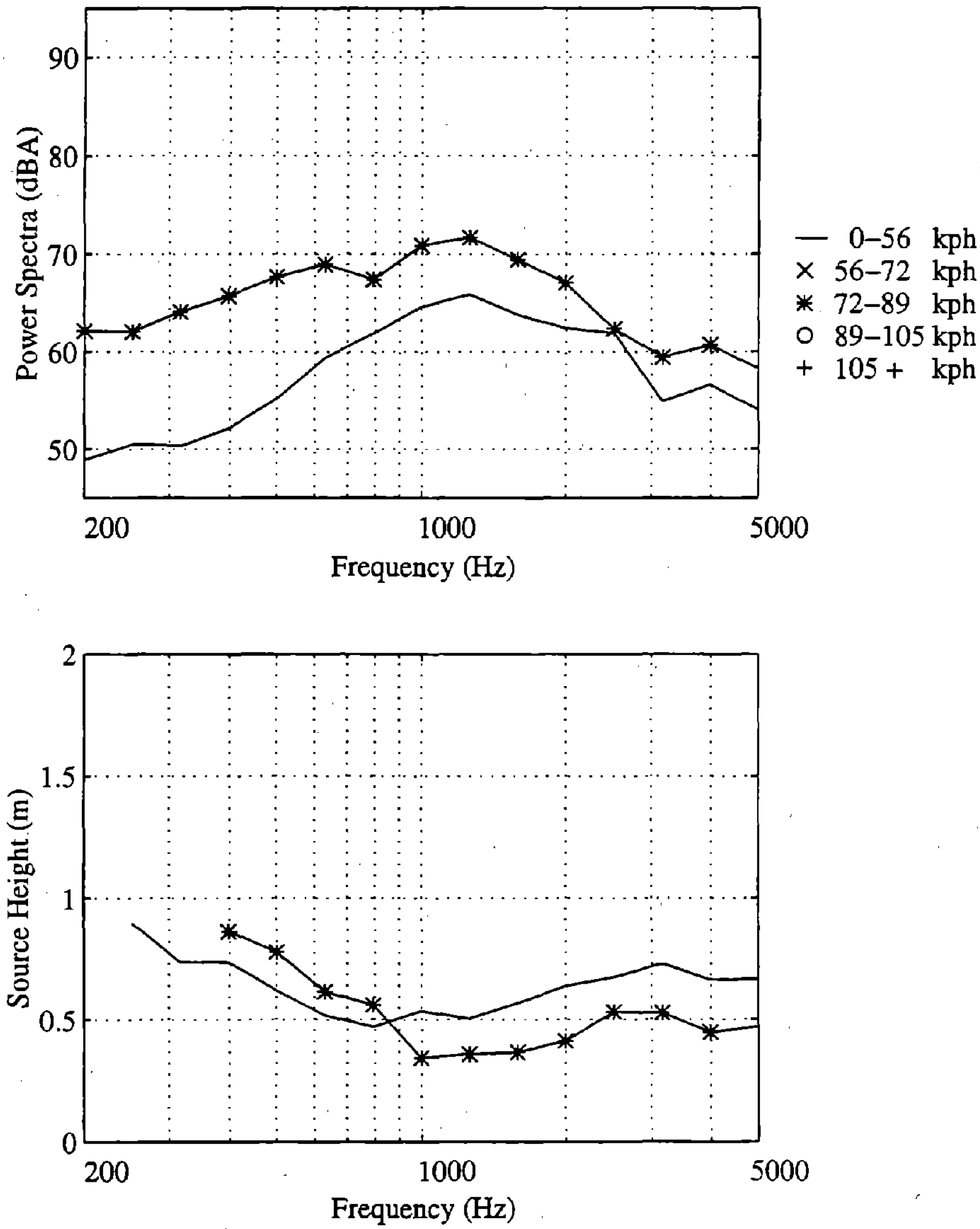

Figure 4.31: Averaged Spectra & Source Heights for Vehicle Types 0 to 4 Cruising on Level Concrete Roadways.
(Using the Highest Microphone Pair Criteria)

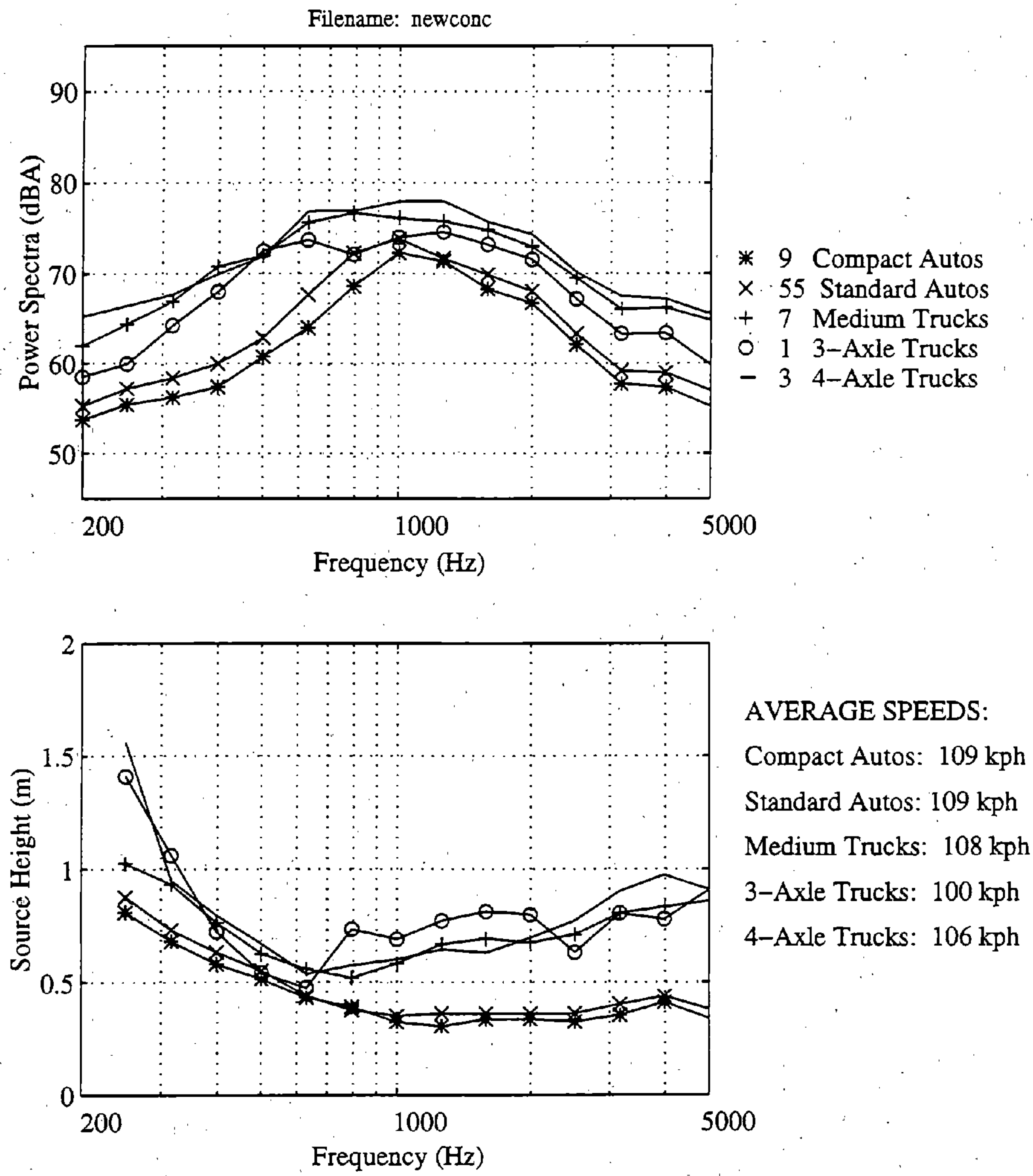

Figure 4.32: Averaged Spectra & Source Heights for Vehicle Types 5 & 6 Cruising on Level Concrete Roadways.
(Using the Highest Microphone Pair Criteria)

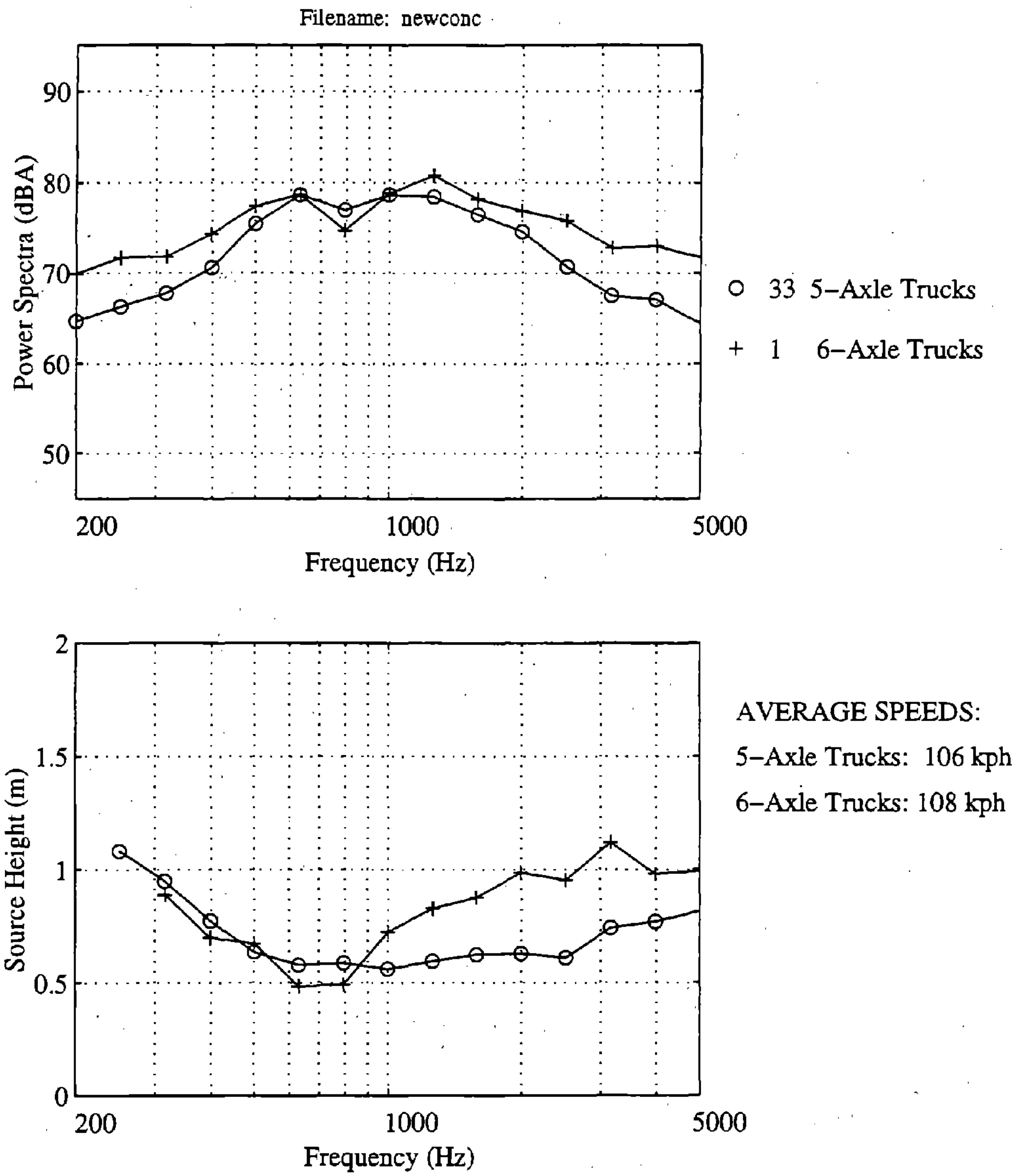

Figure 4.33: Averaged Spectra & Source Heights for Vehicle Types 0 to 4 Climbing on Graded Asphalt Roadways. (Using the Highest Microphone Pair Criteria)

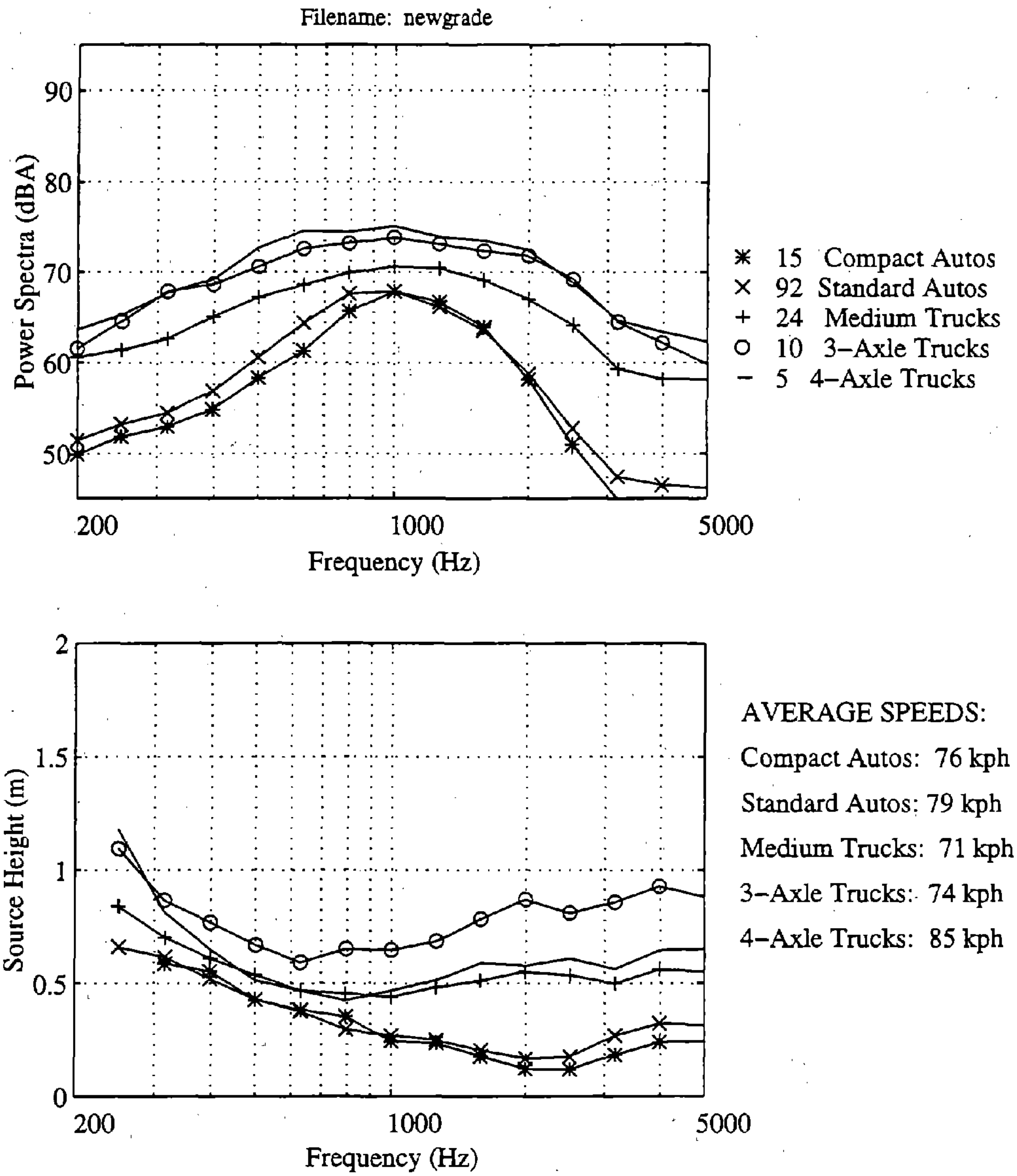

Figure 4.34: Averaged Spectra & Source Heights for Vehicle Types 5 to 9 Climbing on Graded Asphalt Roadways.
(Using the Highest Microphone Pair Criteria)

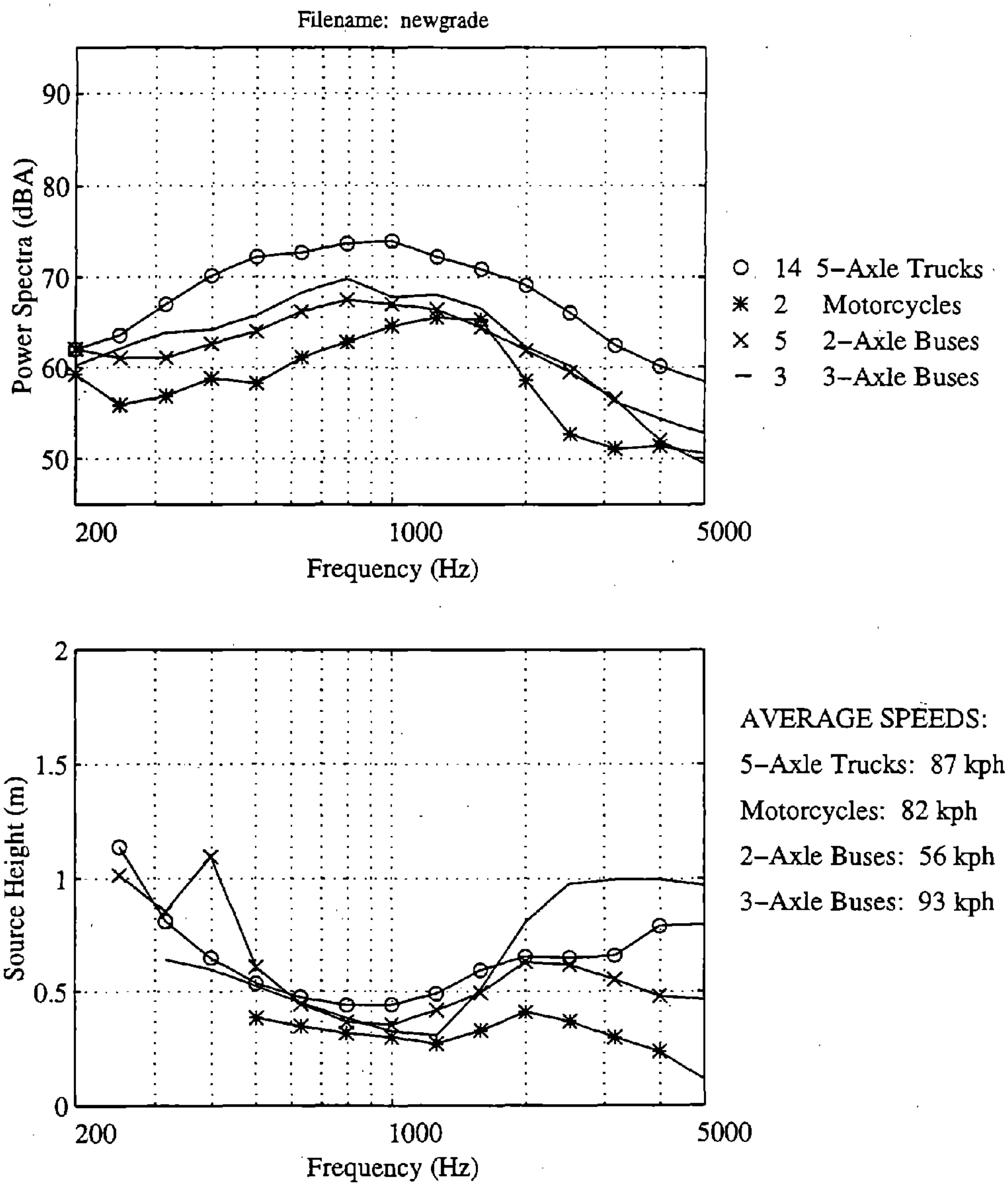

Figure 4.35: Comparison of Averaged Spectra & Source Heights for Standard Autos on Level Asphalt, Level Concrete and Graded Asphalt Roadways, for the 89-105 kph Speed Range. (Using the Highest Microphone Pair Criteria)

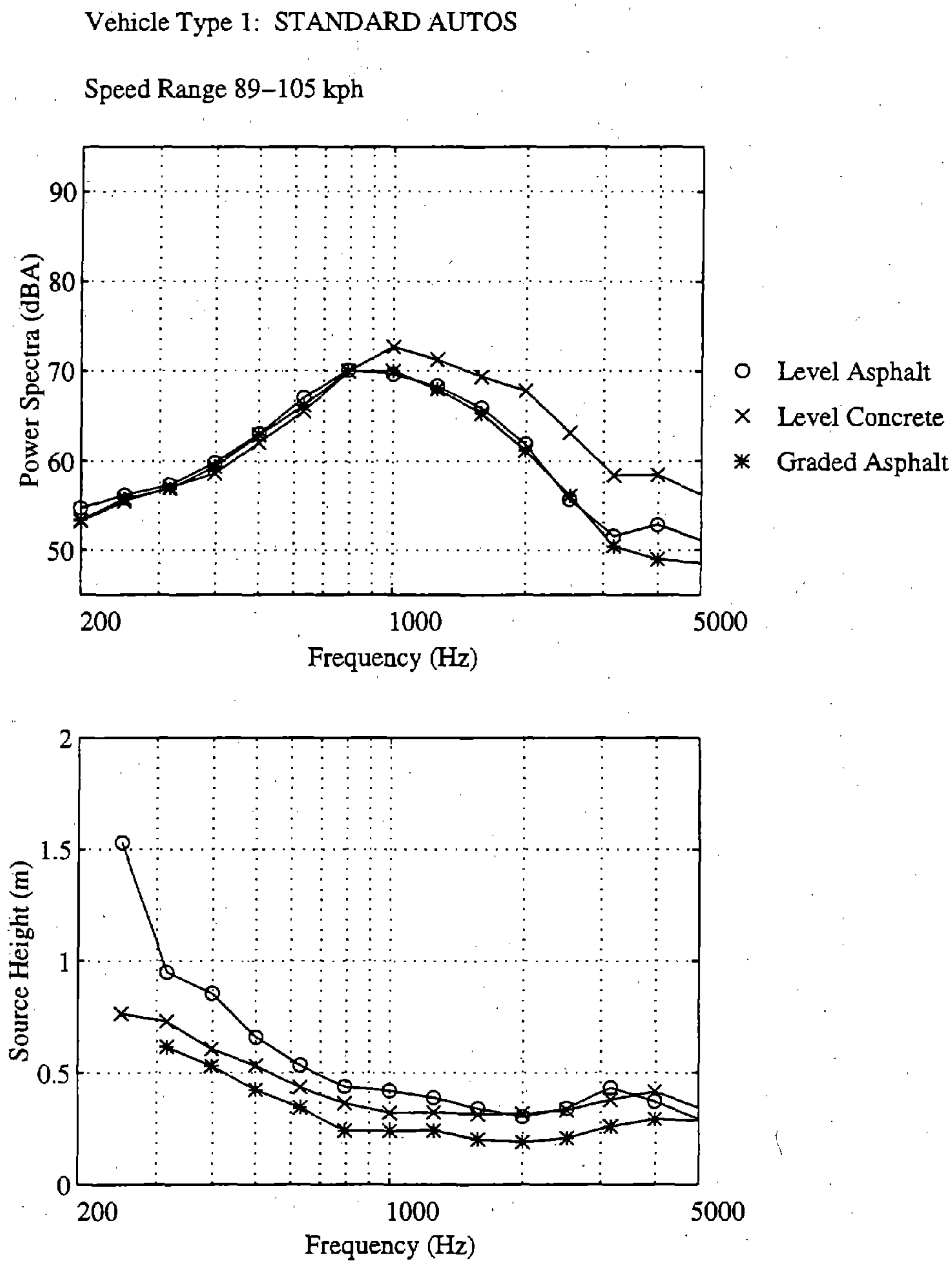

Figure 4.36: Comparison of Averaged Spectra & Source Heights for Medium Trucks on Level Asphalt, Level Concrete and Graded Asphalt Roadways, for the 89-105 kph Speed Range. (Using the Highest Microphone Pair Criteria)

Vehicle Type 2: MEDIUM TRUCKS

Speed Range 89–105 kph

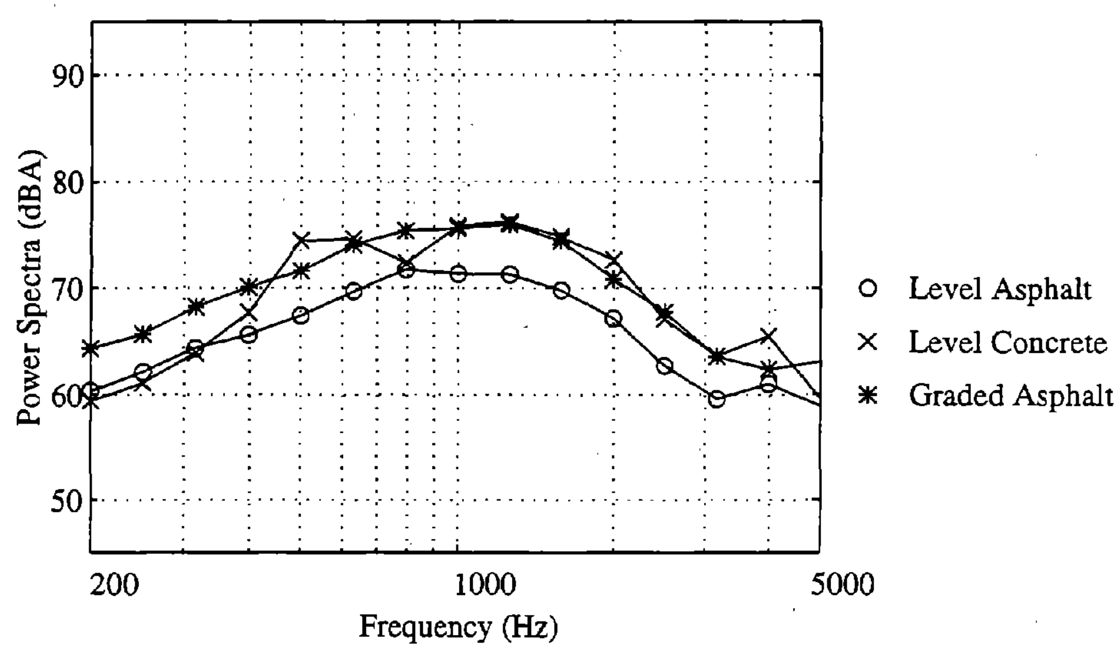

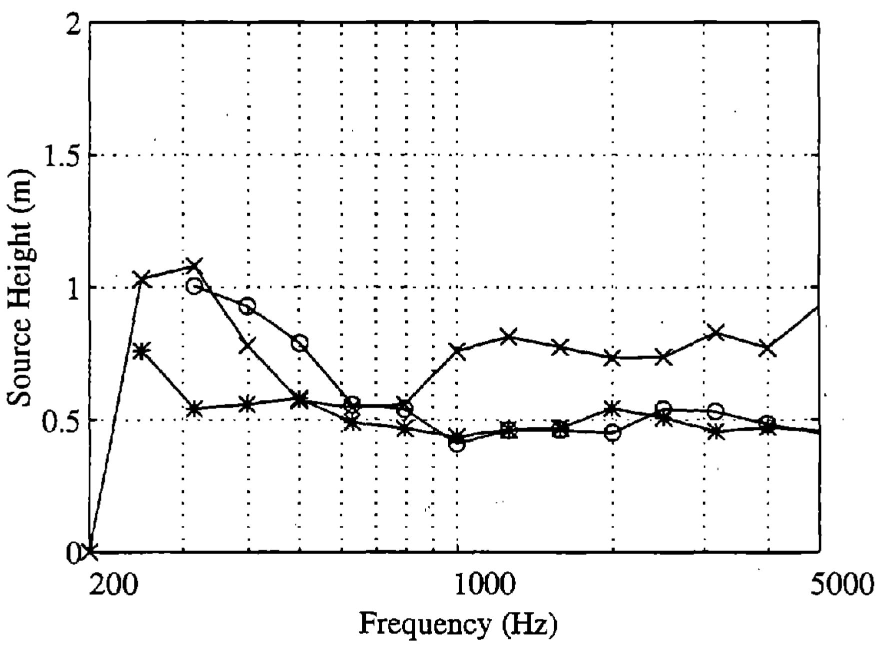

Figure 4.37: Comparison of Averaged Spectra & Source Heights for 5-Axle Heavy Trucks on Level Asphalt, Level Concrete and Graded Asphalt Roadways, for the 89-105 kph Speed Range. (Using the Highest Microphone Pair Criteria)

Vehicle Type 5: 5–AXLE HEAVY TRUCKS

Speed Range 89–105 kph

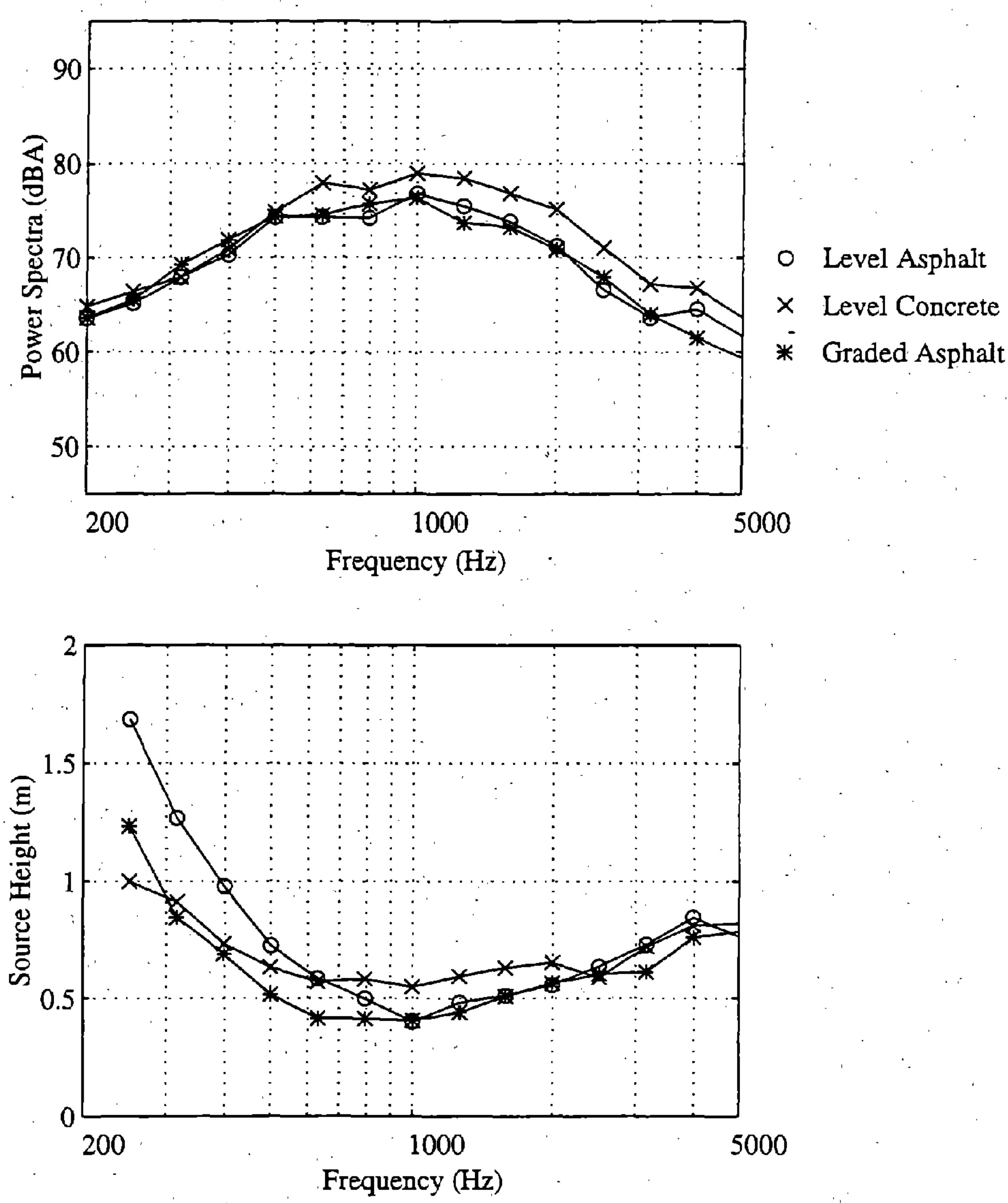

Figure 4.38: Averaged Spectra & Source Heights for Accelerating Vehicle Types 0 to 4 Measured at a point 30.5 m from a Stationary Start. (Using the Highest Microphone Pair Criteria)

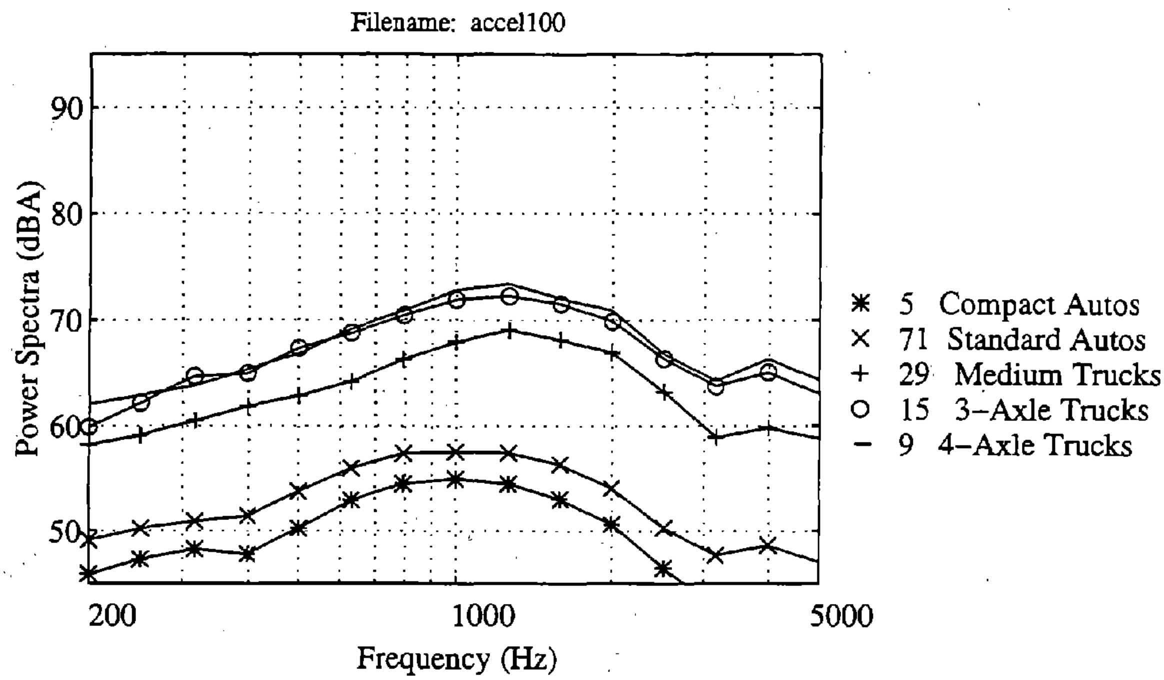

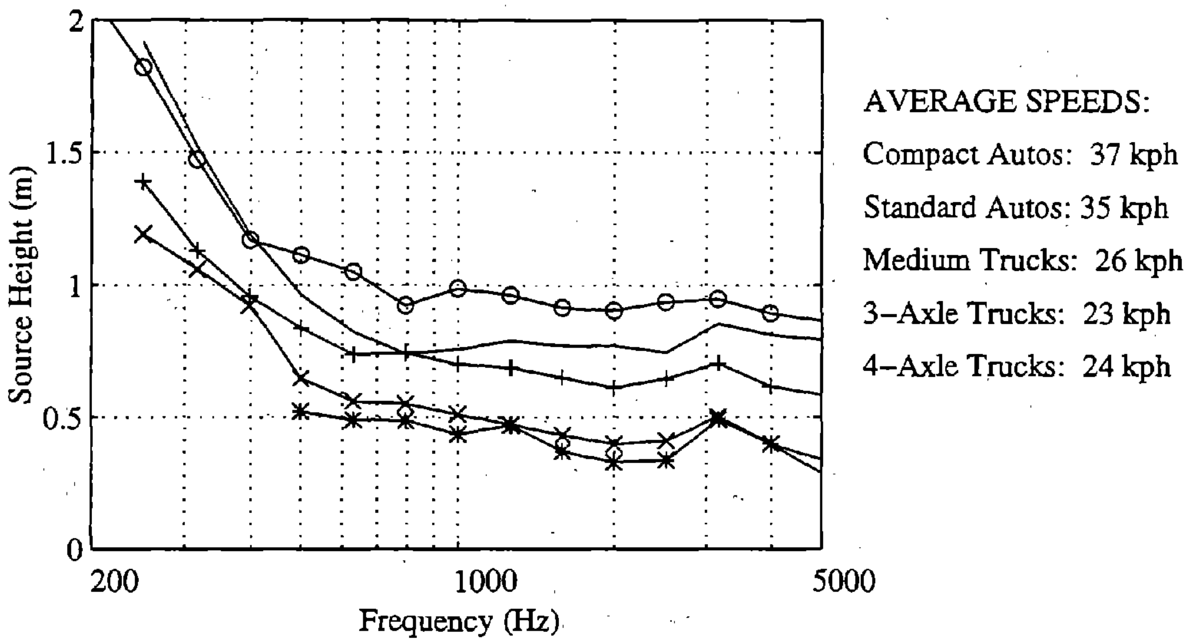

Figure 4.39: Averaged Spectra & Source Heights for Accelerating Vehicle Types 5 to 9 Measured at a point 30.5 m from a Stationary Start. (Using the Highest Microphone Pair Criteria)

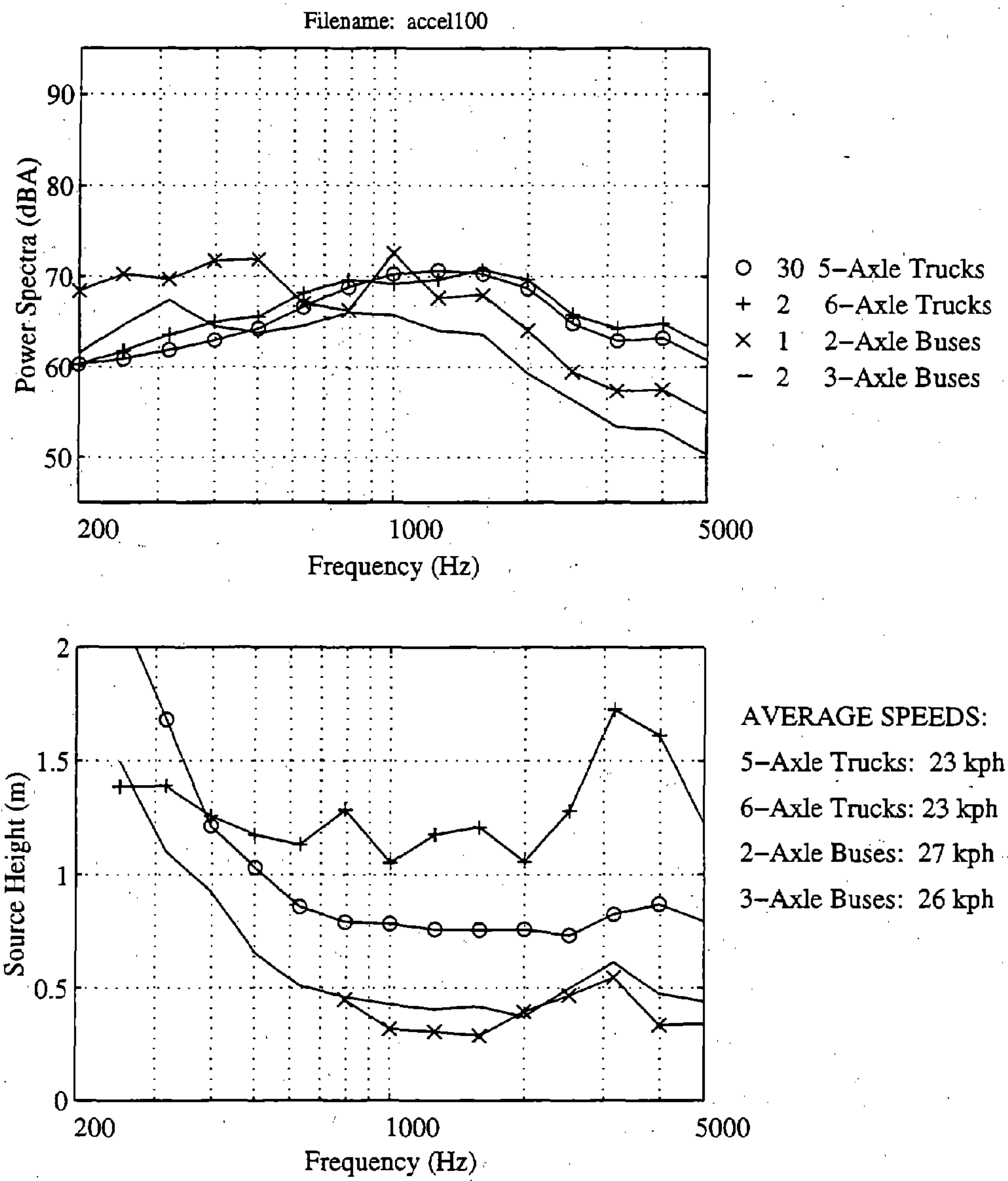

Figure 4.40: Averaged Spectra & Source Heights for Accelerating Vehicle Types 0 to 4 Measured at a point 45.7 m from a Stationary Start. (Using the Highest Microphone Pair Criteria)

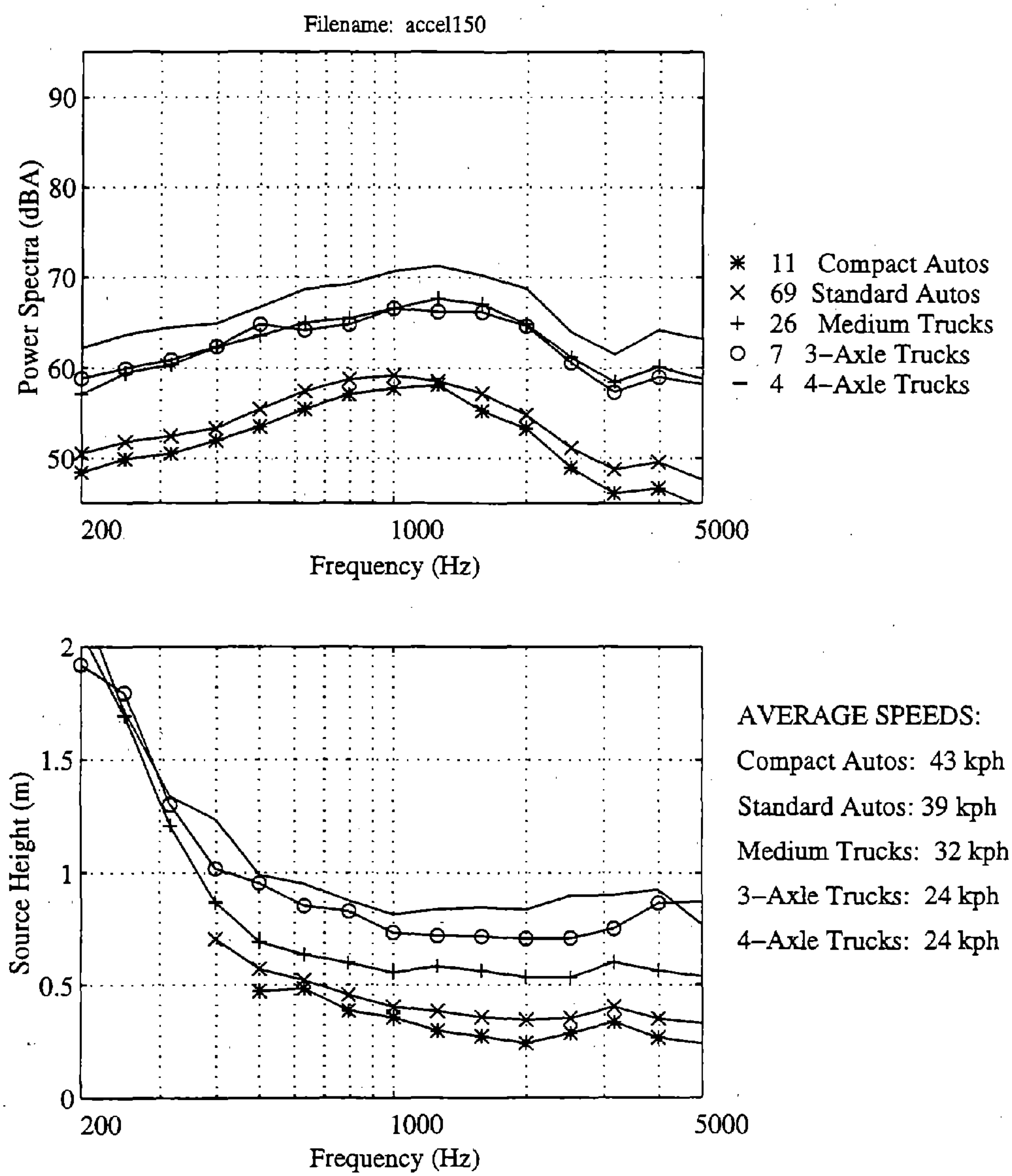

Figure 4.41: Averaged Spectra & Source Heights for Accelerating Vehicle Types 5 to 9 Measured at a point 45.7 m from a Stationary Start. (Using the Highest Microphone Pair Criteria)

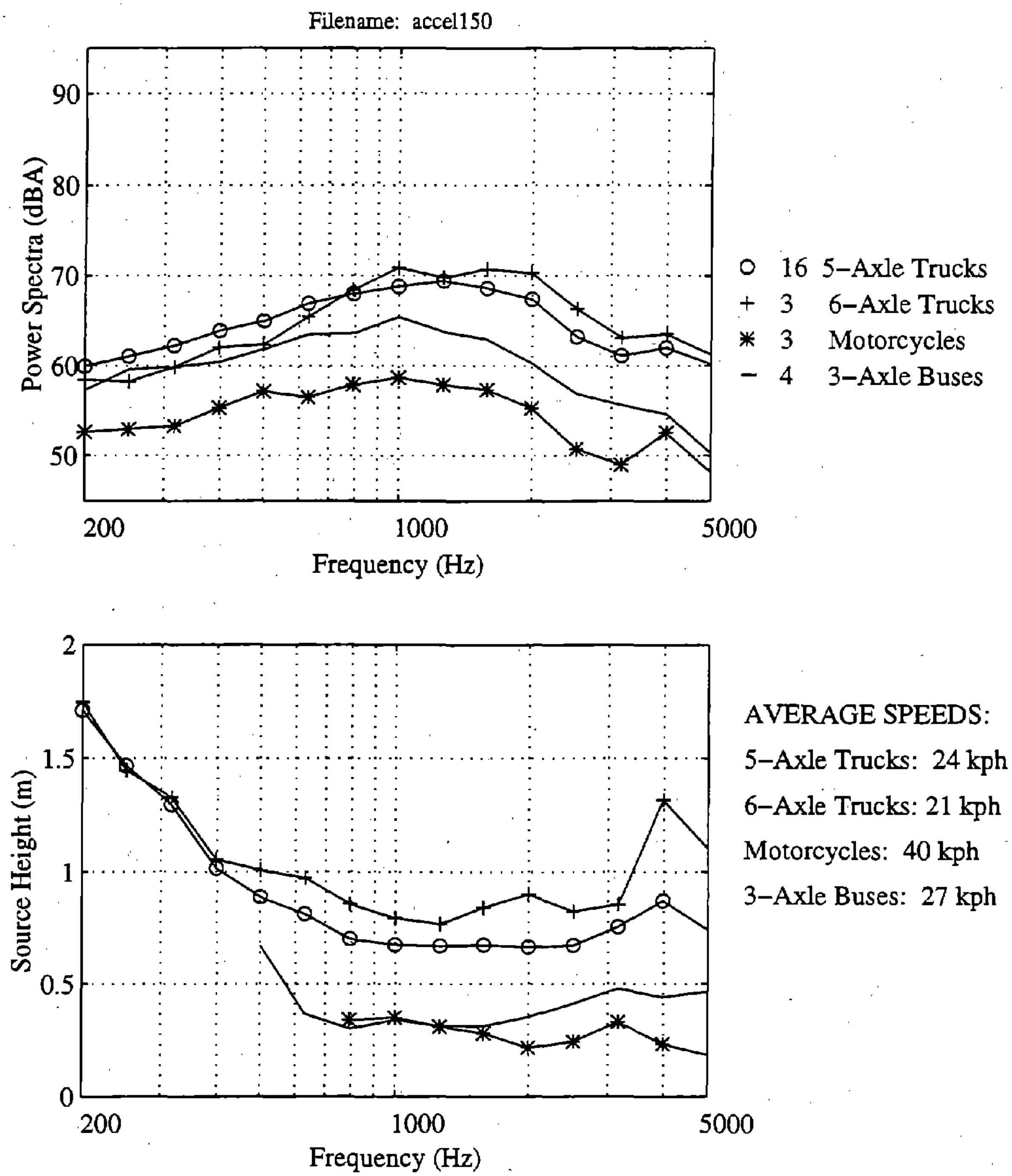

Figure 4.42: Averaged Spectra & Source Heights for Accelerating Vehicle Types 0 to 4 Measured at a point 61.0 m from a Stationary Start. (Using the Highest Microphone Pair Criteria)

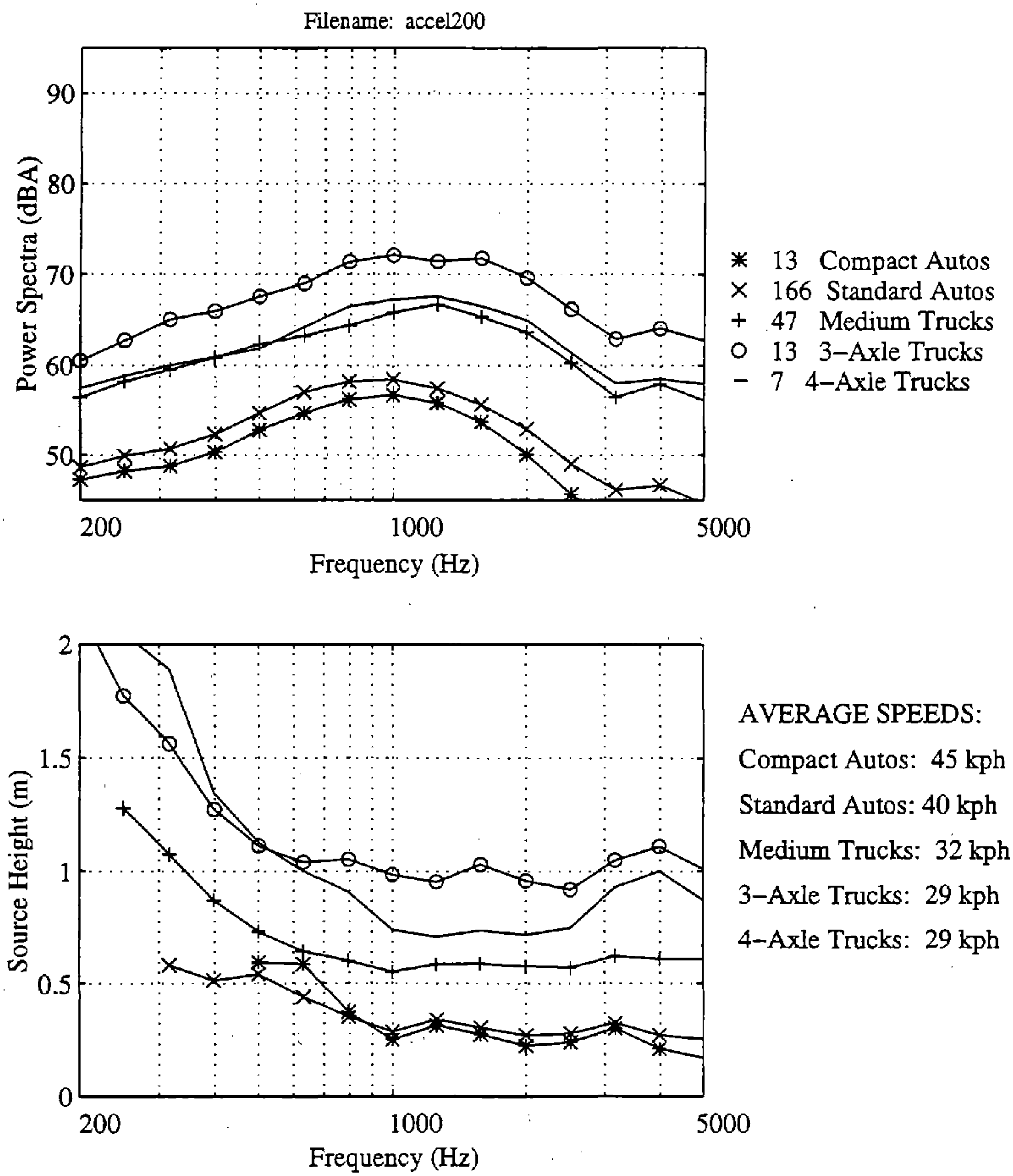

Figure 4.43: Averaged Spectra & Source Heights for Accelerating Vehicle Types 5 to 9 Measured at a point 61.0 m from a Stationary Start. (Using the Highest Microphone Pair Criteria)

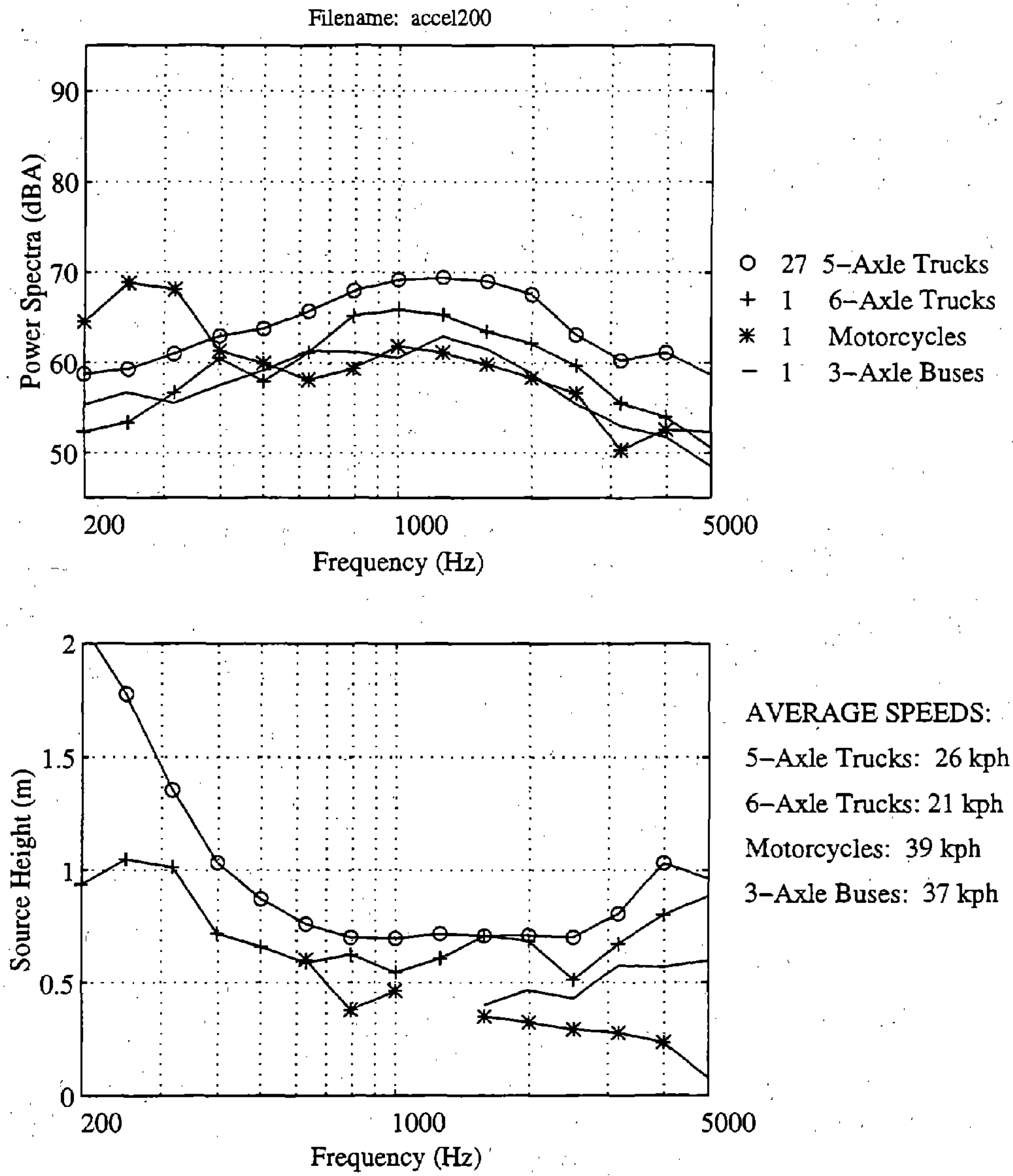

Figure 4.44: Spectra & Source Height Comparison for Accelerating Standard Autos at Three Different Ranges from a Stationary Start. (Using the Highest Microphone Pair Criteria)

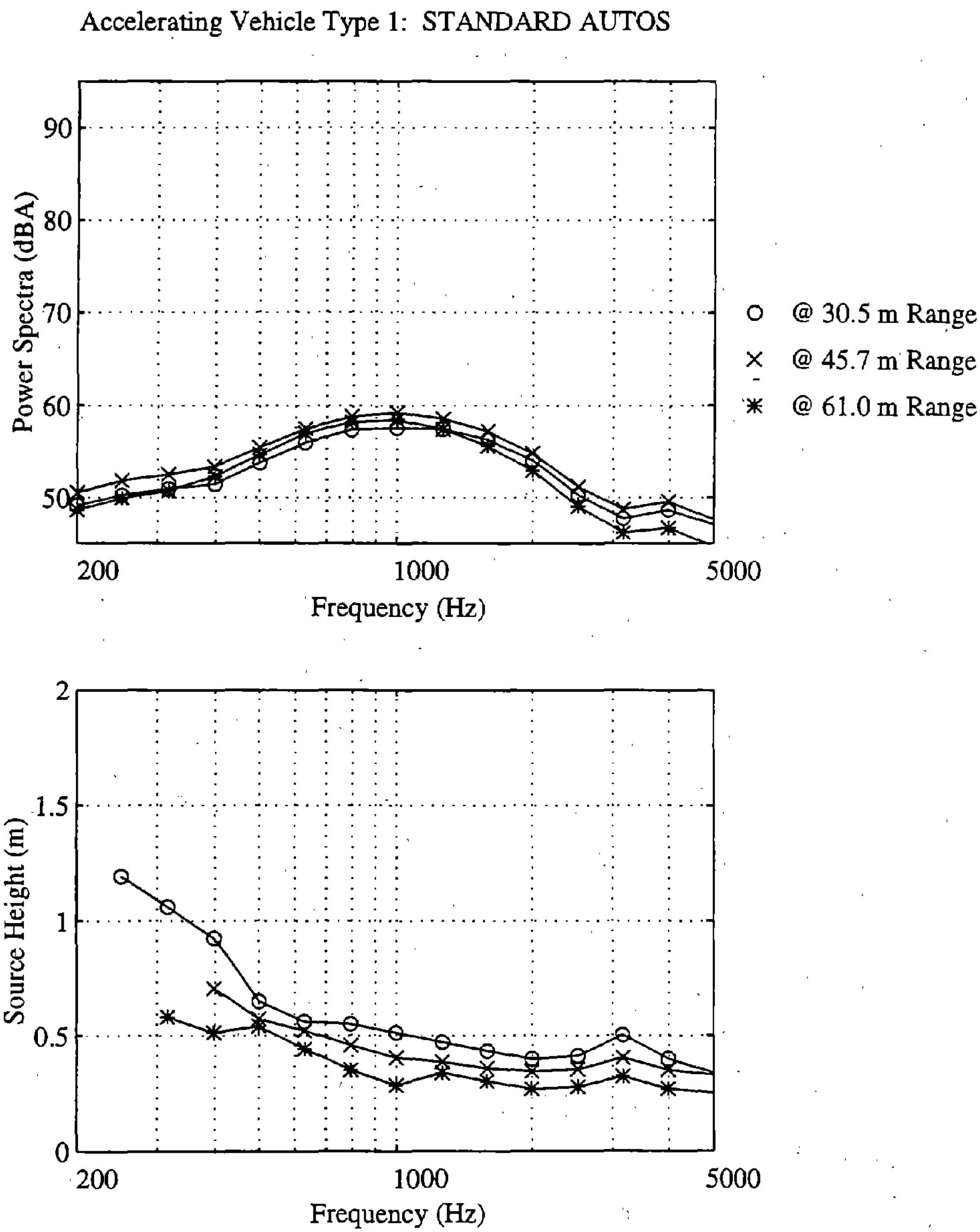

Figure 4.45: Spectra & Source Height Comparison for Accelerating Medium Trucks at Three Different Ranges from a Stationary Start. (Using the Highest Microphone Pair Criteria)

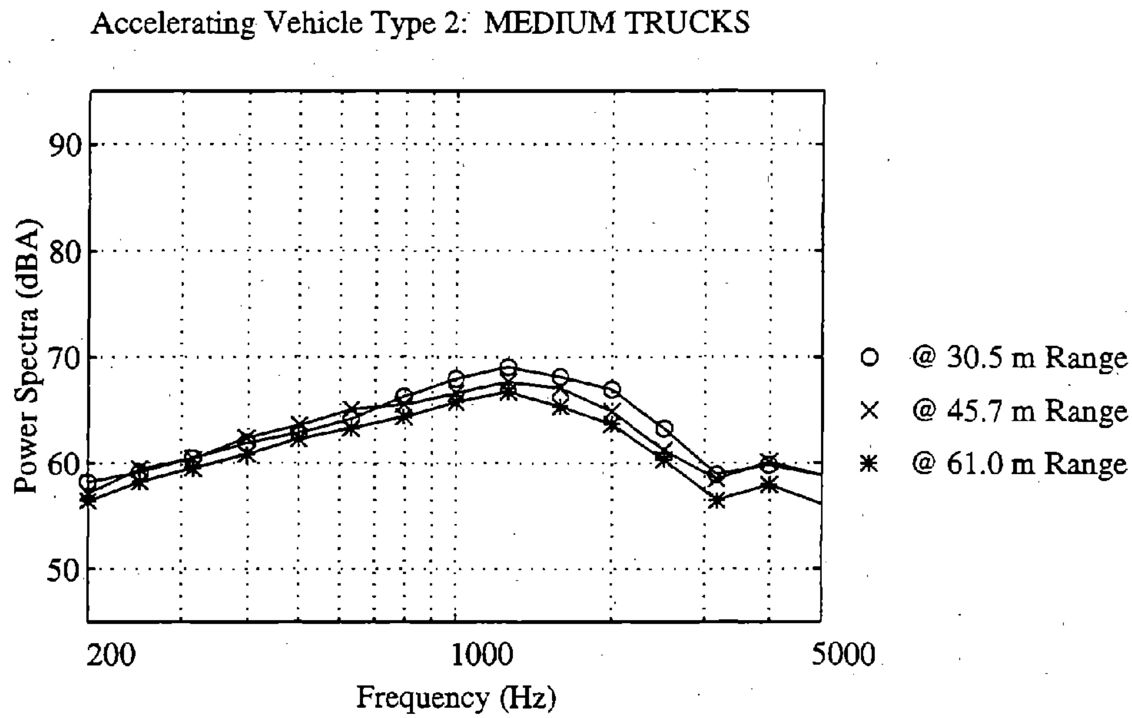

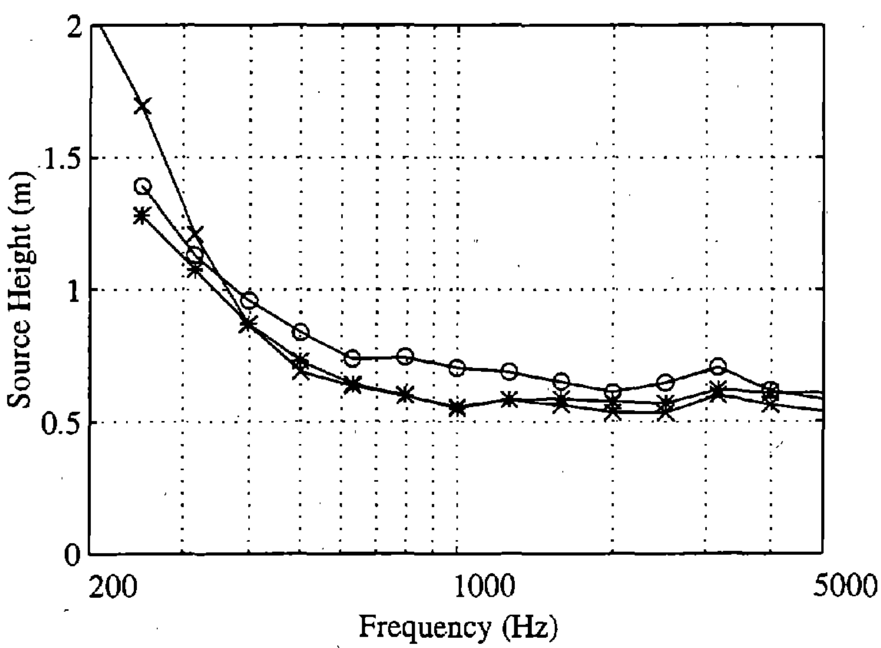

Figure 4.46: Spectra & Source Height Comparison for Accelerating 5-Axle Heavy Trucks at Three Different Ranges from a Stationary Start. (Using the Highest Microphone Pair Criteria)

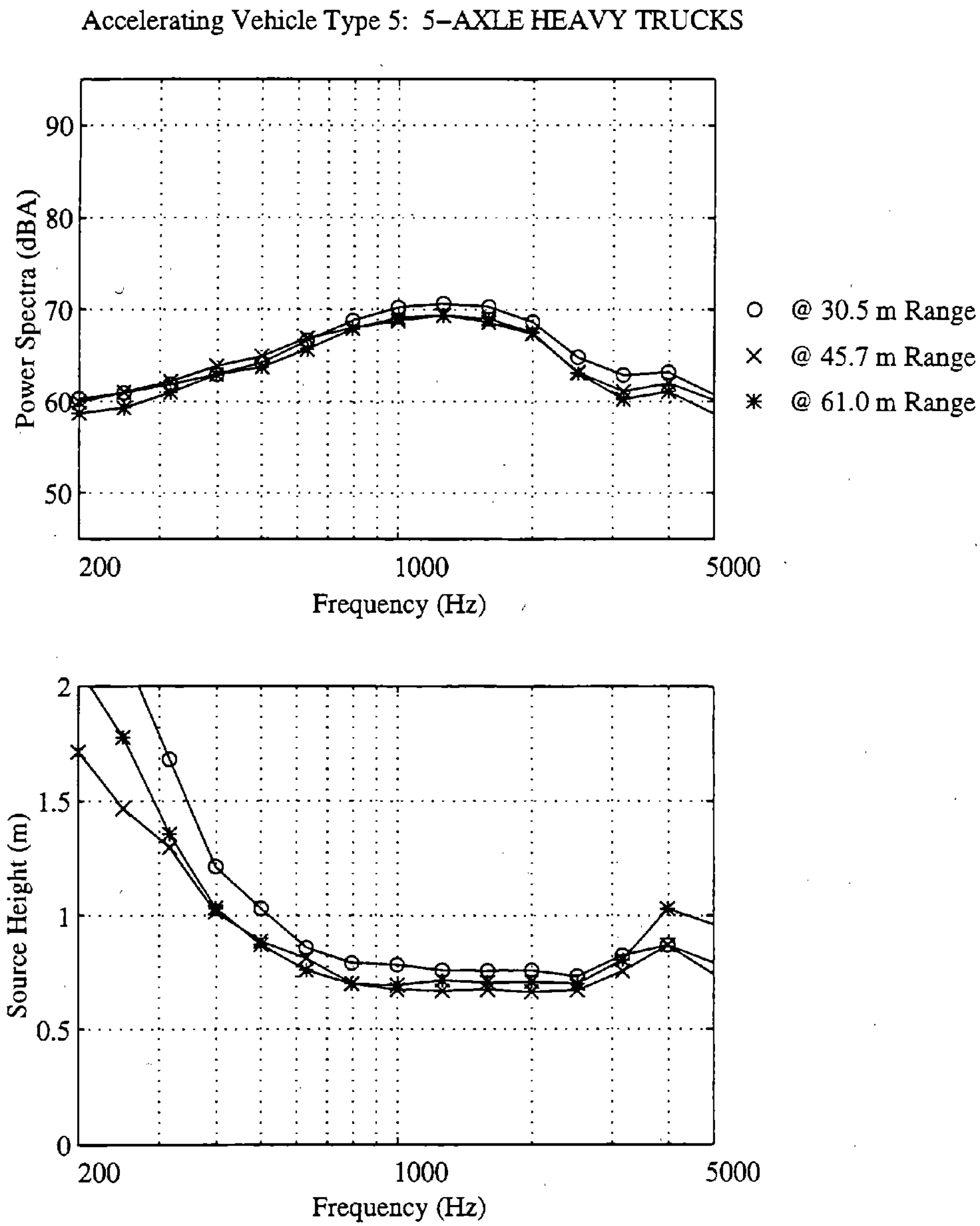

Figure 4.47: Comparison Between Cruising and Accelerating Vehicle Spectra & Source Heights for Vehicle Types 1,2 &5 in the 0-56 kph Speed Band. (Using the Highest Microphone Pair Criteria)

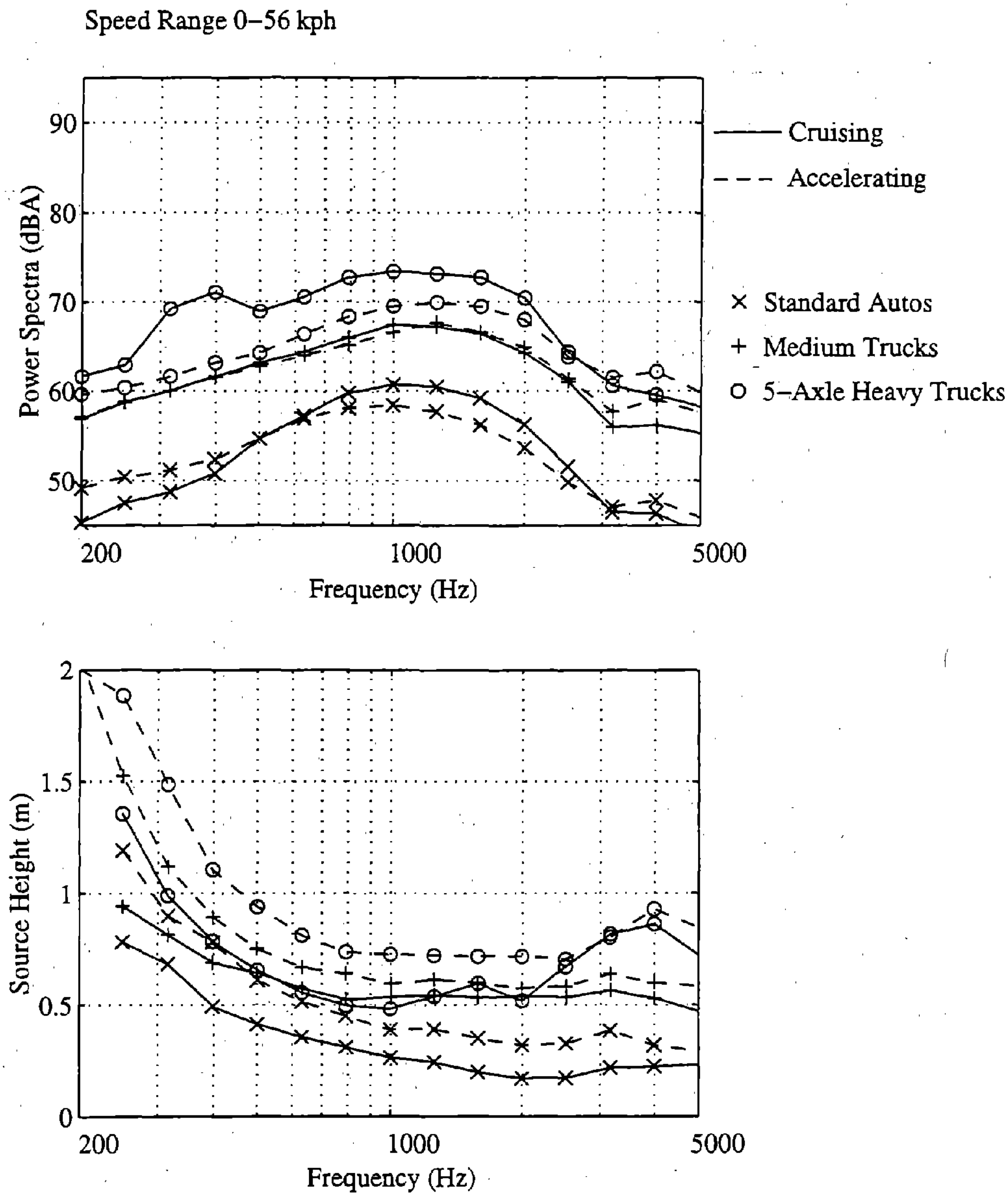

Figure 4.48: Average Sub-Source Spectra & Sub-Source Strength Ratio for Standard Autos Cruising on Level Asphalt Roadways.
(Using the Highest Microphone Pair Criteria)

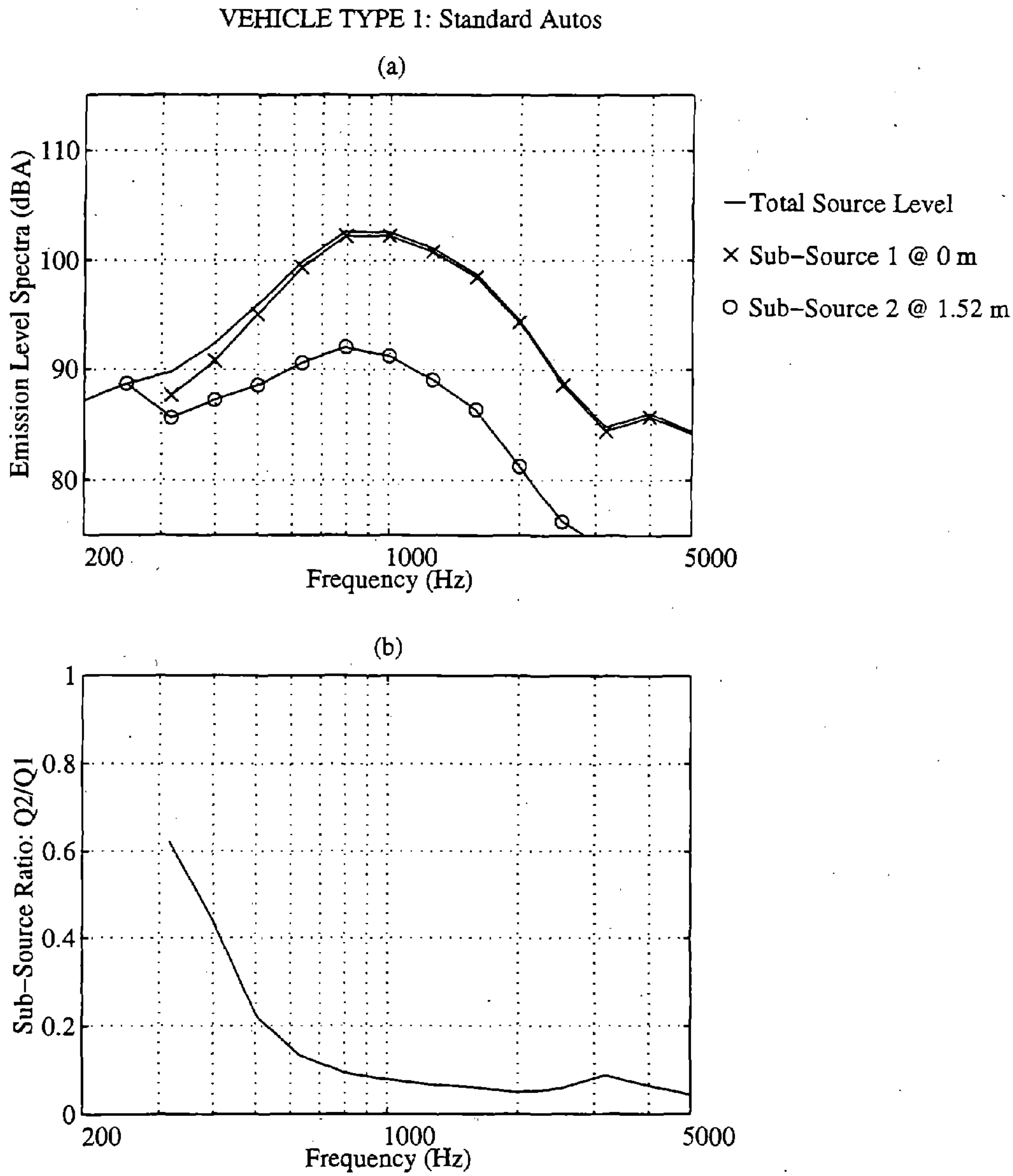

Figure 4.49: Average Sub-Source Spectra & Sub-Source Strength Ratio for Medium Trucks Cruising on Level Asphalt Roadways. (Using the Highest Microphone Pair Criteria)

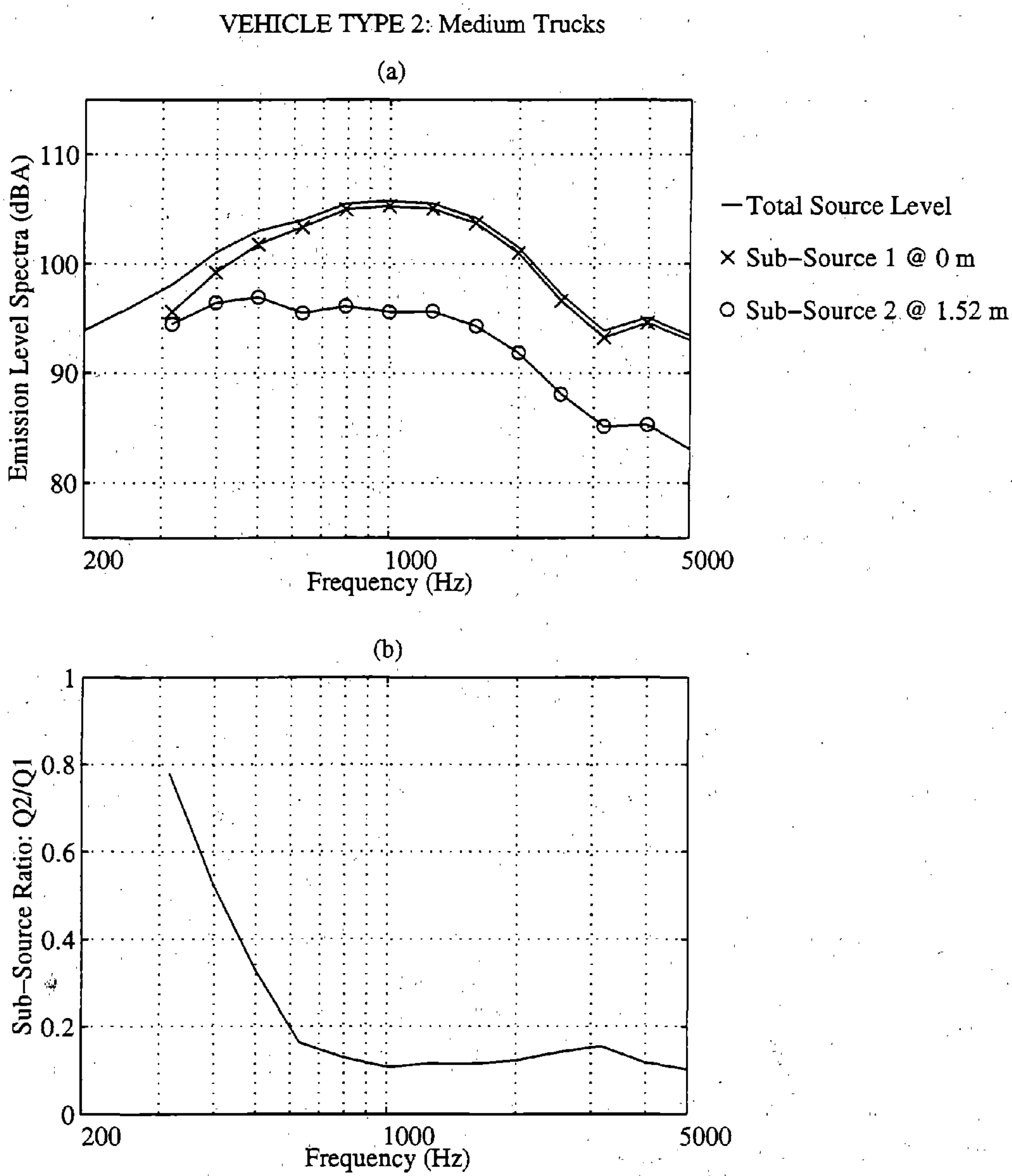

Figure 4.50: Average Sub-Source Spectra & Sub-Source Strength Ratio for 5-Axle Heavy Trucks Cruising on Level Asphalt Roadways. (Using the Highest Microphone Pair Criteria)

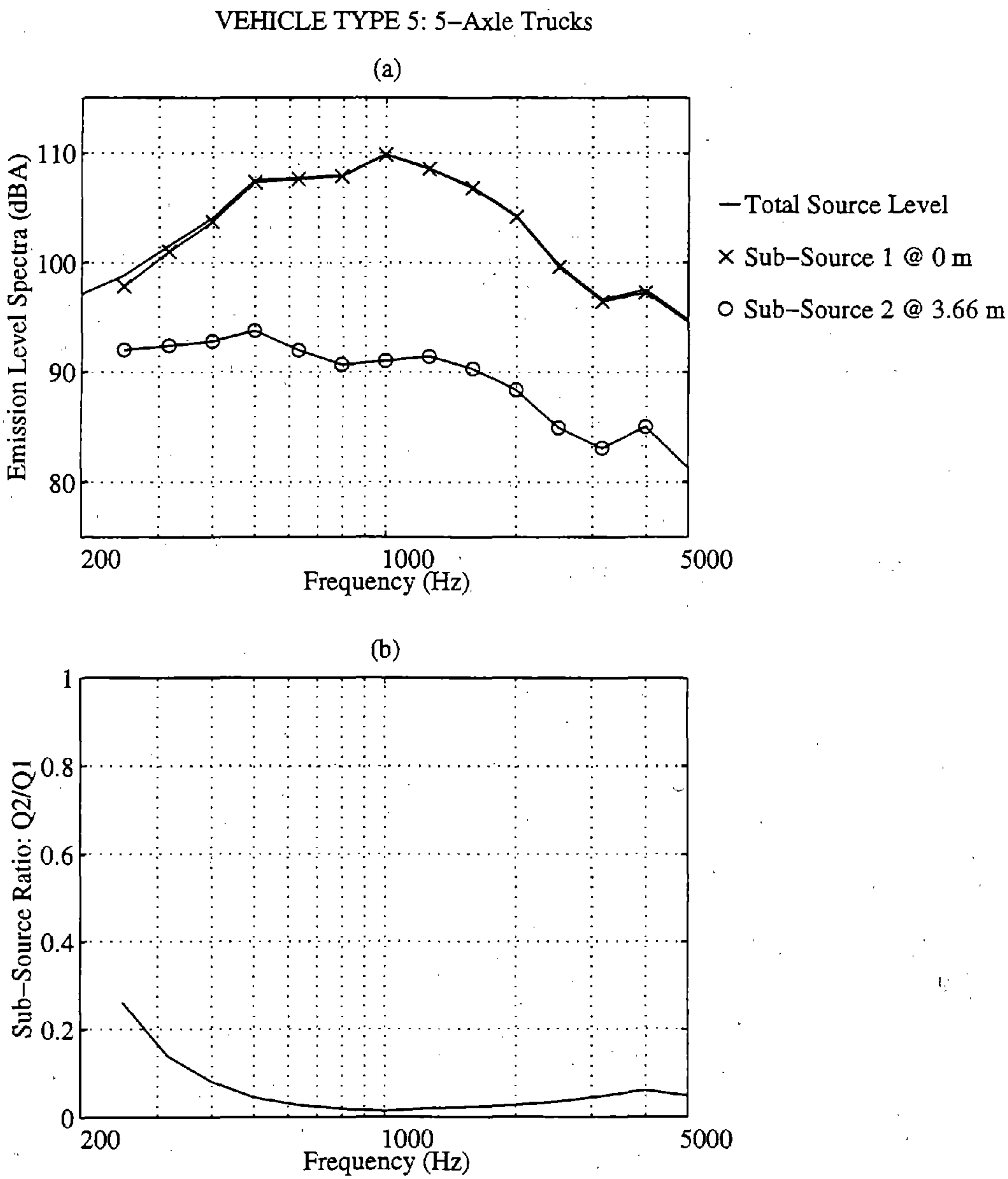

Figure 4.51: Overall Average Spectra & Source Heights for Vehicle Types 0 to 4. Cruising, Accelerating, Asphalt, Concrete, Level and Graded Roadways Combined. (Using the Highest Microphone Pair Criteria)

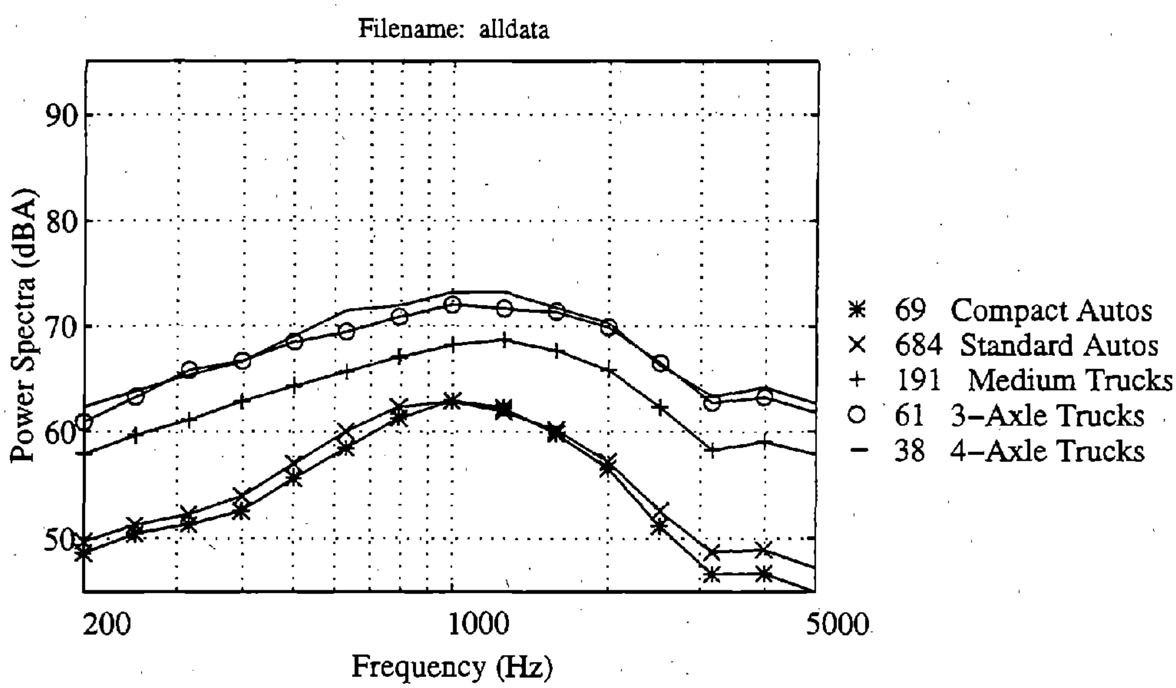

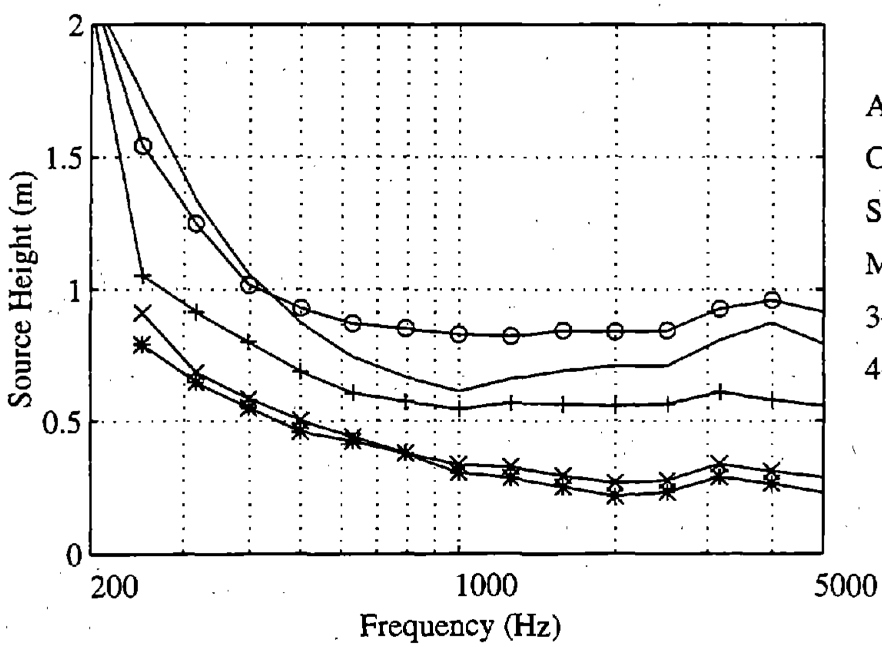

AVERAGE SPEEDS:

Compact Autos: 66 kph

Standard Autos: 60 kph

Medium Trucks: 50 kph

3-Axle Trucks: 47 kph

4-Axle Trucks: 60 kph

Figure 4.52: Overall Average Spectra & Source Heights for Vehicle Types 5 to 9.
Cruising, Accelerating, Asphalt, Concrete, Level and Graded Roadways Combined.
(Using the Highest Microphone Pair Criteria)

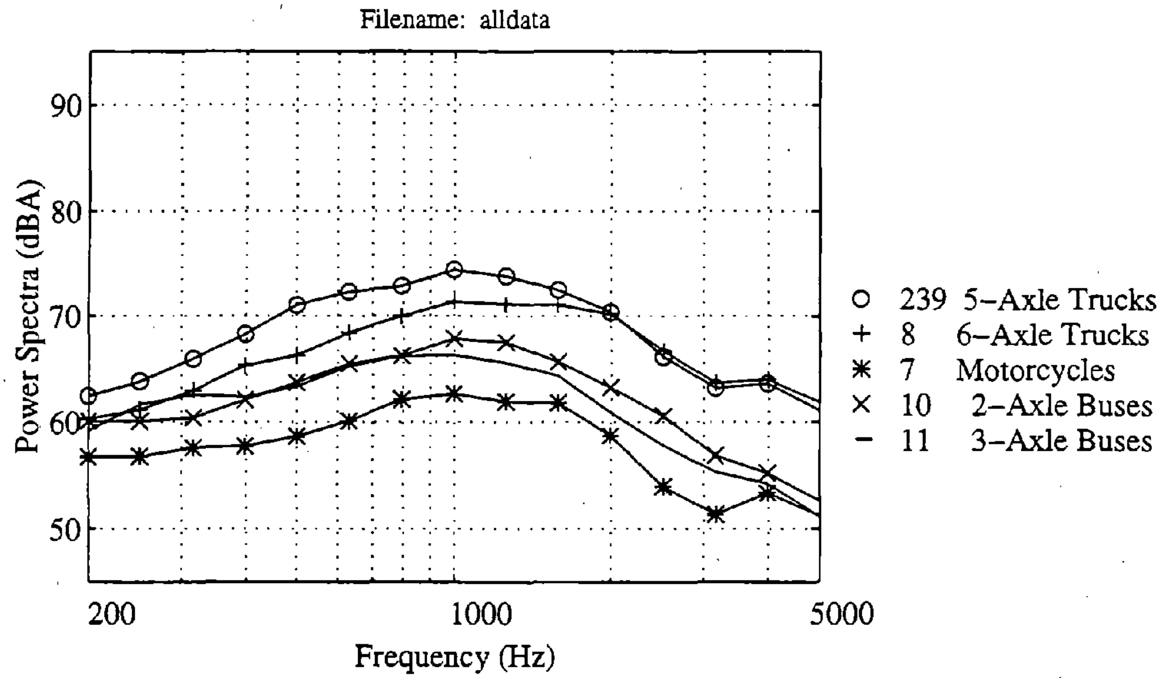

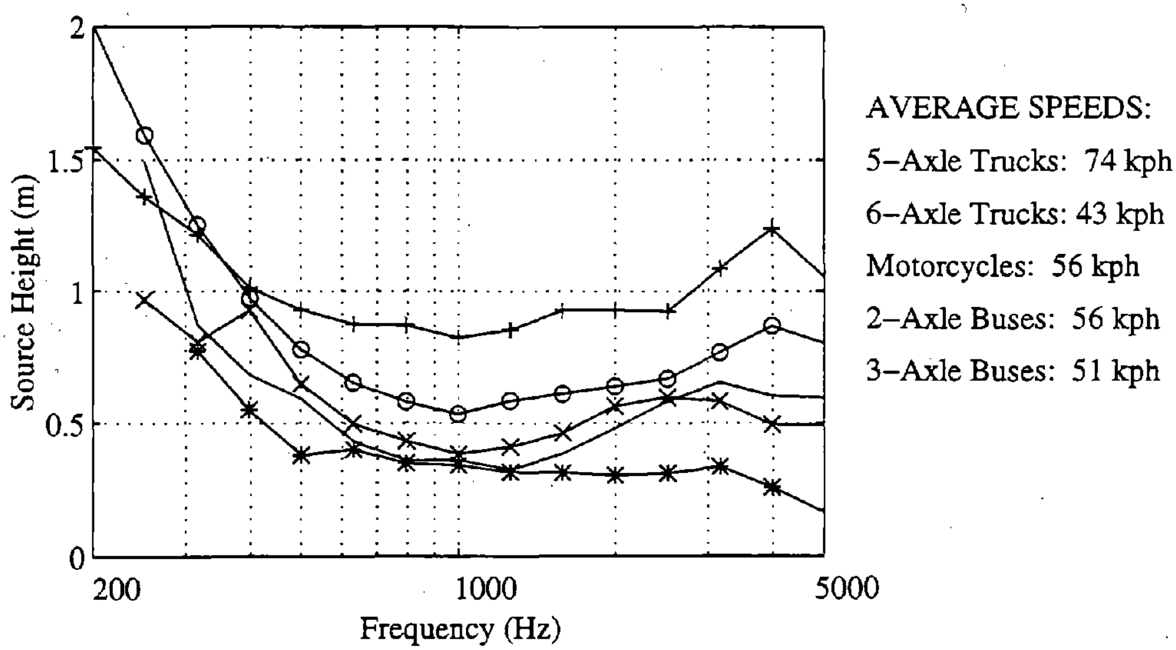

Figure 5.1: Comparison of the Source Heights Obtained for a Standard Auto with the Turn-key System & the Matched Field Processor.

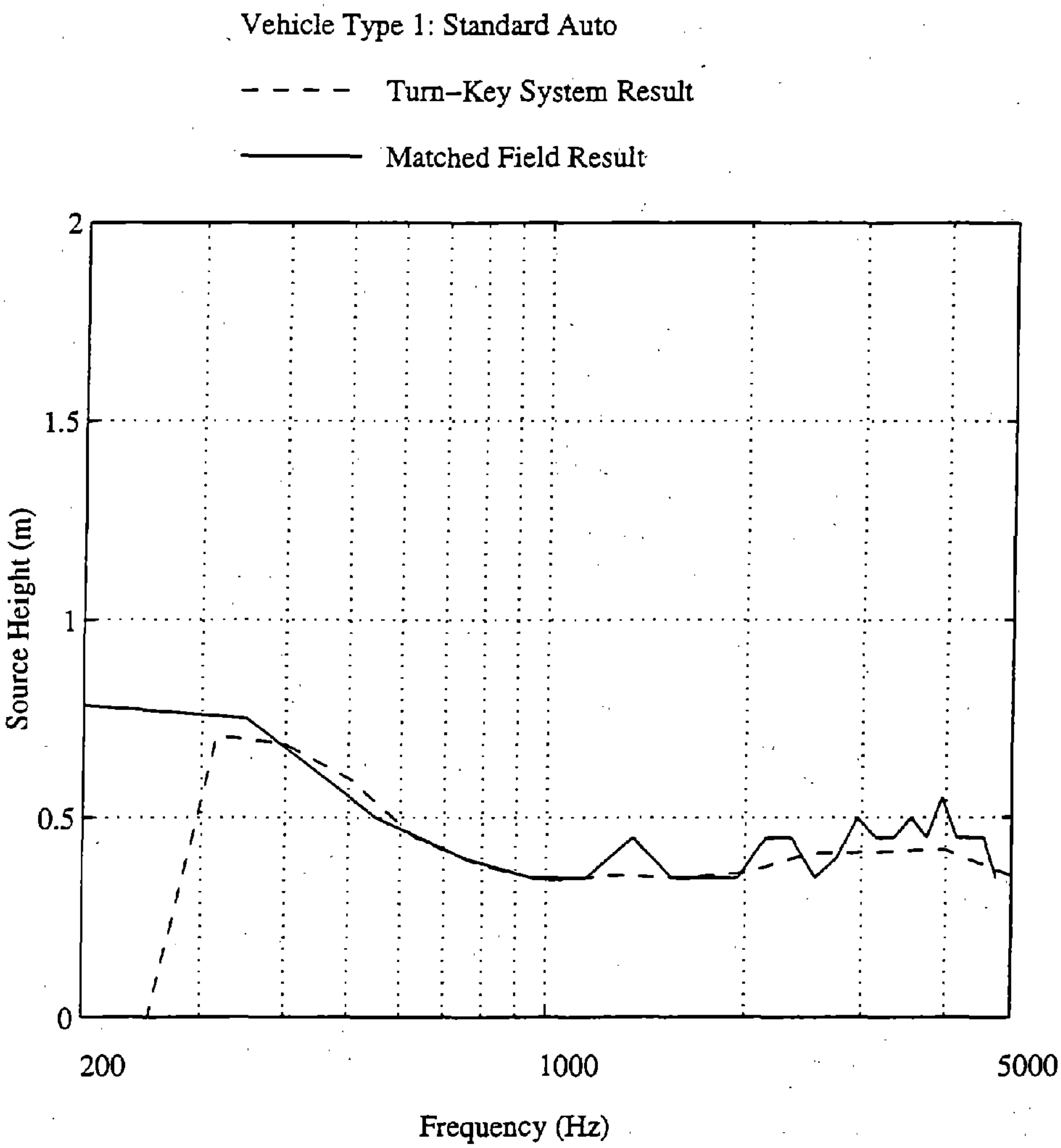

Figure 5.2: Comparison of the Source Heights Obtained for a Medium Truck with the Turn-key System & the Matched Field Processor.

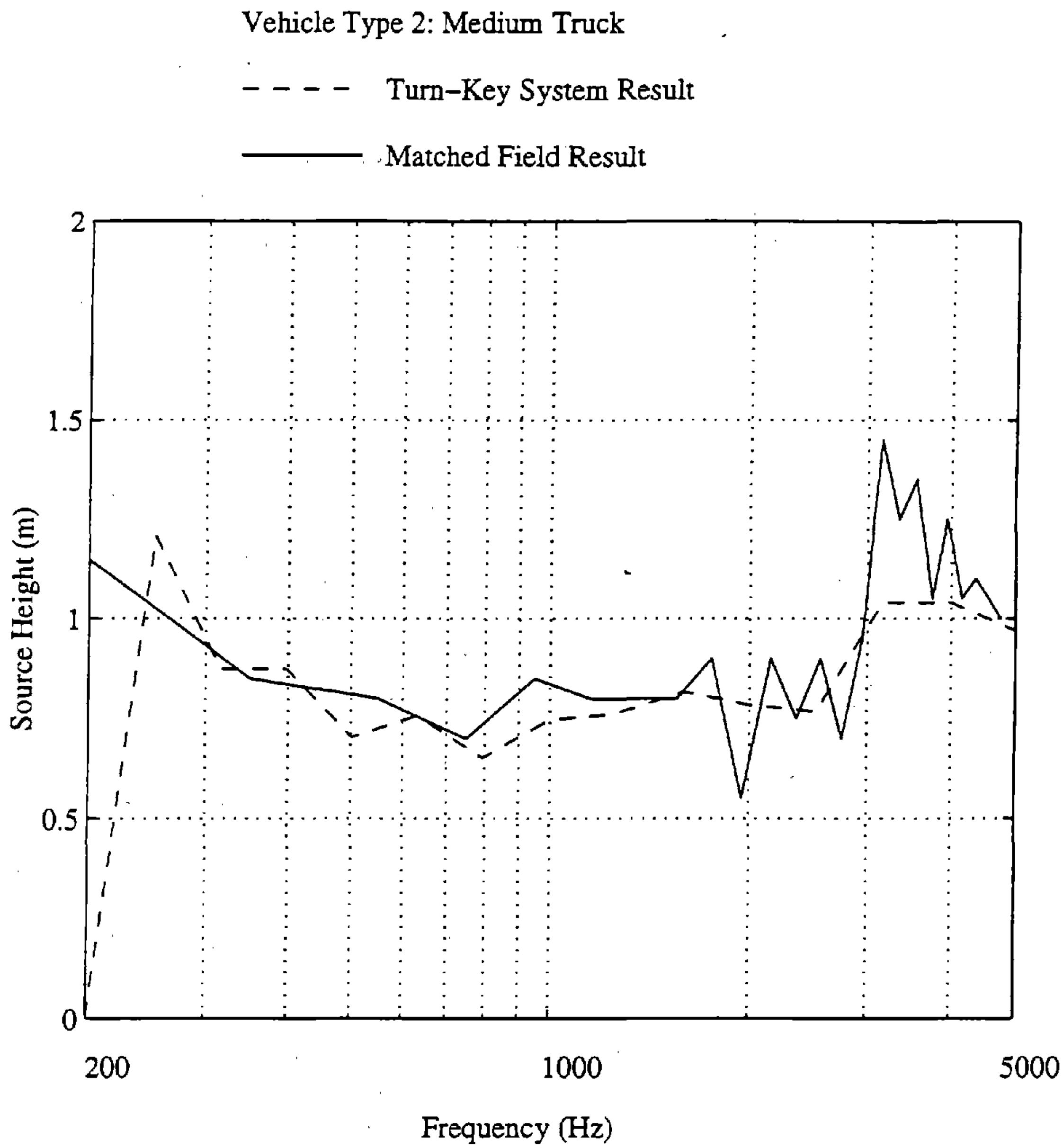

Figure 5.3: Comparison of the Source Heights Obtained for a 5-Axle Heavy Truck with the Turn-key System & the Matched Field Processor.